

**GEOCHEMISTRY OF HYDROTHERMAL Th-U-REE  
QUARTZ/FLUORITE VEINS  
FROM THE CAPITAN PLUTON**

By

Randall S. Phillips

Submitted in Partial Fulfillment of the  
Requirement for the Degree of Master of Science  
in Geochemistry

New Mexico Institute of Mining and Technology

Socorro, New Mexico

December 10, 1990

## ABSTRACT

The Capitan Mountains, south-central New Mexico, contain several, widely distributed Th-U-REE vein deposits near the western end and along the flanks of an east-west trending Tertiary (26.5Ma) alkali feldspar granitic pluton. The Capitan pluton has intruded Permian sedimentary rocks of the Yeso and San Andres Formations.

Mineralization associated with the Th-U-REE veins consist of smoky and clear quartz, fluorite, adularia, hematite, calcite, thorite, titanite, allanite, chlorite and clay minerals. Four main types of fluid inclusions occur in the quartz and fluorite. The inclusions show a large range in temperature and salinity. The dominant and most important type of inclusions are type 1 inclusions, which consist of halite, sylvite, vapor, liquid, anhydrite, hematite plus several other solid phases. Type 1 inclusions represent high temperature-high salinity fluids, Th and TmNaCl >600°C, bulk salinities up to 84 eq wt% NaCl + KCl; type 2 inclusions represent high to moderate temperature-high salinity fluids; type 3 inclusions represent moderate temperature-moderate salinity fluids; type 4 inclusions represent lower temperature-lower salinity fluids. The higher temperature, higher salinity inclusions define a halite trend when plotted in the NaCl-KCl-H<sub>2</sub>O system. This halite trend is a result of crystallizing of KCl-bearing halite from solution prior to entrapment. Most fluid inclusion types define a trend when plotted on Th vs salinity diagrams. The observed trends suggest a type of fluid evolution from the original parent fluid by cooling and crystallization of halite. The lowest temperature inclusions (type 4) suggest a mixing of two different types of fluids. The bulk chemistry of type 1 inclusions indicate K/Na ratios of 0.19 to 0.27. These values correspond to K/Na ratios which are near or at equilibrium with granitic rocks at

temperatures of 600°C.  $\delta^{18}\text{O}$  (from quartz) and  $\delta\text{D}$  (from inclusion fluids in quartz) of the fluids are 7.08‰ to 8.58‰ and -22‰ to -86‰, respectively. The isotopic data suggests that magmatic water was an important and possibly dominant source for the mineralizing fluids. Based on field relations, fluid inclusion microthermometry, stable isotope data, petrographic data, and inclusion fluid chemistry, it is suggested that the fluids responsible for the Th-U-REE mineralized zones in the western half of the Capitan Mountains are of magmatic origin. The fluids were derived as a result of contraction and cracking of the Capitan pluton during cooling, followed by injection of the exsolved magmatic fluids into the brecciated zones. Type 1 inclusions represent this exsolved fluid. Type 2 and 3 inclusion fluids evolved from the cooling type 1 fluids. A late-stage, post-mineralization fluid (type 4 inclusion fluids), which appears to be restricted to the west end of the pluton, may represent a mixture of an evolved magmatic fluid with a meteoric water.

## ACKNOWLEDGEMENTS

Financial aid in the form of grants-in-aid was supplied by the New Mexico Tech Research Council, the New Mexico Geological Society and the Albuquerque Gem and Mineral Club. Financial support was also provided by the Chemistry department, in the form of a Teaching assistantship, for four of the six semesters in residence at New Mexico Tech, and the Geoscience department for a teaching assistantship during the last semester at Tech.

I would like to thank Andrew Campbell, who suggested the thesis topic to me, offered guidance to me throughout the length of the project, quickly reviewed an early version of the thesis text, financially supported me for a semester and a summer at New Mexico Tech, and allowed me to use the stable isotope facilities. I would like to thank Virginia McLemore for support in the field, financial aid during the summer of 1989, guidance on the general geology and petrography pertaining to igneous petrology and a host of other things. I would like to specially thank the New Mexico Bureau of Mines and Mineral Resources who, through Virginia McLemore, helped support the project in the form of drafting figures (a special thanks to the drafting crew , Becky Titus and John Robinson), photography (thanks to Monty Brown), summer assistance, xeroxing facilities, and allowing me to use the instruments in the chemistry division. Within the chemistry division, I would like to thank Lynn Brandvold for helpful ideas pertaining to my crush-leach analyses; Jeannie Verploegh, for showing me how to run the Dionex; and Barbara Popp, for running samples for me on the ICP. I would

also like to thank Stacie Stowe, a chemistry undergraduate, for helping me run samples on the AA spectrophotometer.

Numerous other people I would like to thank are as follows. Chris Fedo, who ran the "SALTY" program for me using R.J. Bodnar's computer at VPI. John Lucio, who sent me many MAC programs and sort of helped me learn how to use them. Dave Mitcheltree and Lucho Changkuon, both of whom encouraged my studies very much ( hey Dave, lets go mineral collecting ; hey Lucho, give me another beer). Sonia Salgado, sort of a special friend, who helped me to keep my sanity (or insanity ?) during my last semester at Tech.

A special thanks to my parents - especially for my dad, Delbert Phillips, for continued support and understanding. This thesis is dedicated to my mother, Ruby Phillips.



## TABLE OF CONTENTS

<b>Abstract</b>	<b>ii</b>
<b>Acknowledgements</b>	<b>iii</b>
<b>Table of Contents</b>	<b>v</b>
<b>List of Figures</b>	<b>viii</b>
<b>List of Tables</b>	<b>x</b>
<b>Introduction</b>	<b>1</b>
<b>Geology and Mineralization</b>	<b>2</b>
<b>Fluid Inclusion Studies</b>	<b>15</b>
Sample Selection and Measurements	15
Fluid Inclusion Types	16
Origin, Size, Occurrence and Heating/Freezing Data	17
Quartz	26
Fluorite	29
Calcite	31
Titanite	31
Salinities of Fluid Inclusions	31
Quartz	52
Fluorite	54
Calcite and Titanite	54
Pressure-Depth Estimates	58
<b>Fluid Inclusion Leachate Analyses</b>	<b>59</b>
Experimental Procedures	60
Results of Crush-Leach Analyses	62

Preliminary Crush-Leach Analyses	62
HF Acid - Quartz Dissolution Analyses	63
Sc(NO <sub>3</sub> ) <sub>3</sub> Crush-Leach Analyses	64
<b>Stable Isotope Studies</b>	<b>74</b>
Experimental Procedures	74
Results of O Isotopes for Quartz, Adularia and Whole Rocks	76
Results of C and O Isotope Analyses on Vein Calcites	77
Results of H Isotope Analyses from Fluid Inclusion Waters	82
<b>Discussion of Fluid Inclusion Data</b>	<b>82</b>
Origin of Type 1 and 2 Fluid Inclusions (Halite Trend)	82
Origin of Type 3 Fluid Inclusions	92
Origin of Type 4 Fluid Inclusions	93
Summary of Fluid Inclusion Origins	93
<b>Chemical Composition of the Capitan Mineralizing Fluids</b>	<b>95</b>
<b>Discussion of Stable Isotope Data</b>	<b>98</b>
$\delta^{18}\text{O}$ of Quartz and Adularia and $\delta\text{D}$ on Inclusion Fluids	98
$\delta^{18}\text{O}$ of Pluton Whole Rocks and Vein Clasts	100
$\delta^{18}\text{O}$ and $\delta^{13}\text{C}$ of Vein Calcites	100
<b>Summary and Conclusions</b>	<b>101</b>
<b>References</b>	<b>106</b>
<b>Appendix A - Chemical, Textural and Mineralogical Descriptions for Representative Samples of the Capitan Pluton</b>	<b>111</b>
<b>Appendix B - Individual Prospect Descriptions</b>	<b>114</b>
<b>Appendix C - Fluid Inclusion Samples Used for Heating/Freezing Measurements and Fluid Inclusion Data</b>	<b>127</b>
<b>Appendix D - Fluid Inclusion Crush-Leach Analysis</b>	<b>159</b>
Sample Preparation	159

Experimental Procedures	160
Analysis of REE's by ICP	162
Hydrofluoric Acid Dissolution Technique	164
Crush-Leach Sample Descriptions	167
<b>Appendix E - Stable Isotope Data</b>	<b>171</b>
$\delta^{18}\text{O}$ on Silicates-Experimental Procedures	176
Oxygen Isotope Sample Descriptions for Quartz	178
Oxygen Isotope Sample Descriptions for Adularia	183
Oxygen Isotope Descriptions for Whole Rocks	186
Oxygen Isotope Descriptions for Whole Rocks on Vein Clasts and Plutonic Rock Adjacent to Veins	188
$\delta\text{D}$ Analyses on Fluid Inclusion Waters Experimental Procedures	191
Hydrogen Isotope Descriptions for Quartz	193
Oxygen and Carbon Isotopes on Carbonates Experimental Procedures	197
C and O Isotope Sample Descriptions of Carbonates	198
<b>Appendix F - Construction of a P-T Diagram to Illustrate the Phase Equilibria for the Capitan Halite Trend Inclusions</b>	<b>201</b>
<b>References Cited in Appendices</b>	<b>202</b>

## LIST OF FIGURES

Figure		Page
1	Geologic/Prospect/Sample Locality Map	3
2	Overview of southern Capitan Mountains	5
3a	Brecciation and hematization at McCory prospect	8
3b	Mineralization at the Hot Hill prospect	9
4	Paragenetic diagram for minerals of MTE prospect	13
5	Paragenetic diagram for minerals of other prospects	14
6a	Type 1 fluid inclusions in clear quartz	18
6b	Type 1 fluid inclusions in smoky quartz	19
6c	Type 1 fluid inclusion in fluorite	20
6d	Anhydrite daughter mineral in type 1 inclusion	21
6e	Hematite daughter mineral in type 1 inclusion	22
6f	Type 2 fluid inclusions in fluorite	23
6g	Plane of type 3 fluid inclusions in quartz	24
6h	Plane of type 4 fluid inclusions in fluorite	25
7	Fluid inclusion histogram for quartz - MTE prospect	33
8	Fluid inclusion histogram for quartz - W3-3 prospect	34
9	Fluid inclusion histogram for quartz - CMX prospect	35
10	Fluid inclusion histogram for quartz - CPU-2 prospect	36
11	Fluid inclusion histogram for quartz - BS prospect	37
12	Fluid inclusion histogram for quartz - CM 104 prospect	38
13	Fluid inclusion histogram for fluorite - CPU-1 prospect	39
14	Fluid inclusion histogram for fluorite - McCory prospect	40
15	Fluid inclusion histogram for fluorite - Koprian Springs prospect	41

16	Fluid inclusion histogram for fluorite - W3-4 prospect	42
17	Fluid inclusion histogram for quartz - W3-4 prospect	43
18	Fluid inclusion histogram for quartz - Fuzzy Nut prospect	44
19	Fluid inclusion histogram for fluorite - Fuzzy Nut prospect	45
20	Fluid inclusion histogram for quartz - Hot Hill prospect	46
21	Fluid inclusion histogram for fluorite - Hot Hill prospect	47
22	Fluid inclusion histogram for quartz - CM 235 prospect	48
23	Fluid inclusion histogram for fluorite - CM 235 prospect	49
24	Fluid inclusion histogram for all quartz data	50
25	Fluid inclusion histogram for all fluorite data	51
26	Th vs Salinity plot for all quartz data	55
27	Th vs Salinity plot for all fluorite data	56
28	NaCl-KCl-H <sub>2</sub> O phase diagram	57
29	$\delta^{18}\text{O}$ vs frequency for quartz and adularia	79
30	Plot of $\delta\text{D}$ versus $\delta^{18}\text{O}$	83
31	Pressure-Temperature diagram	86
32	P-T diagram to illustrate origin of type 1 fluids	89
33	P-T diagram to illustrate origin of type 2 fluids	91
34	P-T diagram to illustrate origin of type 3 fluids	94
35	Plot of K/Na vs temperature	97
36	Cartoon illustrating vein formation	104

## LIST OF TABLES

Table		Page
1	REE data on vein material from various prospects	7
2	Electron probe analyses on titanite and allanite from the MTE prospect	11
3	Summary of fluid inclusion data	32
4A	Concentrations of fluid inclusion leachate solutions normalized to 10 ppm total concentration for vein quartz using various leaching solutions	66
4B	Molalities, charge balances and anion deficiencies for fluid inclusion leachate solutions of vein quartz using various leaching solutions. Concentrations normalized to 10 ppm total concentration	67
4C	Molar ratios of cations and anions analyzed for preliminary crush-leach data using MTE quartz and various leaching solutions	68
5	Concentrations normalized to 10 ppm total concentration, molalities, charge balances and anion deficiencies for fluid inclusion chemical analyses using the hydrofluoric acid-quartz dissolution technique	69
6A	Concentrations of fluid inclusion leachate solutions normalized to 10 ppm total concentration for vein quartz (Sc leaching solution)	70
6B	Molalities for fluid inclusion leachate solutions of vein quartz using a 250 ppm Sc leachate solution in 0.25 wt% HNO <sub>3</sub> Values normalized to 10 ppm total concentration	71
6C	Charge balances and charge deficiencies for fluid inclusion leachate solutions of vein quartz using a 250 ppm Sc leach solution Values normalized to 10 ppm total concentration	72
6D	Molar ratios of cations and chloride on fluid inclusion crush-leach analyses of vein quartz using a 250 ppm Sc solution in 0.25 wt% HNO <sub>3</sub>	73
7	Oxygen isotopic values on quartz and hydrogen isotopic values on fluid inclusion waters in quartz (values vs SMOW)	78
8	Oxygen isotopic ratios (vs SMOW) for vein adularia, whole rock pluton, pluton vein clasts and pluton rock adjacent to veins	80

9	Carbon and oxygen isotopic composition of vein carbonates and limestone	81
A1	Representative chemical analyses for Capitan pluton samples	113
D1	Atomic absorption calibration data for preliminary crush-leach analyses on MTE quartz	168
D2	Anion chromatography data for preliminary crush-leach analyses on MTE quartz	170
D3	Atomic absorption calibration data for fluid inclusion leachate solutions on vein quartz using a 250 ppm Sc in 0.25 wt% HNO <sub>3</sub> leaching solution	171
D4	Anion chromatography calibration data for fluid inclusion leachates on vein quartz using a 250 ppm Sc in 0.25 wt% HNO <sub>3</sub> leaching solution	172
D5	Preliminary crush-leach data using MTE quartz and various leaching solutions	173
D6	Experimental data on fluid inclusion crush-leach analyses of vein quartz using a 250 ppm Sc solution in 0.25 wt% HNO <sub>3</sub>	174
D7	Experimental data for the hydrofluoric acid-quartz dissolution technique	175
E1	Oxygen isotope data for quartz	181
E2	Oxygen isotope data for vein adularia	185
E3	Oxygen isotope data for pluton whole rocks	187
E4	Oxygen isotope data for whole rock vein clasts and plutonic rock adjacent to veins	190
E5	Hydrogen isotope data for quartz and fluorite	195
E6	Carbon and oxygen isotope data on vein carbonates and limestone	199

## INTRODUCTION

Fluid inclusion and stable isotope investigations of various ore deposits have shown that magmatic fluids, fluids which have exsolved from a crystallizing granitic melt, can be an important and even dominant constituent of various ore fluids. Examples include the early-stage mineralization event in the cores of porphyry-type deposits (Sheppard et al., 1969, 1971; Hall et al., 1974; Sheppard and Taylor, 1974; Sheppard and Gustafson, 1976; Larson, 1987) and base and precious metal deposits (Rye, 1966; Landis and Rye, 1974; Rye and Sawkins, 1974; Bethke and Rye, 1979; Kelly and Rye, 1979; Burrows and Spooner, 1987; Thorn, 1988; Paterson et al., 1989; Richards and Spooner, 1989). However, for some of these deposits, it is often difficult to determine the geochemical properties for the magmatic component of the ore fluid involved in the mineralization event because the geochemical signature of the magmatic fluid has been partially contaminated through the interaction of meteoric groundwater, either by mixing before mineral deposition or by an overprint of a later-stage fluid as the hydrothermal system collapses.

Thorium-uranium-rare earth element (Th-U-REE) mineralization in the Capitan Mountains provide an opportunity for direct investigation of the geochemistry of a mineralizing magmatic fluid. The Th-U-REE veins contain an abundance of primary and related pseudosecondary fluid inclusions in quartz and/or fluorite. Willis et al. (1989) initially described the primary/pseudosecondary inclusions in quartz, worked on identifying daughter minerals and did preliminary microthermometric studies of 30 fluid inclusions in quartz from a single vein (Mina Tiro Estrella prospect - MTE).



The purpose of this paper is to chemically and physically characterize the fluids responsible for the Th-U-REE deposits; which in turn, will help to define the physico-chemical conditions responsible for the Th-U-REE quartz/fluorite veins. The methods of investigation used to achieve the goals of this study were: 30 days of field work, which involved locating Th-U-REE deposits and collecting suitable samples for fluid inclusion and stable isotope studies; microthermometric studies of 638 fluid inclusions in quartz and fluorite from 14 different vein systems of the Capitan Mountains; oxygen isotopes on vein quartz, adularia and calcite, hydrogen isotopes on fluid inclusion waters in quartz and fluorite, and carbon isotopes on calcites; and a chemical analysis of the mineralizing fluids which formed the quartz from six vein systems by bulk analysis of fluid inclusions employing a crush-leach procedure.

## **GEOLOGY AND MINERALIZATION**

The Capitan Mountain Th-U-REE deposits are located within the Lincoln National Forest, 5 km northeast of Capitan, Lincoln County, south-central New Mexico (Fig. 1). Access to the deposits are provided by graded dirt roads, jeep trails, pack trails and foot. The mineral potential of the Capitan Mountains consists of thorium, uranium, rare-earth elements, iron, manganese, feldspar and mineral specimens (Collins, 1956; Altshuler, 1959; Hamer and Kelley, 1963; Griswold, 1964; McLemore, 1983; Tuftin, 1984; McLemore and Phillips, in press). Extensive prospecting for radioactive ore deposits was conducted during the 1950's which resulted in the discovery of a number of Th-U-REE anomalies, most of which occur near the western edge of the Capitan Mountains. A thorium mill was partially

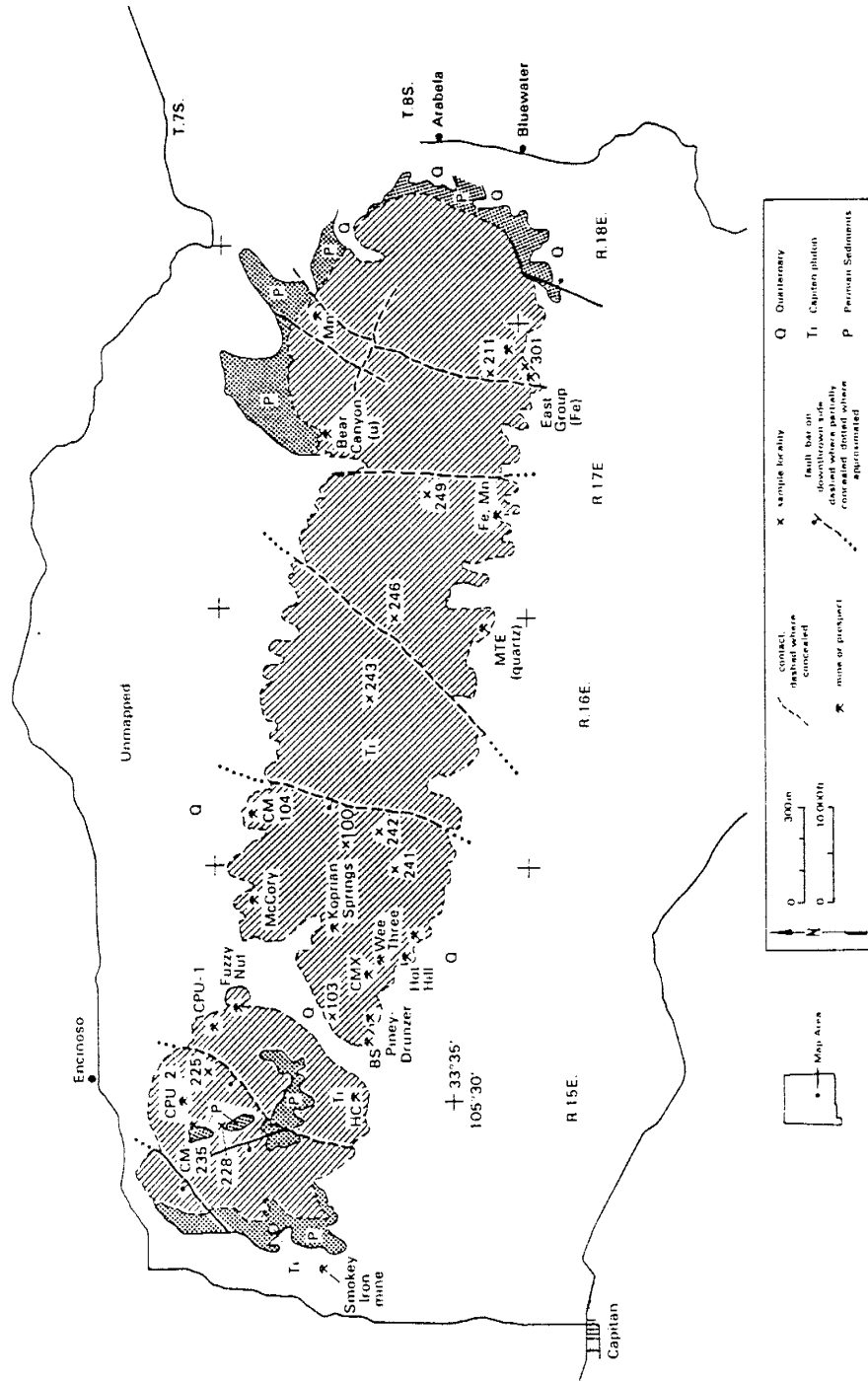


FIG. 1. Generalized geologic map of the Capitan Mountains showing the location of the Capitan pluton, prospect localities and sample localities. Geologic map modified from Kelley (1971).

constructed during the 1950's by the New Mexico Thorium Company, but no ore was ever processed (McLemore, 1983). Most of the Th-U-REE, Mn and Fe deposits are low-tonnage and currently inactive. The Smokey iron mine (Fig. 1; Kelley, 1952) is sporadically producing material for cement. One particular REE quartz-allanite-titanite vein (MTE prospect; Hanson, 1989) is presently being produced for mineral specimens of Japanese-law twinned quartz crystals.

The Capitan Mountains consist of an east (core) - west (apex) trending Tertiary (26.5 Ma, K/Ar, biotite; Allen, 1988) peraluminous alkali granitic pluton which is approximately 32 km long and 5 to 8 km wide (Fig. 1). Elevations range from 1700 to 3100 meters (Fig. 2). The Capitan pluton is one of the largest Tertiary plutons in New Mexico and is a prominent feature of the Capitan lineament (Chapin et al., 1978). The Capitan pluton is one of at least eight Tertiary igneous complexes (referred to as the Lincoln County porphyry belt by Thompson, 1972) in the region. The pluton has intruded carbonates, sandstones and shales of the Permian Yeso and San Andres Formations (Kelley, 1971). The Rio Bonito member (?) of the San Andres Formation overlies the pluton on the west end, forming a roof pendant (Fig. 1; Kelley, 1971). Contact-metasomatic iron-replacement bodies (skarns) occur near the intrusive contact at several places on the west end of the pluton. The sedimentary rocks of the Yeso Formation are overturned or dip steeply away from the intrusive contact at the east end, suggesting a forceful intrusion (Allen, 1988).

The Capitan pluton exhibits textural, chemical and mineralogical zonation trending west to east (Allen, 1988; V. McLemore, pers. comm., 1990). Textural zones have been divided into three types: granophyre, aplite and porphyry (Allen, 1988; Allen and McLemore, 1991). The top of the pluton on the west end is characterized by a granophyric granite containing subequal amounts of quartz, plagioclase and K-feldspar with trace amounts of biotite, epidote, magnetite, zircon

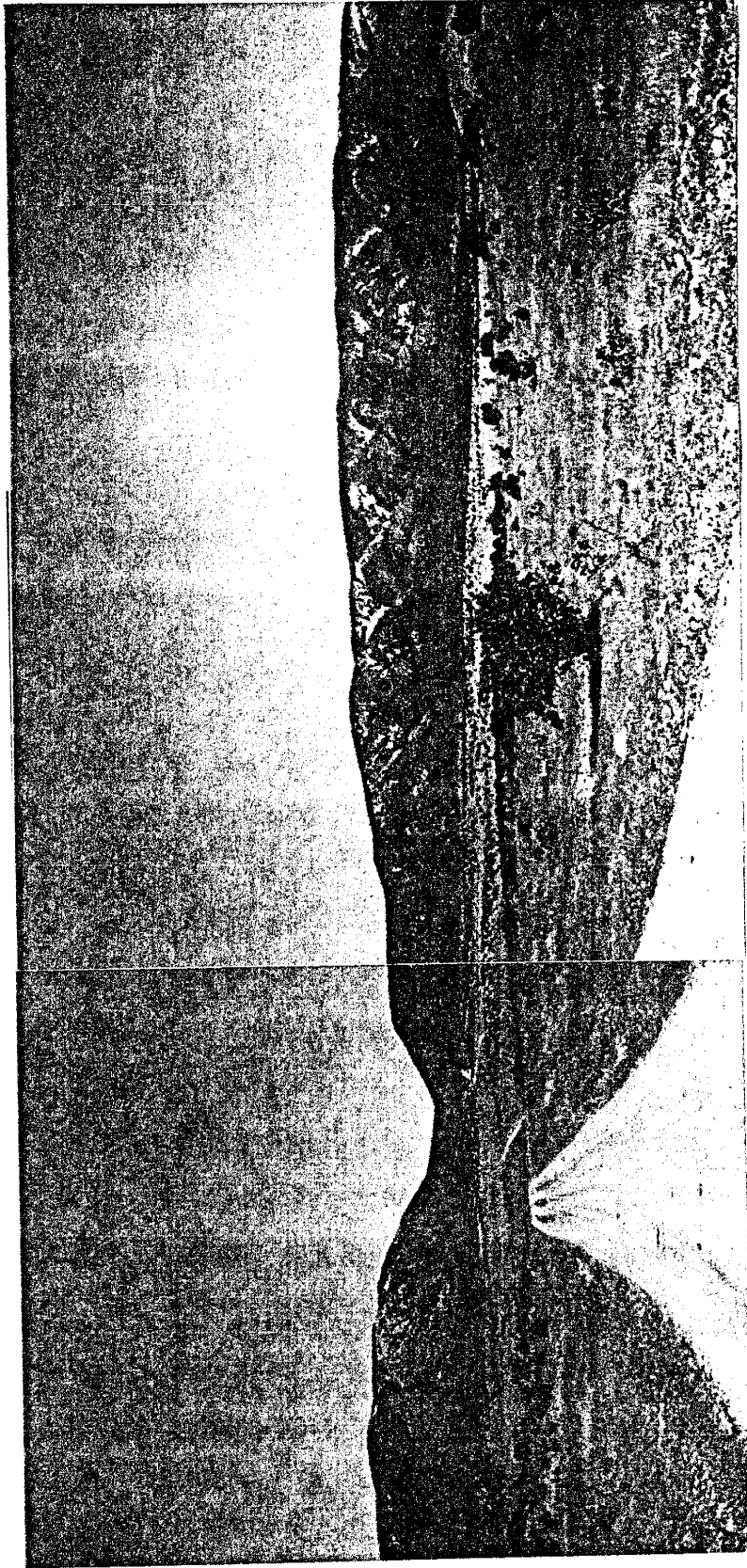


FIG. 2. Southern view of the Capitan Mountains, home of Smoky Bear.

and possibly allanite. The granophyric granite grades into an aplitic granite. The mineralogy of the aplitic granite is similar to the granophyric granite but contains less mafic minerals. The aplitic granite grades into a core (east end) of porphyritic granite containing relatively large phenocrysts of K-feldspar and quartz surrounded by a finer-grained matrix of quartz, plagioclase and K-feldspar. The porphyritic granite also contains numerous crystal aggregates of biotite, apatite, zircon, magnetite, titanite and richterite. Silica varies from 77 % in the granophyric granite (west end) to 68 % in the porphyritic granite (core, east end). Nb and Th decreases from the apex to the core, whereas Fe<sub>2</sub>O<sub>3</sub>, CaO, TiO<sub>2</sub>, Al<sub>2</sub>O<sub>3</sub>, Zr and Sr increase from the apex to the core. Representative chemical analyses for the Capitan pluton and mineralogical descriptions for the three textural zones are given in Appendix A.

The Capitan pluton is cut by several faults, and numerous brecciated and mineralized zones occur along the flanks and west end (Fig.1). Five types of mineralization occur: 1) a quartz vein with REE's, 2) quartz and/or fluorite veins with Th-U-REE's, 3) feldspar, 4) iron skarns near the intrusive contact and magnetite veins within the pluton, and 5) manganese veins. Only the first two types of mineralization will be discussed.

The quartz vein with REE's and quartz and/or fluorite veins with Th-U-REE's occur only in the granophyric granite and aplitic granite. Some areas of the porphyritic granite were examined for Th-U-REE's without much success. Some iron skarns and magnetite veins also contain anomalous U and Th. Th-U-REE analyses for some of the prospects are summarized in Table 1. The veins occur as fillings in brecciated zones (Fig. 3a) and as joint or fracture fillings in the pluton. In most prospects, the brecciated zones lie parallel with near-vertical joints in the pluton. The veins vary from less than a few centimeters to several meters in width and can be traced for as much as 300 meters in length.

Table 1. Rare Earth Element Data on Vein Material from Various Prospects

Prospect	Concentrations in ppm												
	Th	La	Ce	Pr	Nd	Sm	Gd	Tb	Dy	Ho	Yb	Lu	Y
CM 235	NA	13	91	BD	BD	BD	BD	BD	BD	BD	BD	BD	NA
CPU-2	NA	BD	86	8	58	57	7	2	7	6	3	BD	58
Fuzzy Nut	NA	BD	89	BD	56	59	7	2	6	6	3	BD	60
Kopm Spgs	NA	BD	85	21	323	316	48	3	48	48	15	BD	344
McCory-1	217	2500	4350	303	954	96	125	BD	87	BD	32	5	330
McCory-2	NA	91	139	18	88	20	25	2	24	BD	11	1	140
Piney-1	2460	13	91	BD	40	11	17	BD	BD	BD	4	BD	87
Piney-2	5	8	55	BD	21	4	7	BD	BD	BD	BD	BD	10
Piney-3	740	25	59	BD	46	11	16	BD	BD	BD	4	BD	61
Piney-4	245	50	74	BD	110	30	38	BD	BD	BD	12	BD	131
Wee Three	NA	BD	12	BD	BD	1	1	3	BD	BD	BD	BD	1

Rare Earth Elements by Inductively Coupled Plasma Spectrophotometry, courtesy of New Mexico Bureau of Mines and Mineral Resources

Data from McLemore and Phillips (in press)

BD - below detection limit

NA - not analyzed



FIG. 3a. Brecciation and hematization of vein material, McCory prospect.



FIG. 3b. Mineralization at the Hot Hill prospect. Visible minerals are clear fluorite, white calcite as vug material and as overgrowths on brown tabular minerals and adularia. Also present is Fe-Mn oxide staining.



Based on field observations and hand sample identifications, the quartz vein with REE's (Mina Tiro Estrella prospect, MTE) consists of quartz, adularia, allanite, titanite, chlorite, epidote and clay minerals. Actinolite, hematite, magnetite and microlite have been reported by Hanson (1989), but were not observed in the field by the author. Quartz occurs as massive, somewhat transparent vein-filling material; clear to smoky single crystals up to 3 cm filling open spaces; and as clear to smoky Japanese-law twinned crystals. Titanite occurs as reddish-brown, euhedral crystals up to 0.5 cm in length filling open spaces and as crystal aggregates within a massive adularia matrix. Titanite is also found growing on the surfaces of the various types of vein quartz. Black specks (allanite ?) have been observed as solid inclusions in the titanite. Allanite occurs as black, euhedral tabular crystals up to 1 cm in length filling open spaces. Allanite generally occurs as euhedral crystals growing on vein quartz. Allanite and titanite are the host minerals for REE's (Table 2) and both exhibit complex chemical zonation, as evidenced by back scatter electron mapping (M. Willis, pers. comm. 1989; Willis et al., 1989). The adularia is pink to white and occurs as massive intergrowths with quartz and as euhedral crystals filling open spaces. Adularia also occurs as growths of euhedral crystals on vein quartz surfaces. Clay minerals are present within the vein material and may be related to the alteration of the feldspars. Based on overgrowth/intergrowth relations for minerals from visual observations of dump samples from the MTE prospect, the following preliminary generalized paragenetic sequence is proposed (Fig. 4). Because of the lack of fresh vein material to define a detailed paragenesis, Figure 4 is meant to be only tentative.

Based on field observations and hand sample identifications, the quartz-fluorite veins with Th-U-REE's (CM 235, Fuzzy Nut, CPU-1, CPU-2, HC, McCory, Wee Three, Koprian Springs and Hot Hill prospects) consist of quartz, fluorite,

Table 2. Electron Probe Analyses on Titanite and Allanite from the MTE Prospect

Oxide	Titanite (1) (Wt%)	Titanite (2) (Wt%)	Allanite (1) (Wt%)	Allanite (2) (Wt%)
SiO <sub>2</sub>	27.73	28.80	28.35	30.33
TiO <sub>2</sub>	29.71	31.03	1.65	0.59
Al <sub>2</sub> O <sub>3</sub>	1.05	0.91	6.85	10.61
Fe <sub>2</sub> O <sub>3</sub>				11.71
FeO	4.67	4.29	21.60	7.69
CaO	24.08	24.95	9.23	10.38
MgO	0.24	0.14	1.29	1.16
MnO	0.10	0.12	0.49	
La <sub>2</sub> O <sub>3</sub>	0.52	0.50	12.20	9.73
Ce <sub>2</sub> O <sub>3</sub>	2.08	1.65	11.77	14.89
Pr <sub>2</sub> O <sub>3</sub>				0.58
Nd <sub>2</sub> O <sub>3</sub>	1.20	0.93	1.59	1.95
Sm <sub>2</sub> O <sub>3</sub>				0.24
ThO <sub>2</sub>				0.17
P <sub>2</sub> O <sub>5</sub>				0.01
Nb <sub>2</sub> O <sub>5</sub>	0.98	0.81	0.01	
ZrO <sub>2</sub>	0.26	0.97	0.03	
Y <sub>2</sub> O <sub>3</sub>	0.89	0.79	0.25	
F <sub>2</sub>	1.04	1.17	0.72	0.32
H <sub>2</sub> O				1.38
Totals	94.55	96.96	96.03	101.74

Titanite (1), Titanite (2) and Allanite (1) were analyzed at the Dept. of Earth and Planetary Sciences, Washington University, St. Louis, MO (Willis et al., 1989).

Allanite (2) was analyzed at the Dept. of Geological Sciences, University of Michigan, Ann Arbor, MI (E. Essene, pers. comm., 1990).

adularia, hematite/maghemite, thorite (identified by XRD from mineral separates; V. McLemore, pers. comm., 1990) and allanite(?). Quartz occurs as clear to smoky crystals up to 2 cm lining fractures and open spaces and as massive material filling brecciated zones. Fluorite occurs as green, blue, purple and colorless cubes up to 2 cm filling vugs and fractures and as massive, vein-filling material. Adularia generally occurs as pink to white, euhedral crystals up to 7mm lining fractures. Primary hematite/maghemite occurs as specular plates coating fractured surfaces and as massive material filling brecciated zones. Th-U-REE prospects containing quartz, adularia, thorite and allanite(?) are CM 104, BS, Piney-Drunzer and CMX. Calcite was observed as a late-stage, fine-grained, vug-filling mineral at the Fuzzy Nut, HC, Hot Hill (Fig. 3b) and Wee Three prospects. Apatite and garnet were found at the Fuzzy Nut prospect. Brown nodular to tabular masses up to a few centimeters were seen in veins at the CM 235, HC, Hot Hill, Wee Three and Fuzzy Nut prospects. These masses may contain the Th-U-REE mineral phases. The higher grade Th occurrences appear to be localized in the hematite-cemented parts of the brecciated veins. A preliminary generalized paragenetic sequence based on field observations and hand samples for the more common minerals in the prospects is proposed in Figure 5. Due to a lack of adequate samples which would enable a detailed paragenesis to be defined, the paragenetic sequence in Figure 5 is tentative. Numerous other small prospect pits occur throughout the western end of the Capitan pluton. For a more detailed description of the individual prospects, refer to Appendix B and McLemore and Phillips (in press).

Mineralization is localized to the fractured/brecciated zones within the pluton. Alteration associated with the mineralization appears to be absent or at a minimum in the host plutonic rock adjacent to the veins.

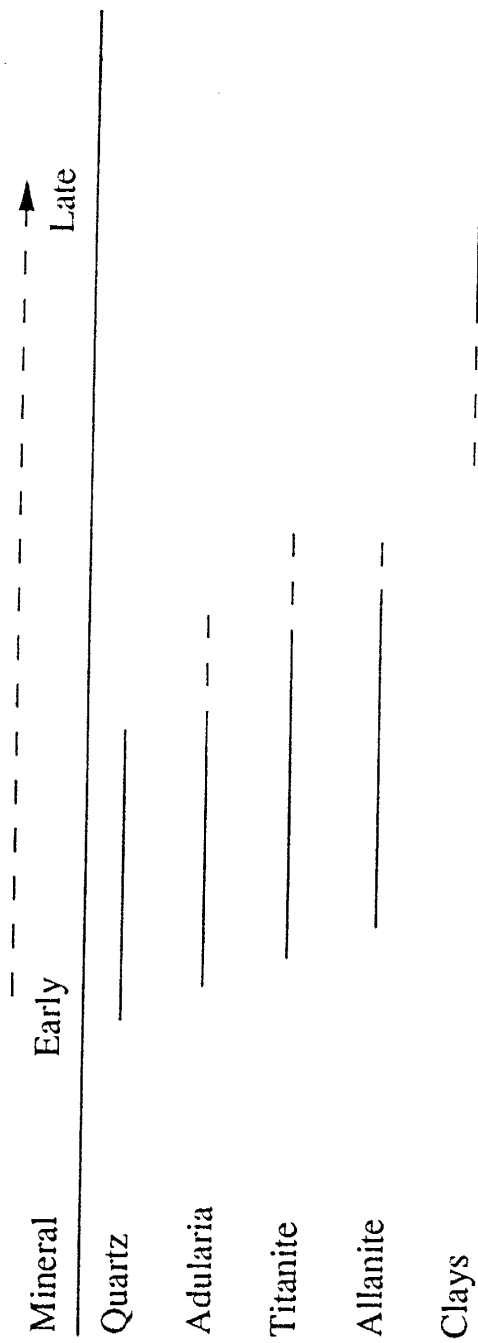


FIG. 4. Preliminary generalized paragenetic diagram for minerals at the MTE prospect. Paragenesis is based on visual observations from dump samples and should be regarded as tentative until further thin section studies of exposed vein material are conducted.

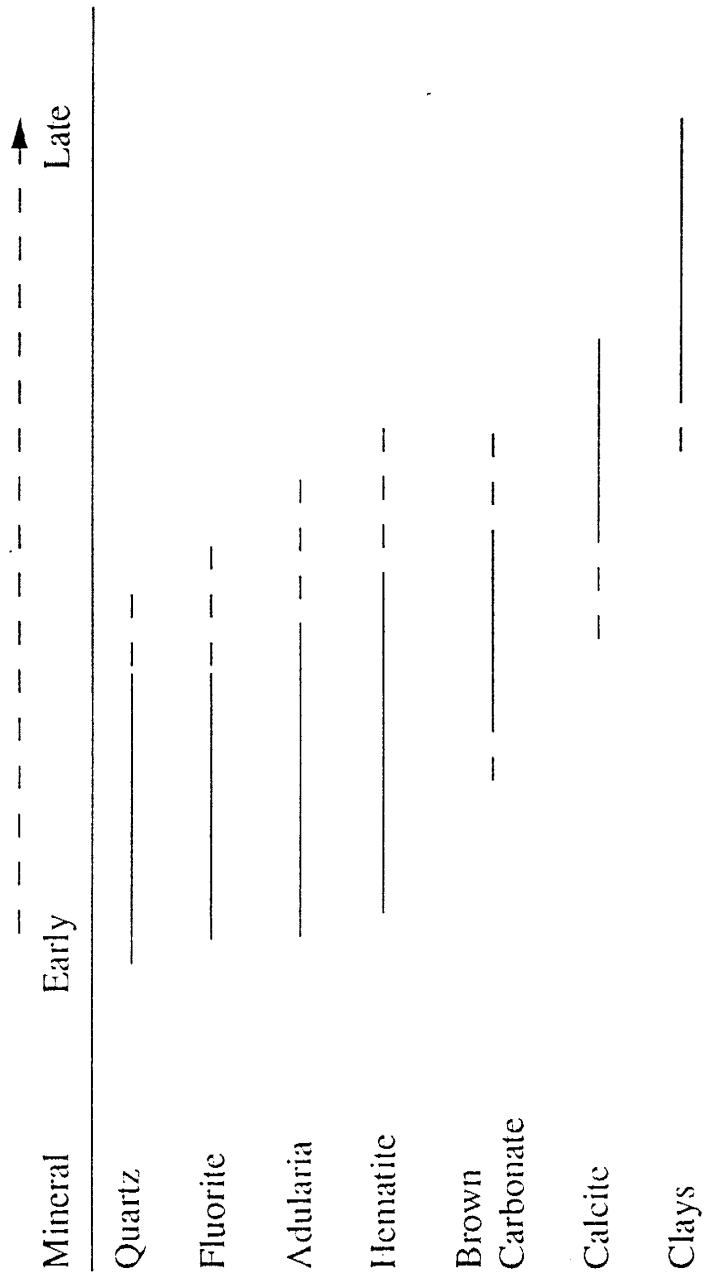


FIG. 5. Preliminary generalized paragenetic diagram for commonly observed minerals at the Th-U-REE prospects. Paragenesis is based on visual observations from dump samples and should be regarded as tentative until further thin section studies of exposed vein material are conducted.

## FLUID INCLUSION STUDIES

### SAMPLE SELECTION AND MEASUREMENTS

Samples for fluid inclusion microthermometric measurements were selected from vein quartz, fluorite, titanite and calcite. Garnets within a magnetite skarn, near CM 235 prospect, contain inclusions similar to quartz, but were not measured due to the small size of the inclusions. An attempt was made to identify fluid inclusions in doubly-polished thick sections of vein adularia and allanite crystals and thin plates ( $< 0.1$  mm) of magnetite using transmitted infrared and visible light, but none were observed. Small, vuggy quartz crystals within miarolitic cavities of the plutonic rock and igneous quartz contain small inclusions, but were not measured due to the small size of the inclusions. Forty doubly-polished thick sections of euhedral quartz crystals, massive quartz within brecciated vein material and single fluorite cubes were prepared for microthermometric studies. Small cleavage fragments (0.1-0.5 mm in thickness) of fluorite and calcite and small grains (0.2-0.4mm in thickness) of titanite were also used for microthermometric measurements. Detailed descriptions of samples used for microthermometric measurements are given in Appendix C.

Microthermometric studies of fluid inclusions were performed on a Linkham TH 600 heating/freezing stage. Calibration for heating measurements was achieved with various organic and inorganic compounds with melting temperatures 82, 115, 135, 165, 192, 236, 306, 398, 455 and 560°C. Precision for temperatures less than 150°C was  $\pm 1^\circ\text{C}$ , for temperatures between 150 to 300°C was  $\pm 2^\circ\text{C}$ , and for temperatures greater than 300°C was  $\pm 6^\circ\text{C}$ . Calibration for freezing measurements was obtained using triply distilled/deionized water.

## FLUID INCLUSION TYPES

Optical microscopy of phase assemblages of 638 fluid inclusions in quartz and fluorite reveal four major types of inclusions.

1) Type 1 inclusions are multiphase inclusions [ liquid (L) + vapor (V) + halite (H) + sylvite (S) + three or more other daughter minerals; Figs. 6a-d.] that homogenize by either halite dissolution or vapor homogenization, the former being more dominant. Type 1 inclusions are the most abundant of the four types. The vapor phase constitutes 8 to 15% of the total fluid inclusion volume. Preliminary laser Raman microprobe work on the vapor phase did not detect any other gases besides water vapor (M. Willis, pers. comm., 1989). Some of the daughter minerals in type 1 inclusions have been positively identified optically, by SEM and laser Raman spectroscopy (Willis et al., 1989) as halite, sylvite, anhydrite and hematite. Titanite, magnetite, barite and an unknown carbonate mineral (G. Wolf, pers. comm., 1990) have been tentatively identified. An attempt was made to use X-ray diffraction on a polished section of quartz to identify daughter minerals, no daughter minerals were detected (C. McKee, pers. comm., 1990). Other daughter minerals may consist of complex Fe-Zn-Mn-Mg-Ca salts, as evidenced by the fluid inclusion chemistry. Halite is the dominant solid phase and is isotropic, colorless and forms sharp to slightly rounded cubic crystals. Sylvite is the second most abundant solid phase and is isotropic, colorless, exhibits slightly lower relief than halite and forms subrounded crystals. Anhydrite occurs as elongated, slightly rounded rectangular prisms with moderate birefringence (Fig. 6d) and usually does not dissolve at temperatures below 600°C. Hematite occurs either as a black opaque solid phase or as a yellow/orange to red thin plate, occasionally exhibits a hexagonal habit (Fig. 6e) and never dissolves upon heating to 600°C. Phase ratio observations of the daughter minerals in hundreds of type 1 inclusions within a given sample of quartz or

fluorite show that the daughter minerals occur in similar ratios in the different inclusions, which suggests that the solid phases are not trapped minerals. Also, no solid inclusions were observed in the host quartz and fluorite.

2) Type 2 inclusions are multiphase inclusions [ L + V + H + S + zero to two other daughter minerals; Fig. 6f] which generally homogenize by halite dissolution. Hematite may be present as a daughter mineral in some quartz samples. The vapor phase accounts for 8-10% of the total inclusion volume.

3) Type 3 inclusions are three phase inclusions [ L + V + H; Fig. 6g]. The vapor phase accounts for 5 to 10% of the total inclusion volume. Type 3 inclusions may homogenize by either halite dissolution or vapor homogenization.

4) Type 4 inclusions are two phase inclusions [L + V; Fig. 6h]. The vapor phase accounts for 5 to 10% of the total inclusion volume.

A fifth type of inclusion was observed in smoky quartz from the Wee Three prospect (W3-3). These inclusions are vapor-rich and may be subdivided as nearly 100% vapor, and 40 to 60% vapor with halite and occasional black opaque daughter minerals. These types of inclusions are very rare.

#### **ORIGIN, SIZE, OCCURENCE AND HEATING/FREEZING DATA**

Fluid inclusion types were classified as primary, pseudosecondary or secondary in origin according to the criteria of Roedder (1984).

The occurrence of the four types of inclusions varies from vein to vein. Type 1 inclusions occur in all quartz and fluorite samples, although they are more abundant in quartz. Types 2, 3 and 4 inclusions are more abundant in fluorite. Quartz/fluorite veins which occur near or on ridge tops (ie., Hot Hill, Koprion Springs prospects), hence closer to the roof of the pluton, contain a slightly higher percentage of type 3 and 4 inclusions as compared to veins which occur on the flanks (MTE prospect)



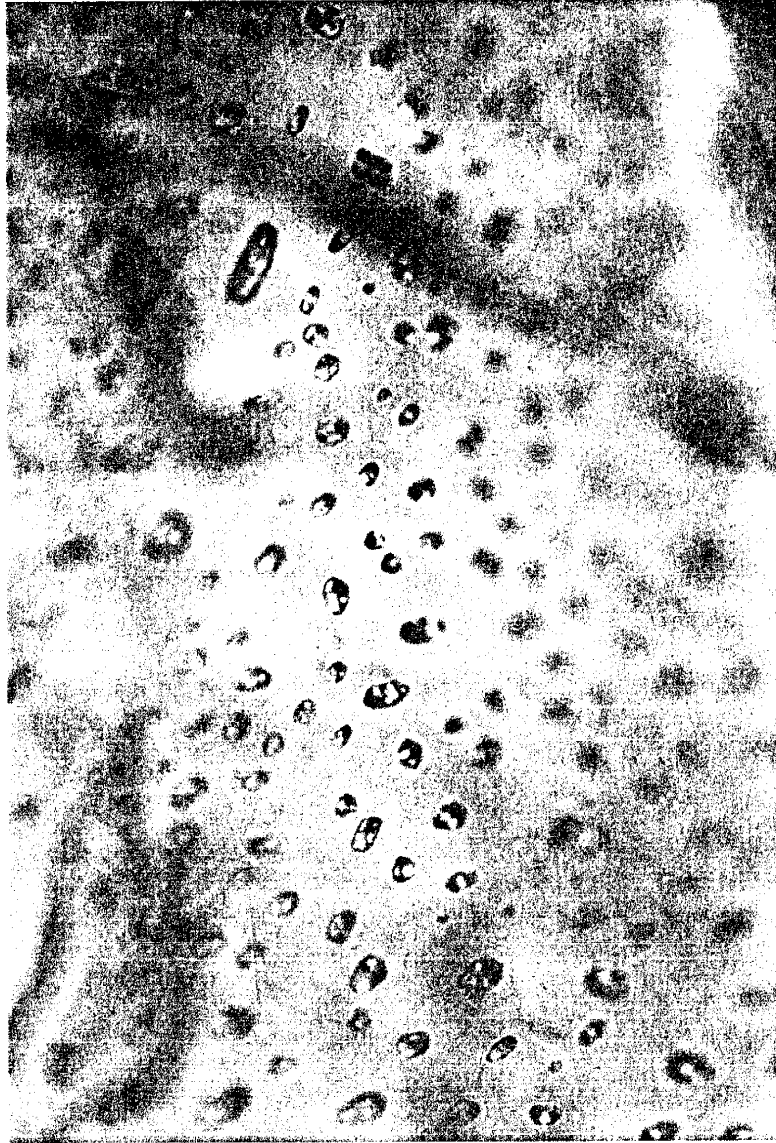


FIG. 6a. Plane of primary type 1 inclusions along growth zones in quartz from the MTE prospect. Inclusions are 5 to 15 microns in size. Picture taken in plane light.



FIG. 6b. Type 1 inclusions in smoky quartz from the Wee Three prospect. Largest inclusion is 75 microns. Halite is largest daughter mineral followed by sylvite.



FIG. 6c. Primary type 1 inclusion in fluorite from the CPU-1 prospect. Inclusion is 90 microns in size. Largest daughter mineral is halite (H). Sylvite (S) is the next largest solid phase. Vapor bubble adjacent to sylvite.

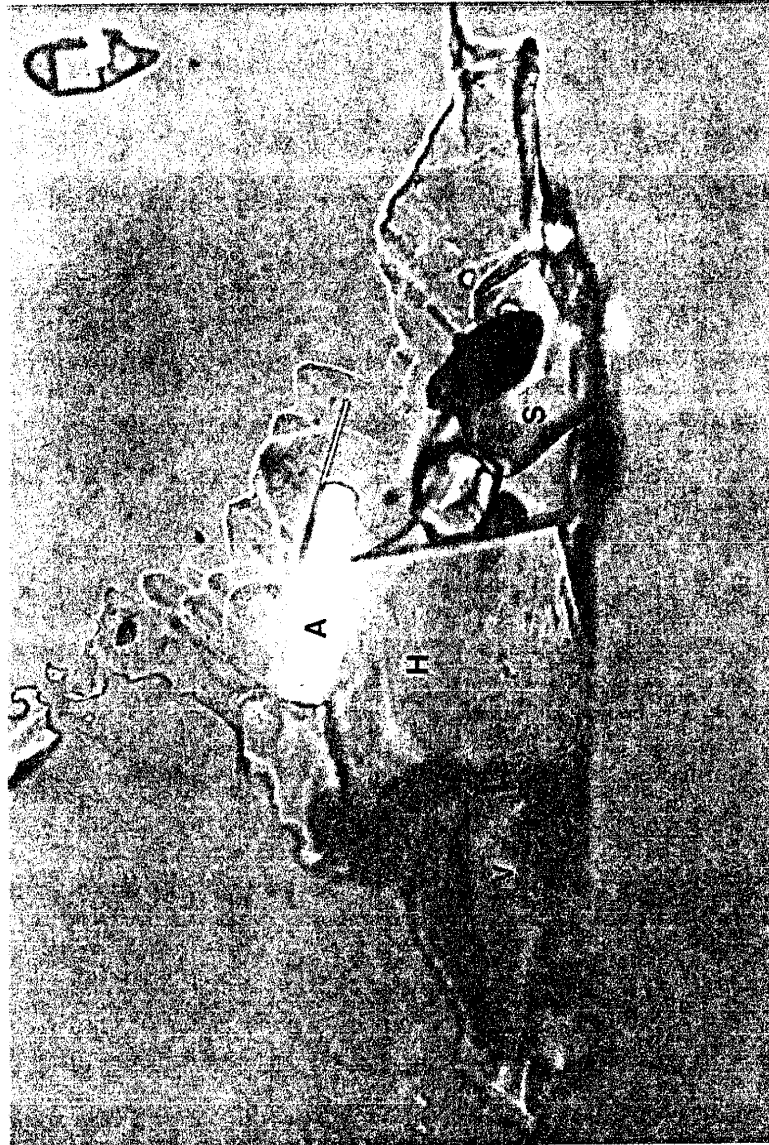


FIG. 6d. Birefringent daughter mineral (anhydrite) in a stretched type 1 inclusion in quartz from the Wee Three prospect. Inclusion is 120 x 55 microns in size. Daughter minerals are halite (H), sylvite (S), hematite (red) and others. Vapor bubble (V) appears adjacent to halite.



FIG. 6e. Hexagonal hematite daughter mineral in a leaked type 1 inclusion in fluorite from the CPU-1 prospect. Hematite is 20 x 20 microns in size. Hematite is always present in type 1 inclusions, but not always in such a euhedral form.



FIG. 6f. Type 2 inclusion in fluorite from the Hot Hill prospect. Inclusion is 110 microns long and contains halite (H), sylvite(S), vapor and liquid.



FIG. 6g. Plane of secondary type 3 inclusions in smoky quartz from the Wee Three prospect. Inclusions are less than 5 to 60 microns in size. Solid phase is halite.



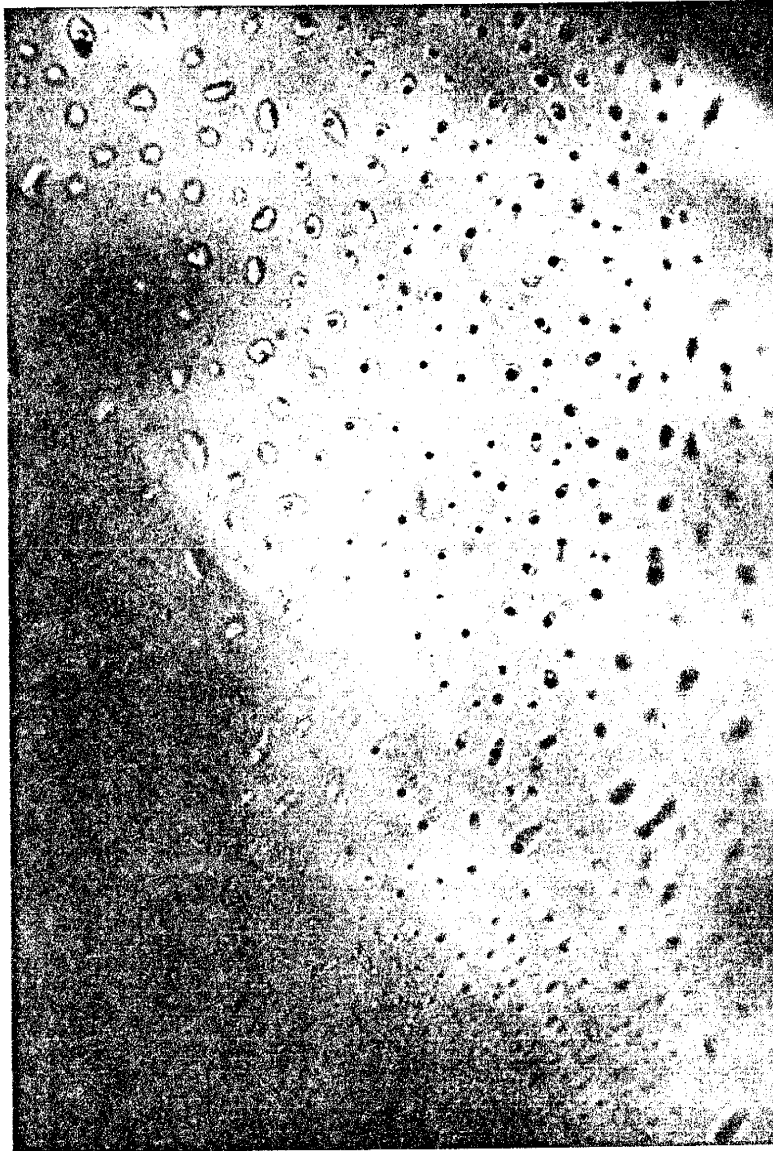


FIG. 6h. Plane of secondary type 4 (L + V) inclusions in fluorite from the Koprion Springs prospect. Individual inclusions are 5 to 10 microns in size.



and in the valleys (Wee Three prospects), which are inferred to be deeper within the pluton. The granophyric granite (apex) on the west end of the pluton is locally altered (a late-stage deuteric alteration?) and fractured and is host to prospects which generally contain a higher percentage (less than 25%) of type 4 inclusions in the quartz and fluorite. As the pluton grades into an aplitic granite, less to no alteration is apparent and the prospects hosted by the aplitic granite generally contain a lower percentage (less than 10%) of type 4 inclusions in the quartz and fluorite.

Vapor homogenization temperatures ( $T_h$ ), halite dissolution temperatures ( $T_m$  NaCl) and sylvite dissolution temperatures ( $T_m$  KCl) were measured on 638 fluid inclusions in quartz and fluorite from 14 different vein systems to determine the temperatures and pressures of vein formation and salinities of the vein-forming solutions. Table 3 summarizes the important fluid inclusion data. Appendix C tabulates the raw data for each of the prospects. Histograms for the veins looked at in this study are shown in Figures 7 - 23. Figure 24 shows a histogram with all the quartz data combined and Figure 25 shows a histogram with all the fluorite data combined. Due to a lack of adequate data for complex "salty" systems (type 1 and 2 inclusions), no pressure corrections have been applied to any of the measured temperatures.

### QUARTZ

Type 1 inclusions are the dominant type in quartz from all prospects which were studied. The type 1 inclusions range in size from 150 to less than 5 microns, averaging 10 to 30 microns. They are usually sub-oval to irregular in shape. They occur as isolated inclusions, as planes containing hundreds of inclusions along growth zones which do not cut through grain boundaries (Fig. 6a), as clusters, and

as trails healing fractures which do not cut grain boundaries. Type 1 inclusions in quartz are primary or psuedosecondary in origin. Type 1 inclusions in vein quartz could not always be easily distinguished between primary and psuedosecondary. In cases where this distinction could not be made, a psuedosecondary origin was assigned. Type 1 fluid inclusions in quartz tend to be bigger (average 30 to 40 microns) for the MTE, CMX and WeeThree prospects as compared to type 1 inclusions in the other prospects, which average 10 to 20 microns. Type 1 inclusions account for greater than 90% of the total inclusions in quartz from the MTE, CMX, CM 104 and Wee Three prospects. For the remaining prospects, type 1 inclusions account for 75 to 90% of the total inclusion population. Two-hundred and eighty type 1 inclusions were measured in quartz. Th for type 1 inclusions ranges from 398 to  $>600^{\circ}\text{C}$ .  $T_m$  NaCl for type 1 inclusions ranges from 483 to  $> 600^{\circ}\text{C}$ . Based on the size of the halite cube and/or vapor bubble still present at the  $600^{\circ}\text{C}$  limit of the heating stage, it is estimated that complete homogenization would occur at temperatures less than  $650^{\circ}\text{C}$ , with the majority in the  $610$  to  $620^{\circ}\text{C}$  range.  $T_m$  KCl ranges from  $145$  to  $313^{\circ}\text{C}$ . There is a general increase in halite dissolution temperatures trending west to east, with the westernmost CM 235 prospect having  $T_m$  NaCl up to  $547^{\circ}\text{C}$  and the easternmost MTE prospect having  $T_m$  NaCl  $> 600^{\circ}\text{C}$ .

Type 2 inclusions were only observed and measured from the CM 235, Hot Hill, Fuzzy Nut, CMX and MTE prospects. They account for less than 1% of the total inclusions in the quartz. Sizes range from less than 5 to 15 microns. Type 2 inclusions occur as trails within healed fractures cutting across quartz grains. The majority of type 2 inclusions are secondary in origin. For single quartz crystals, type 2 inclusions could not be observed cutting grain boundaries and hence their origin could not be distinguished between psuedosecondary and secondary. Seventeen

type 2 inclusions were measured in quartz. Th ranges from 343 to 480°C, Tm NaCl ranges from 363 to 509°C and Tm KCl ranges from 96 to 204°C.

Type 3 inclusions occur in all the quartz veins. They are less abundant in the MTE, CM 104, Wee Three and CMX prospects, accounting for less than 1 to 5% of the total inclusions. The other prospects contain 5 to 10% type 3 inclusions as part of the total inclusion volume. Type 3 inclusions are small, less than 20 microns, and generally ovoid in shape. They usually occur as secondary planes of inclusions cutting across mineral grains. Type 3 inclusions are generally classified as secondary in origin. For single quartz crystals, grain boundary crosscutting relations could not be observed; thus, the origin of the type 3 inclusion could not be classified as pseudosecondary or secondary. Forty-six type 3 inclusions were measured in quartz. Th ranges from 119 to 402°C and Tm NaCl ranges from 139 to 389°C. A high-temperature type 3 inclusion was observed from CM 104, Th of 461 °C and Tm NaCl of 469°C. This may be a metastable type 2 inclusion.

Type 4 inclusions are small, less than 10 microns, and generally subrounded in shape. Type 4 inclusions were observed in only a few prospects and account for less than 1 to 5% of the total inclusion volume. They generally occur as planes containing several inclusions cutting across quartz grain boundaries. Type 4 inclusions are classified as secondary in origin. Thirteen type 4 inclusions were measured in quartz. Th varies from 113 to 208°C. Freezing point depressions for type 4 inclusions range from -15.8 to -14.1°C.

Vapor-rich inclusions from the Wee Three (W3-3) prospect are oval to rounded in shape, range from less than 1 micron to 10 microns in size and occur isolated and as inclusion trails along healed fractures within single quartz crystals. They account for less than 1% of the total inclusions and their origin is uncertain. For inclusions which were nearly 100% vapor, it was impossible to observe the

liquid to vapor homogenization. An attempt was made to measure inclusions which contained 40 to 60% vapor plus liquid plus halite, but they usually decipitated/leaked before halite dissolution or liquid to vapor homogenization could be observed.

### FLUORITE

In general, type 1 inclusions are not very abundant in vein fluorite for most of the prospects. An exception occurs in fluorite from the CPU-1 prospect, which contains > 90% type 1 inclusions. Most veins containing fluorite have type 1 inclusions accounting for 5 to 10% of the total inclusions. Type 1 inclusions range from less than 5 to 70 microns, averaging 10 to 20 microns, and are generally oval to irregular in shape. Type 1 inclusions are classified as primary when they occur isolated or in clusters and psuedosecondary when they occur in trails healing fractures within mineral grains. Type 1 inclusions never occur as hundreds of inclusions along growth planes, as is common for quartz. Type 1 inclusions in fluorite are compositionally similiar to those in quartz, which suggests that the quartz and fluorite are cogenetic. Fifty-four type 1 inclusions were measured in fluorite. Th for type 1 inclusions ranges from 329 to > 600°C, Tm NaCl ranges from 483 to >600°C and Tm KCl ranges from 167 to 283°C.

Type 2 inclusions in vein fluorite were observed in all prospects, except CM 235. They account for 0 to 25% of the total inclusions, are sub-rounded and elongated in shape and range in size from less than 5 to 30 microns. Type 2 inclusions generally occur as inclusions trails healing fractures which cut through grain boundaries and are classified as secondary in origin. In some cases where cleavage chips and single crystals were looked at, type 2 inclusions could not be observed to cut grain boundaries and hence they could not be distinguished between

psuedosecondary and secondary. They always contain halite and sylvite and rarely hematite as daughter minerals. One-hundred and eleven type 2 inclusions were measured in fluorite. Th ranges from 268 to 407°C, Tm NaCl ranges from 288 to 407°C and Tm KCl ranges from 51 to 162°C.

Type 3 inclusions were observed in all prospects containing vein fluorite, except the CPU-1 prospect. They account for 0 to 50% of the total inclusions, are oval to sub-rounded in shape and range from less than 1 to 30 microns in size, averaging 5 microns. They occur in planes cutting through grain boundaries and as trails crosscutting grain boundaries. The majority of type 3 inclusions are secondary in origin. When cleavage chips and single fluorite crystals were looked at a distinction between psuedosecondary and secondary could not be determined. Ninety-two type 3 inclusions were measured in fluorite. Th ranges from 119 to 358°C and Tm NaCl ranges from 167 to 351°C.

Type 4 inclusions in fluorite were observed in most prospects. They account for 10 to 30% of the total inclusions, are rounded to oval in shape and range in size from less than 1 micron to 10 microns. They occur in planes containing hundreds of 1 to 2 micron-sized inclusions cutting grain boundaries and are commonly stretched. They also occur within healed fractures cutting grain boundaries. Most type 4 inclusions can be classified as secondary in origin. When cleavage chips and single crystals are looked at, the problem of assigning a psuedosecondary or secondary is encountered as mentioned above. Twenty-two type 4 inclusions were measured in fluorite. The inclusions have Th from 110 to 169°C. Freezing point depressions range from -17.7 to -7.1°C.

### CALCITE

Type 3 and 4 inclusions in late-stage, vug-filling calcite were observed from the Hot Hill prospect. Type 3 inclusions occur as trails in healed cracks, are less than 8 microns in size and are oval in shape. These inclusions appear to be secondary in origin; however, because only cleavage chips were looked at, the distinction between a pseudosecondary versus secondary origin could not be established. Only four type 3 inclusions were measured due to their small size. Th ranges from 225 to 237°C and Tm NaCl ranges from 231 to 233°C. Type 4 inclusions in calcite occur within planes along fractures, are usually oval in shape and are less than 1 micron. Type 4 inclusions appear to be secondary in origin. These were not measured due to their small size.

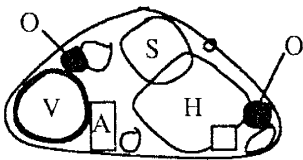
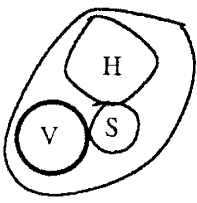
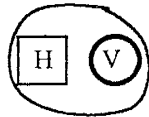
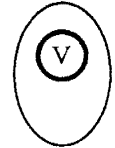
### TITANITE

Type 1 inclusions in titanite from the MTE vein are very small and hard to see due to the dark red cloudiness of the host mineral. In one mineral grain, three type 1 inclusions were observed as a cluster and one was measured. The measured inclusion was a primary inclusion. The inclusion contained at least five daughter minerals. The inclusion is oval in shape and is 12 microns in size. The vapor bubble accounts for 8% of the inclusion volume. This inclusion is similar to type 1 inclusions in the associated quartz, which suggests the two minerals are cogenetic. Th is greater than 600°C, Tm NaCl is 564°C and Tm KCl is 250°C.

### **SALINITIES OF FLUID INCLUSIONS**

Salinities for type 1 and 2 inclusions, best represented by the NaCl-KCl-H<sub>2</sub>O system, were obtained by measuring halite and sylvite dissolution temperatures and using the FORTRAN program SALTY (Bodnar et al., 1989). Salinities for type 3

Table 3. Summary of Fluid Inclusion Data

Type	1	2	3	4
Phases	L+V+H+S + others	L + V + H + S	L + V + H	L + V
				
<b>Th Vapor (C)</b>				
Quartz	398 - > 600	343 - 480	119 - 461	113 - 208
Fluorite	329 - > 600	268 - 407	119 - 358	110 - 169
<b>Bulk Salinity</b>				
	Wt% NaCl + KCl	Wt% NaCl + KCl	Wt% NaCl	Wt% NaCl
Quartz	65.8 - > 83.6	52.4 - 69.6	29.4 - 55.8	18.8 - 19.3
Fluorite	66.8 - > 80.8	45.6 - 56.5	30.8 - 42.7	10.6 - 20.7
<b>K/Na Ratios</b>				
Quartz	0.16 to 0.32	0.24 to 0.40		
Fluorite	0.21 to 0.33	0.21 to 0.43		
<b>Number of Measurements</b>				
Quartz	280	17	46	13
Fluorite	54	111	92	22

H = Halite, V = Vapor bubble, S = Sylvite, A = Anhydrite, O = Opaque

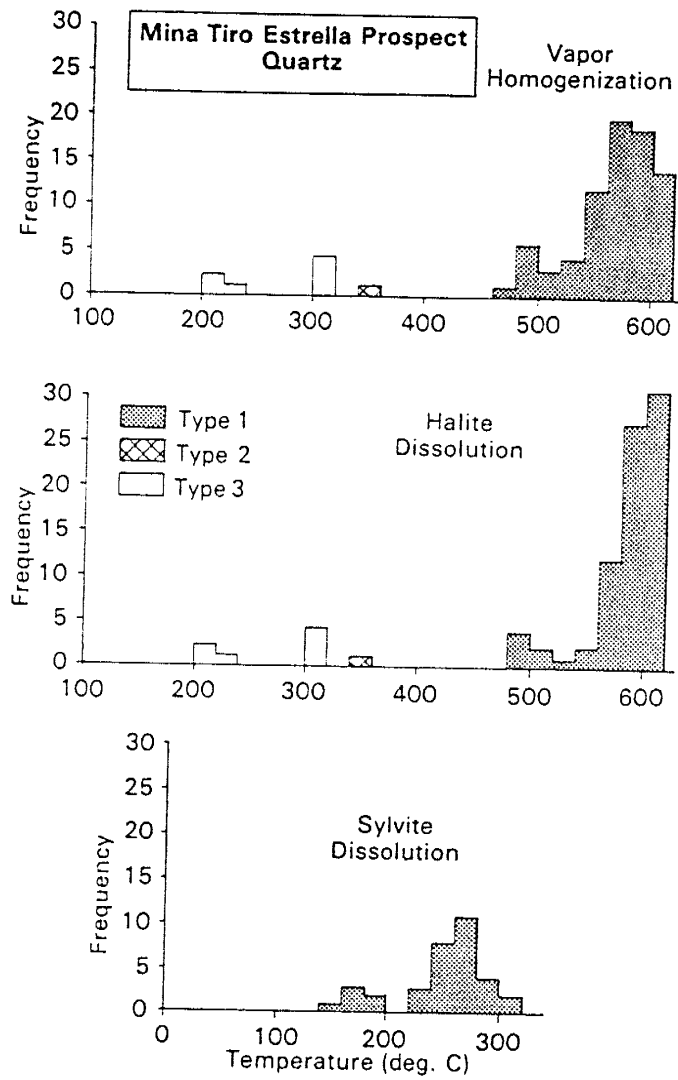


FIG. 7. Vapor homogenization, halite dissolution and sylvite dissolution temperatures for fluid inclusions in quartz from the MTE prospect.



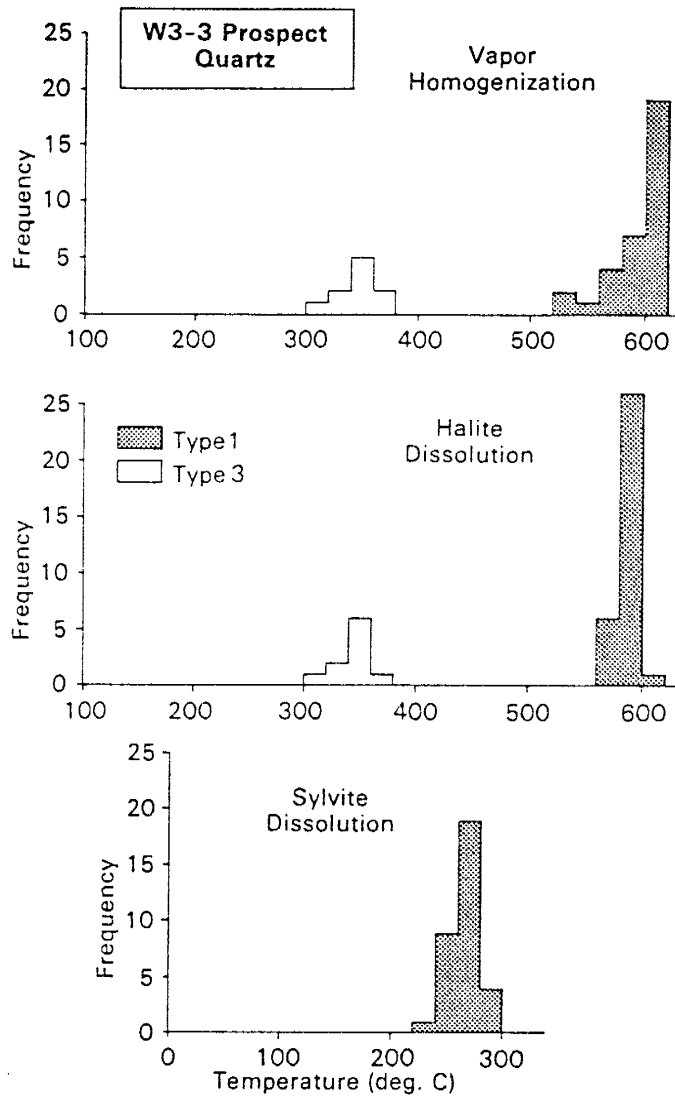


FIG. 8. Vapor homogenization, halite dissolution and sylvite dissolution temperatures for fluid inclusions in smoky quartz from the Wee Three (W3-3) prospect.

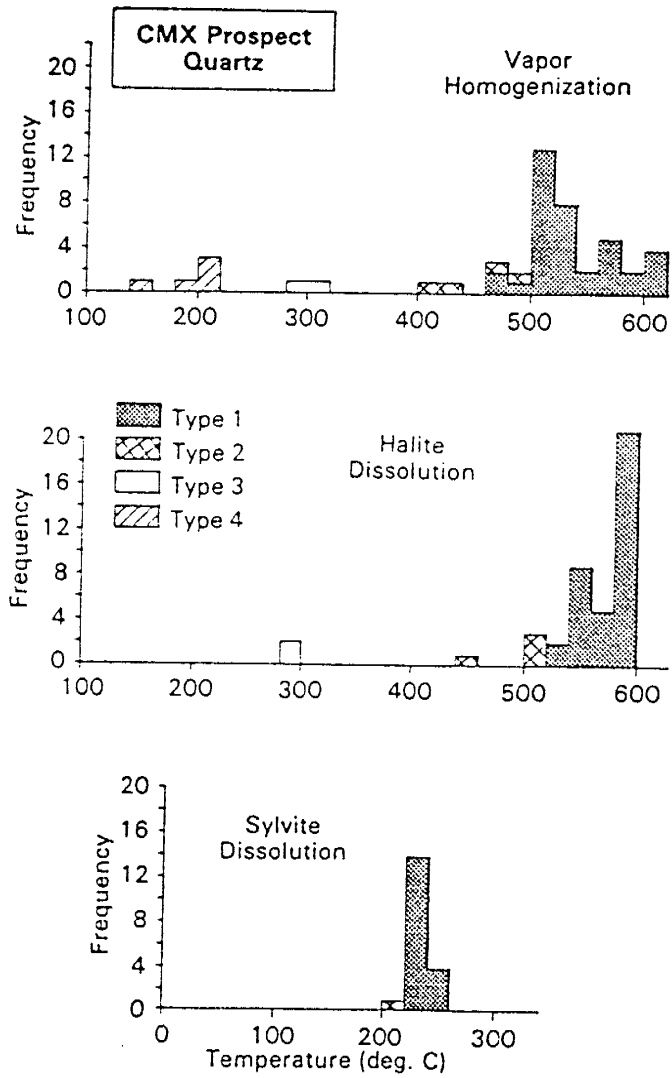


FIG. 9. Vapor homogenization, halite dissolution and sylvite dissolution temperatures for fluid inclusions in smoky quartz from the CMX prospect.

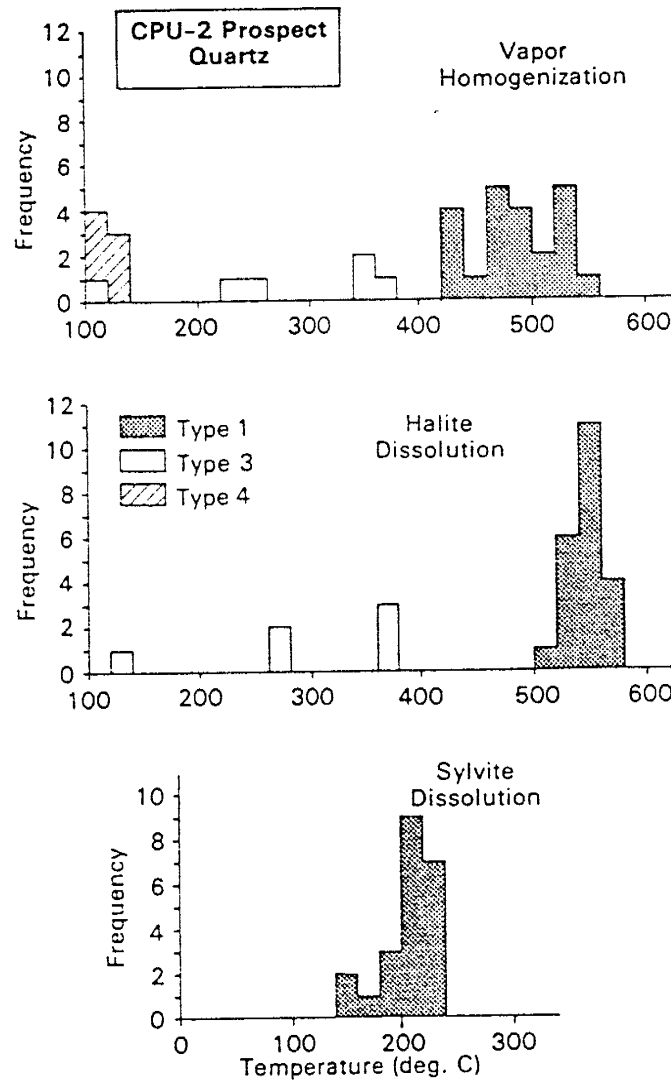


FIG. 10. Vapor homogenization, halite dissolution and sylvite dissolution temperatures for fluid inclusions in quartz from the CPU-2 prospect.

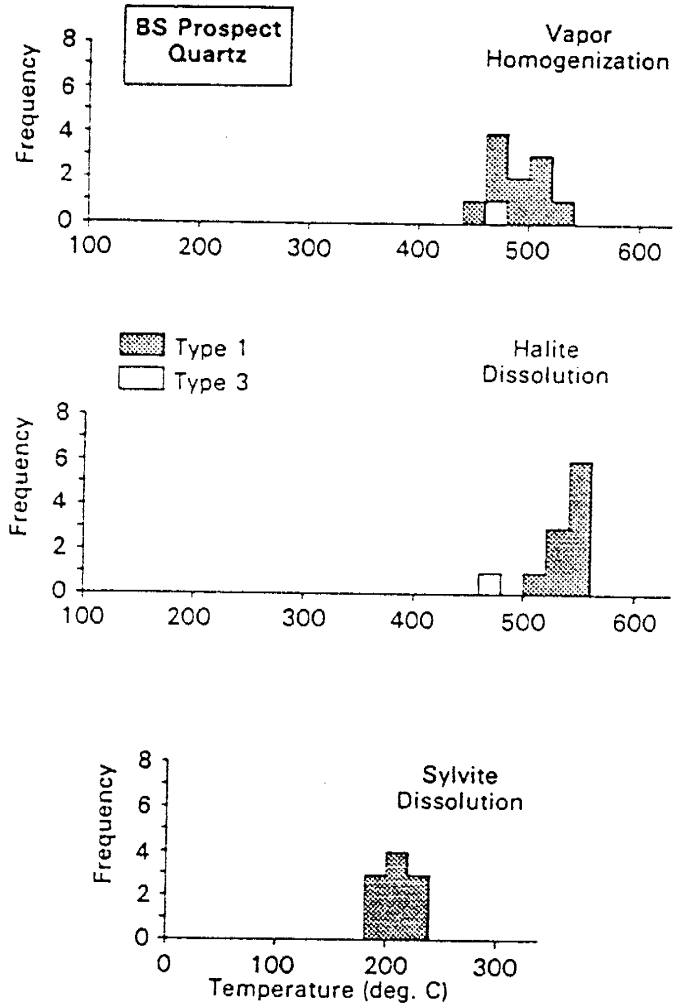


FIG. 11. Vapor homogenization, halite dissolution and sylvite dissolution temperatures for fluid inclusions in quartz from the BS prospect.

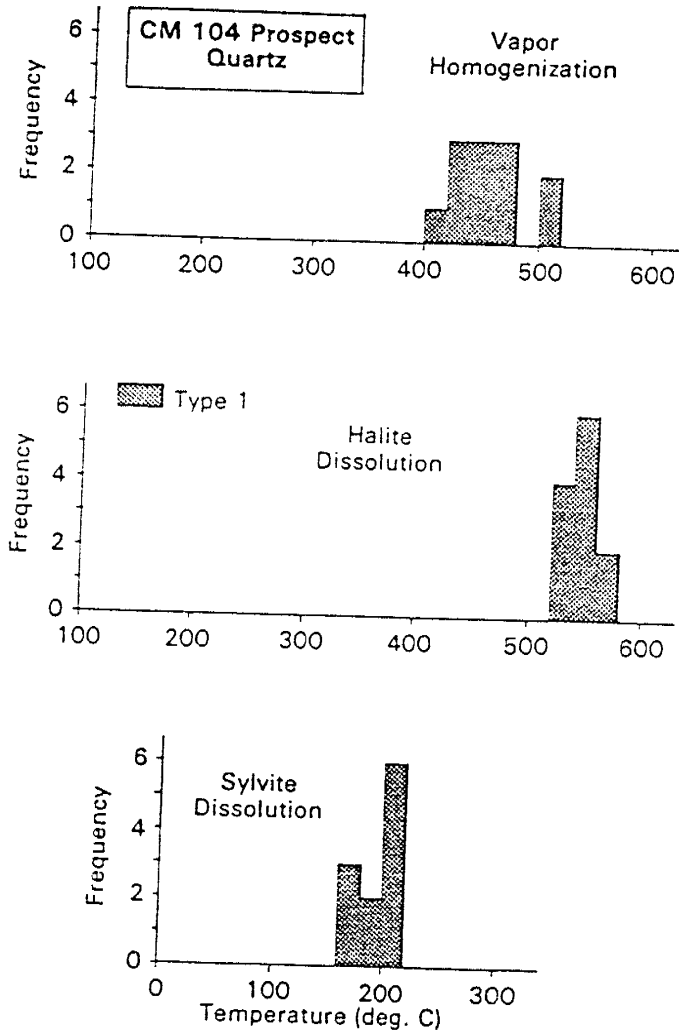


FIG. 12. Vapor homogenization, halite dissolution and sylvite dissolution temperatures for fluid inclusions in quartz from the CM 104 prospect.

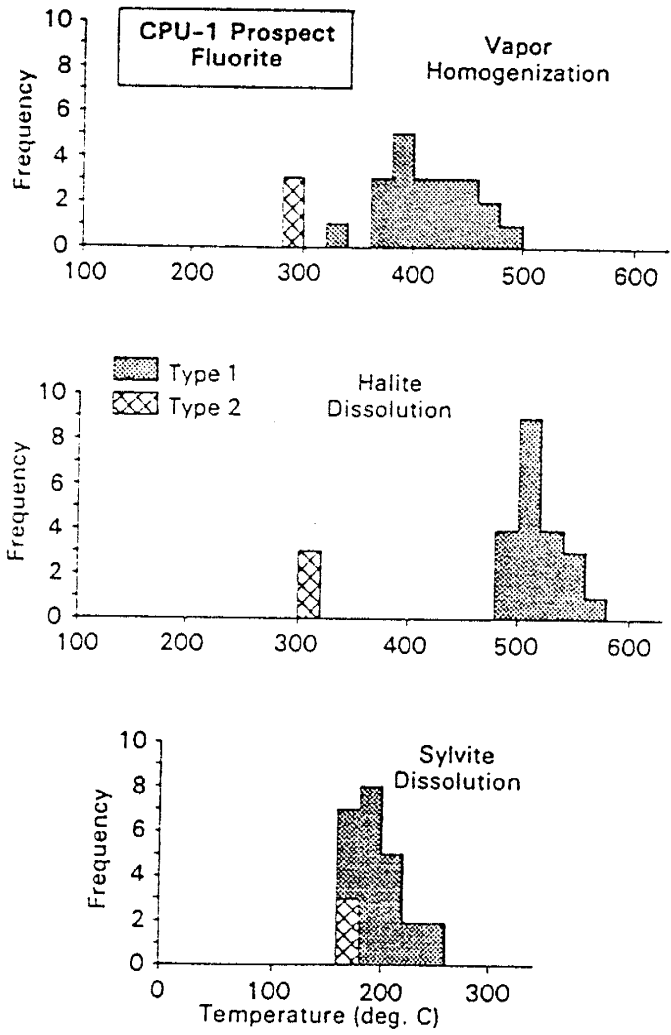


FIG. 13. Vapor homogenization, halite dissolution and sylvite dissolution temperatures for fluid inclusions in fluorite from the CPU-1 prospect.

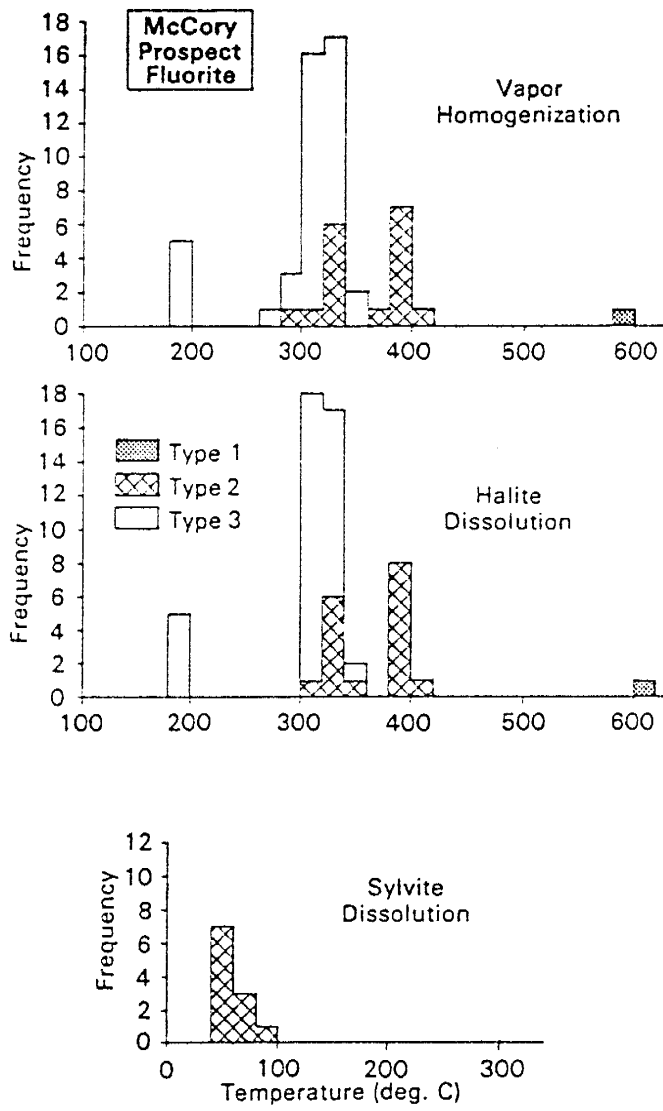


FIG. 14. Vapor homogenization, halite dissolution and sylvite dissolution temperatures for fluid inclusions in fluorite from the McCory prospect.

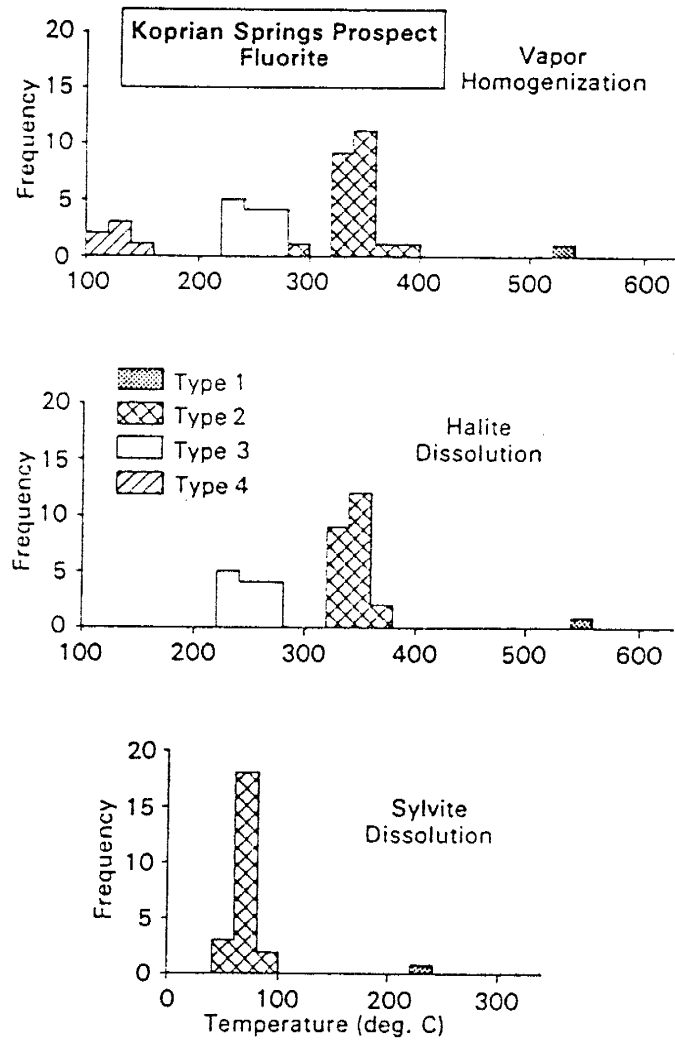


FIG. 15. Vapor homogenization, halite dissolution and sylvite dissolution temperatures for fluid inclusions in fluorite from the Koprian Springs prospect.



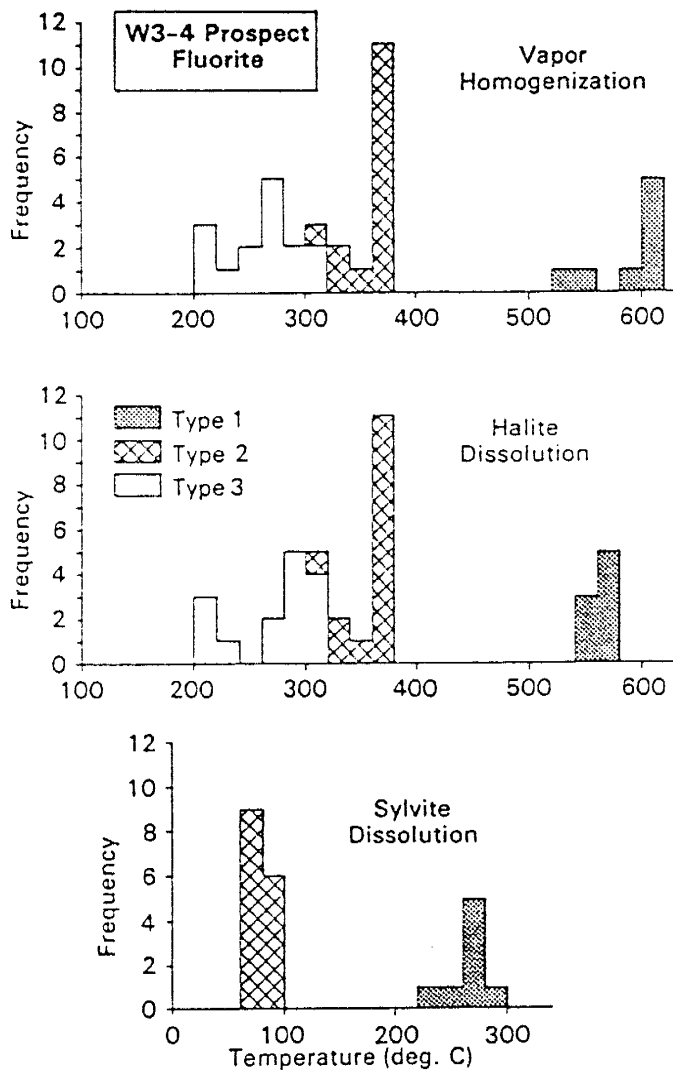


FIG. 16. Vapor homogenization, halite dissolution and sylvite dissolution temperatures for fluid inclusions in fluorite from the Wee Three (W3-4) prospect.

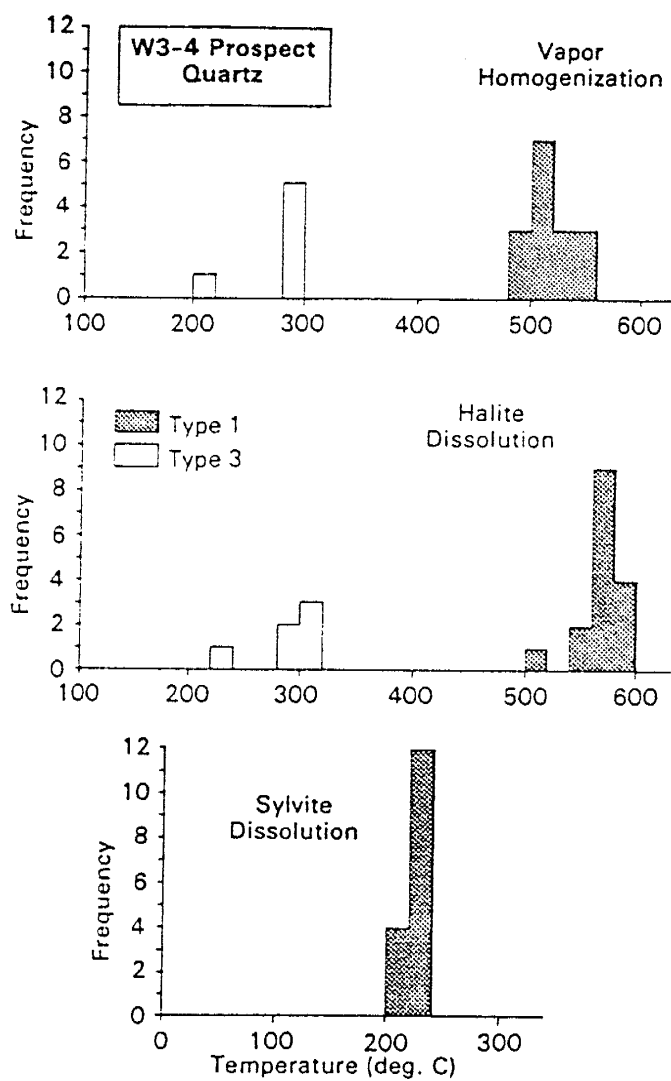


FIG. 17. Vapor homogenization, halite dissolution and sylvite dissolution temperatures for fluid inclusions in smoky quartz from the Wee Three (W3-4) prospect.

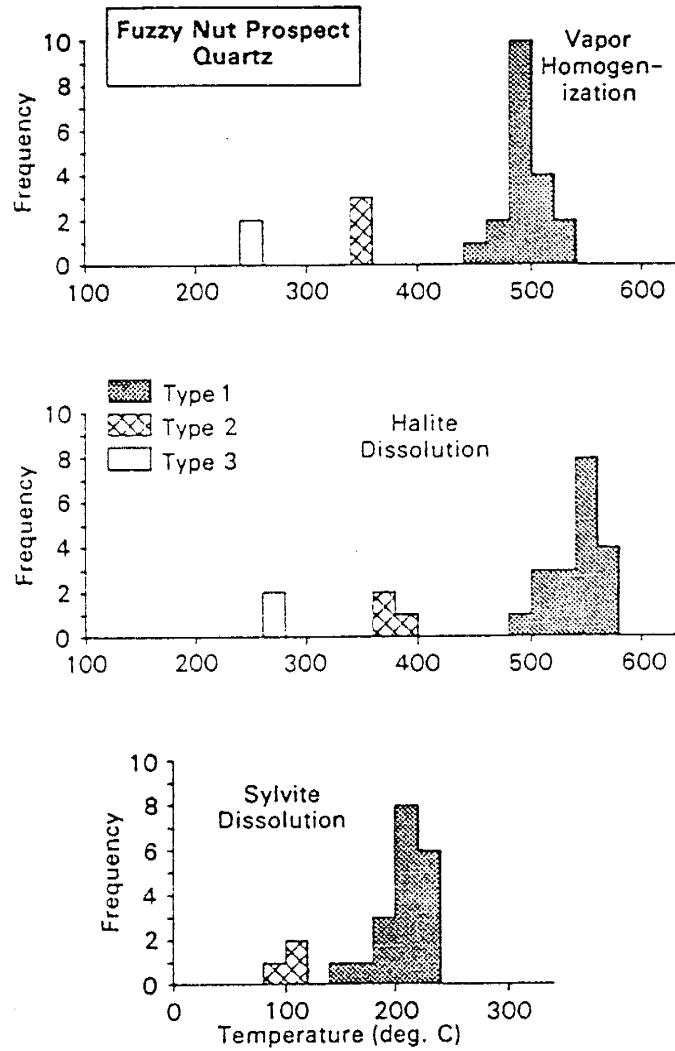


FIG. 18. Vapor homogenization, halite dissolution and sylvite dissolution temperatures for fluid inclusions in quartz from the Fuzzy Nut prospect.

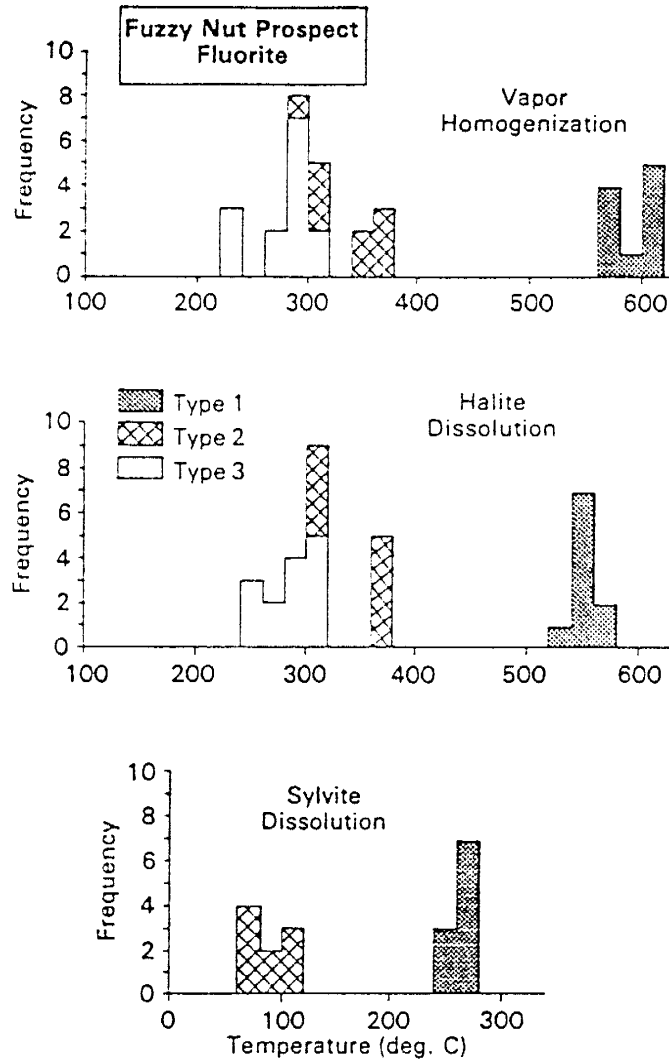


FIG. 19. Vapor homogenization, halite dissolution and sylvite dissolution temperatures for fluid inclusions in fluorite from the Fuzzy Nut prospect.

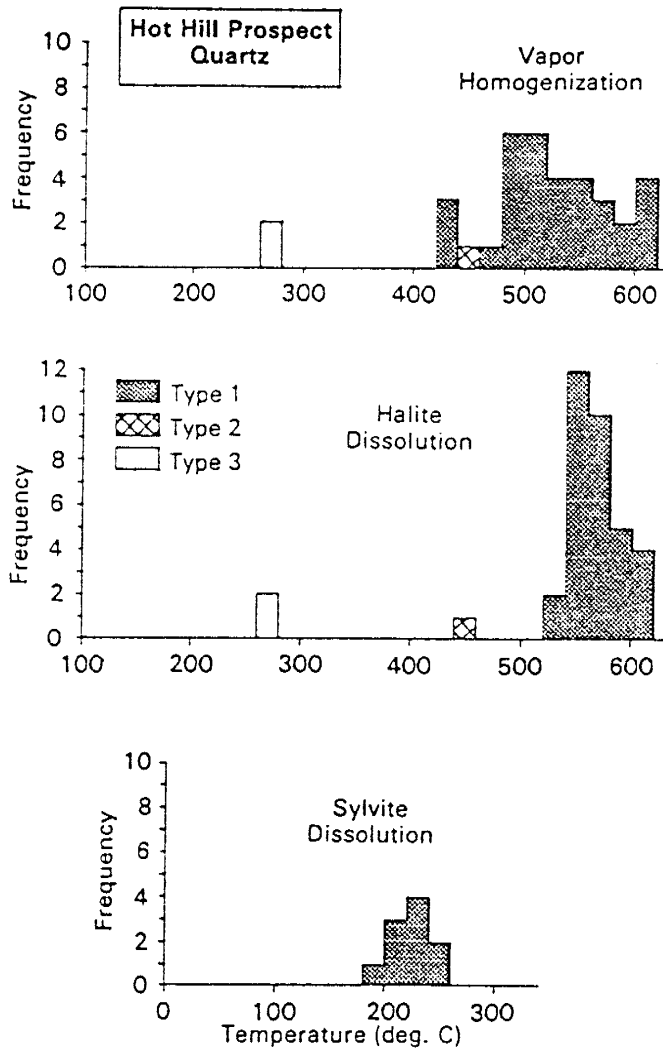


FIG. 20. Vapor homogenization, halite dissolution and sylvite dissolution temperatures for fluid inclusions in smoky quartz from the Hot Hill prospect.

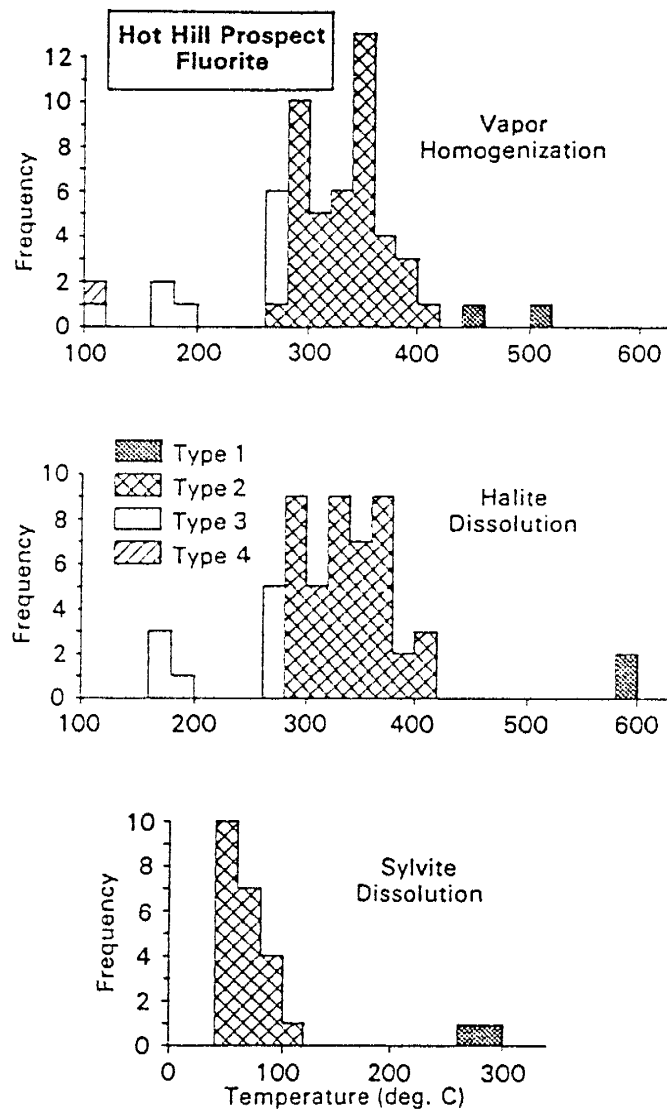


FIG. 21. Vapor homogenization, halite dissolution and sylvite dissolution temperatures for fluid inclusions in fluorite from the Hot Hill prospect.

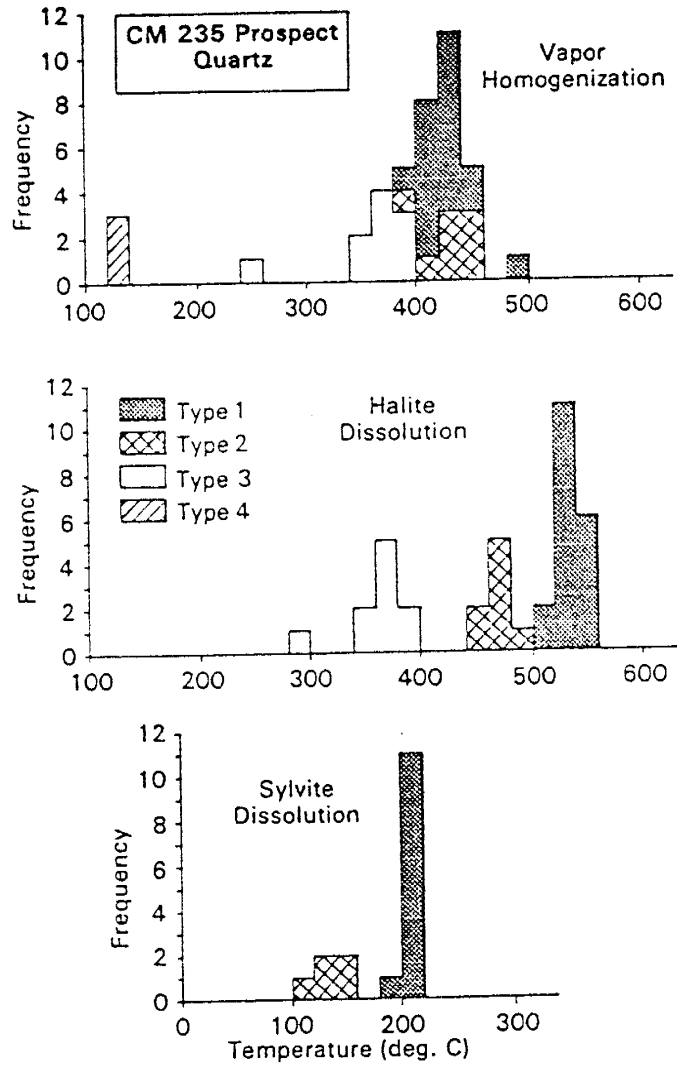


FIG. 22. Vapor homogenization, halite dissolution and sylvite dissolution temperatures for fluid inclusions in quartz from the CM 235 prospect.

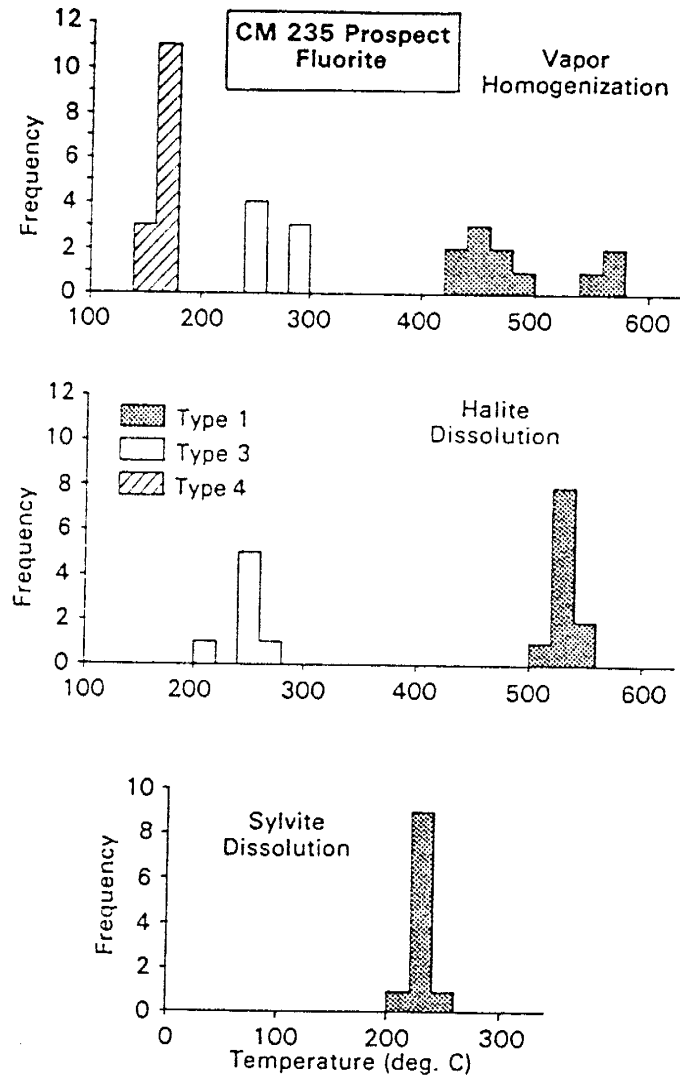


FIG. 23. Vapor homogenization, halite dissolution and sylvite dissolution temperatures for fluid inclusions in fluorite from the CM 235 prospect.



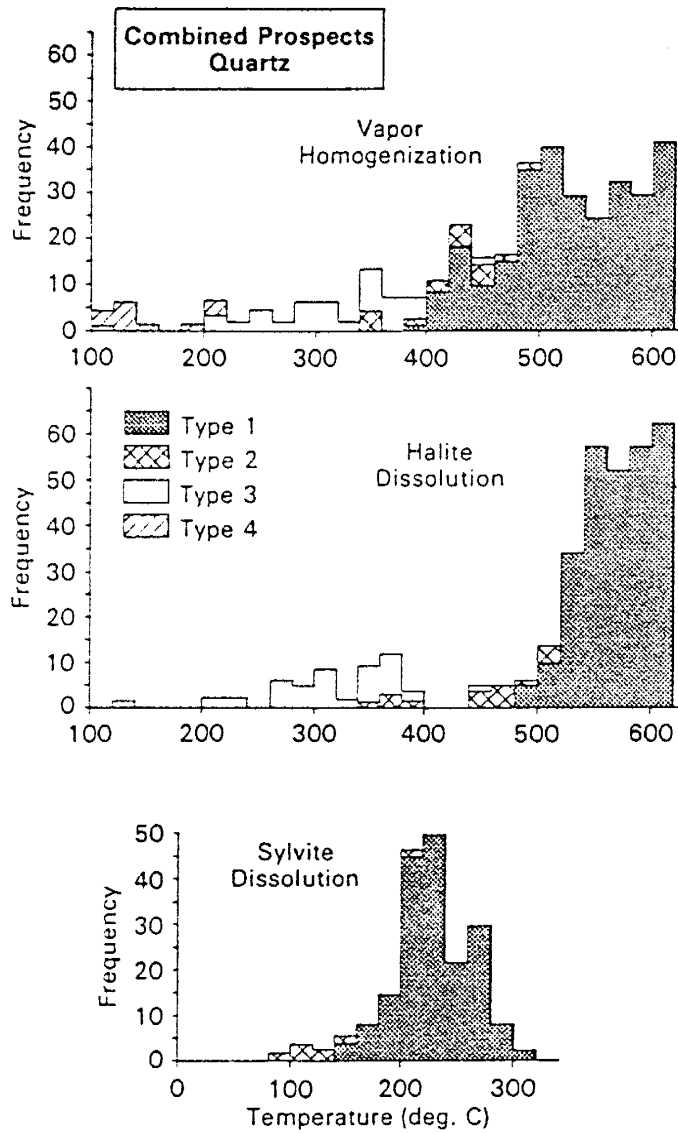


FIG. 24. Histogram showing vapor homogenization, halite dissolution and sylvite dissolution temperatures for all fluid inclusions in quartz from all of the prospects looked at in this study.

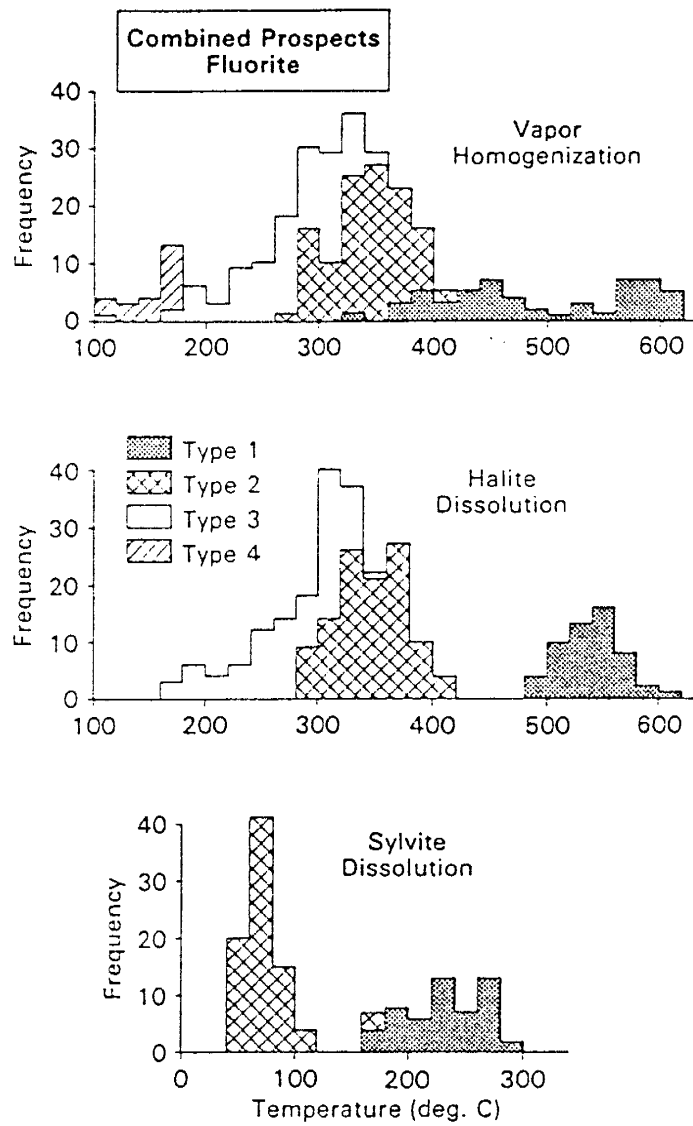


FIG. 25. Histogram showing vapor homogenization, halite dissolution and sylvite dissolution temperatures for all fluid inclusions in fluorite from all of the prospects looked at in this study.

inclusions, best represented by the NaCl-H<sub>2</sub>O system, were determined by measuring halite dissolution temperatures and referring to FLINCOR (Brown, 1989), a Microsoft Windows application (data from Brown and Lamb, 1989). Salinities for type 4 inclusions were determined by measuring the freezing point depression and using FLINCOR (data from Brown and Lamb, 1989).

Homogenization temperature and salinity data for all types of inclusions are summarized for quartz (Fig. 26) and fluorite (Fig. 27) from the different vein systems. All four types of inclusions exhibit separate fields. The gaps observed in Figures 26 and 27 may be due to inadequate sampling, a result of metastability problems (Roedder, 1984), or may indicate a type of fluid evolution. The origin of the observed fields will be discussed in a later section. Salinity fields for type 1 and 2 inclusions in quartz and fluorite are shown on the NaCl-KCl-H<sub>2</sub>O ternary plot (Fig. 28). The observed fields will be discussed in a later section.

### QUARTZ

Salinities for type 1 inclusions range from 49.3 to > 66.6 wt% NaCl and 13.3 to 21.3 wt% KCl (Field A, Fig. 28). Bulk salinities range from 65.8 to > 83.6 wt% NaCl + KCl. Calculated molalities for type 1 inclusions range from 31.2 molal ( 24.7 NaCl and 6.5 KCl) to > 82.9 molal (67.0 NaCl and 15.9 KCl). K/Na ratios for type 1 inclusions range from 0.16 to 0.32, with the majority in the 0.22 to 0.26 range. Bulk compositions of type 1 inclusions are more complex than the simple NaCl-KCl-H<sub>2</sub>O system. Daughter minerals in type 1 inclusions indicate additional components. Ca, Fe and SO<sub>4</sub>, and bulk analysis of fluid inclusion leachates (discussed in a later section) indicates even further additional components, Mn, Mg and Zn. The NaCl-KCl-H<sub>2</sub>O system ignores the effects of these additional components. The additional components may alter the actual bulk salinities for the type 1 inclusions.

Type 1 inclusions probably have higher bulk salinities and lower NaCl and KCl concentrations than from those reported above. Salinities for type 2 inclusions range from 35.4 to 49.8 wt% NaCl and 15.3 to 20.2 wt% KCl (Field C, Fig. 28). Bulk salinities range from 52.4 to 69.6 wt% NaCl+KCl. K/Na ratios for type 2 inclusions range from 0.24 to 0.40, with most falling in the 0.26 to 0.30 range. Calculated molalities for type 2 inclusions range from 17.5 molal (12.7 NaCl and 4.8 KCl) to 37.4 molal (28.4 NaCl and 9.0 KCl). Salinities for type 3 inclusions range from 29.4 to 55.8 eq wt% NaCl. Salinities for type 4 inclusions range from 18.8 to 19.3 eq wt% NaCl.

Densities for type 1 inclusions can be estimated from phase volume measurements of individual inclusions. A typical type 1 inclusion contains roughly 30% halite, 39% liquid (saturated with 26.3 wt% NaCl), 15% water vapor, 7% sylvite, 2% anhydrite, 3% hematite and 4% unknown daughter minerals. Using densities (Klein and Hurlbut, 1977) of  $2.16\text{g/cm}^3$  for halite,  $1.99\text{g/cm}^3$  for sylvite,  $2.89\text{g/cm}^3$  for anhydrite,  $5.26\text{g/cm}^3$  for hematite,  $0.001\text{g/cm}^3$  for water vapor, an average density of  $2.5\text{g/cm}^3$  for the unknown daughter minerals (Roedder, 1971) and  $1.2\text{g/cm}^3$  for liquid (Roedder, 1971), the total density of the inclusion fluid is  $1.57\text{g/cm}^3$ . According to Roedder (1971), such a fluid would be classified as a "hydrosaline melt" rather than a true aqueous fluid. A typical type 2 inclusion contains 72% liquid (saturated with 26.3 wt% NaCl), 14% halite, 12% vapor and 2% sylvite. The total density for such an inclusion is  $1.21\text{g/cm}^3$ . Densities for type 3 inclusions were determined using FLINCOR (Brown and Lamb's data, 1989), they range from 1.07 to  $1.15\text{g/cm}^3$ . Densities for type 4 inclusions were determined using FLINCOR (Brown and Lamb's data, 1989), they average  $1.08\text{g/cm}^3$ .

### FLUORITE

Salinities for type 1 inclusions range from 48.3 to > 62.2 wt% NaCl and 16.6 to 22.2 wt% KCl (Field B, Fig. 28). Bulk salinities range from 66.8 to >80.8 wt% NaCl + KCl. Calculated molalities for type 1 inclusions range from 32.4 molal (24.9 NaCl and 7.5 KCl) to > 68.4 molal (55.4 NaCl and 13.0 KCl). K/Na ratios range from 0.21 to 0.33, with most in the 0.26 to 0.30 range. Salinities for type 2 inclusions range from 31.9 to 41.1 wt% NaCl and 11.4 to 16.9 wt% KCl (Field D, Fig. 28). Bulk salinities range from 45.6 to 56.5 wt% NaCl + KCl. Calculated molalities for type 2 inclusions range from 13.5 molal (10.1 NaCl and 3.4 KCl) to 20.9 molal (15.9 NaCl and 5.0 KCl). K/Na ratios range from 0.21 to 0.43, with most falling in the 0.28 to 0.32 range. Salinities for type 3 inclusions range from 30.8 to 42.7 equiv wt% NaCl. Salinities for type 4 inclusions range from 10.6 to 20.7 eq wt% NaCl. Inclusion fluid densities for types 1-4 in fluorite are similar to those of quartz.

### CALCITE and TITANITE

Salinities for type 3 inclusions in calcite are 34 eq wt% NaCl, corresponding to inclusion fluid densities of 1.11 g/cm<sup>3</sup>.

The salinity for the only measured type 1 inclusion in titanite is 58.2 wt% NaCl, 19.5 wt% KCl, corresponding to a bulk salinity of 77.7 wt% NaCl + KCl. The molality for this inclusion is 56.3 molal (44.6 NaCl and 11.7 KCl). The K/Na ratio is 0.26 and the density is similar to a type 1 inclusion in quartz.

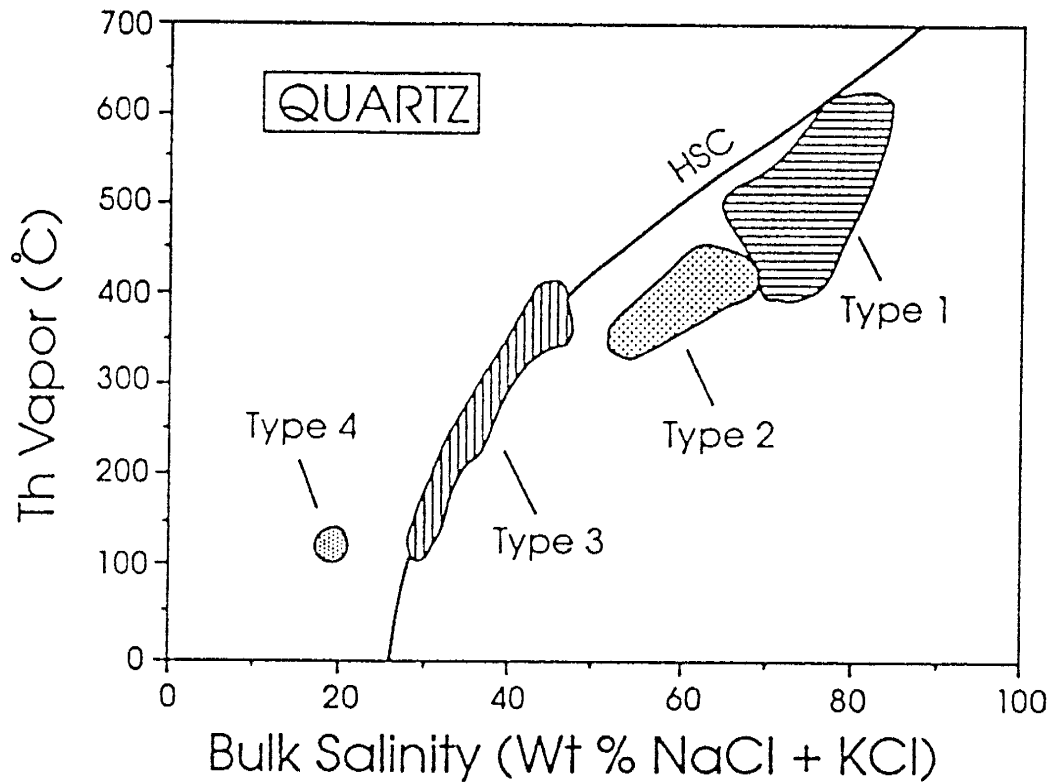


FIG. 26. Plot of combined vapor homogenization temperature versus bulk salinity for types 1, 2, 3 and 4 inclusions in vein quartz from all of the prospects looked at in this study. Salinities for type 1 and 2 inclusions are expressed as eq wt% NaCl + KCl. Salinities for type 3 and 4 inclusions are expressed as eq wt% NaCl. Type 1 inclusions represent 186 measurements, type 2 inclusions represent 6 measurements, type 3 inclusions represent 43 measurements and type 4 inclusions represent 8 measurements. HSC is the halite saturation curve (from Sterner et al., 1988). All four types of inclusions plot in separate fields. Type 1 and 2 inclusions plot off the HSC because  $T_m$  NaCl is greater than  $T_h$  and/or the HSC is not a good representation of the NaCl-KCl-H<sub>2</sub>O system. Type 3 inclusions plot on or near the HSC. Type 4 inclusions plot off the HSC, suggesting some type of mixing trend.

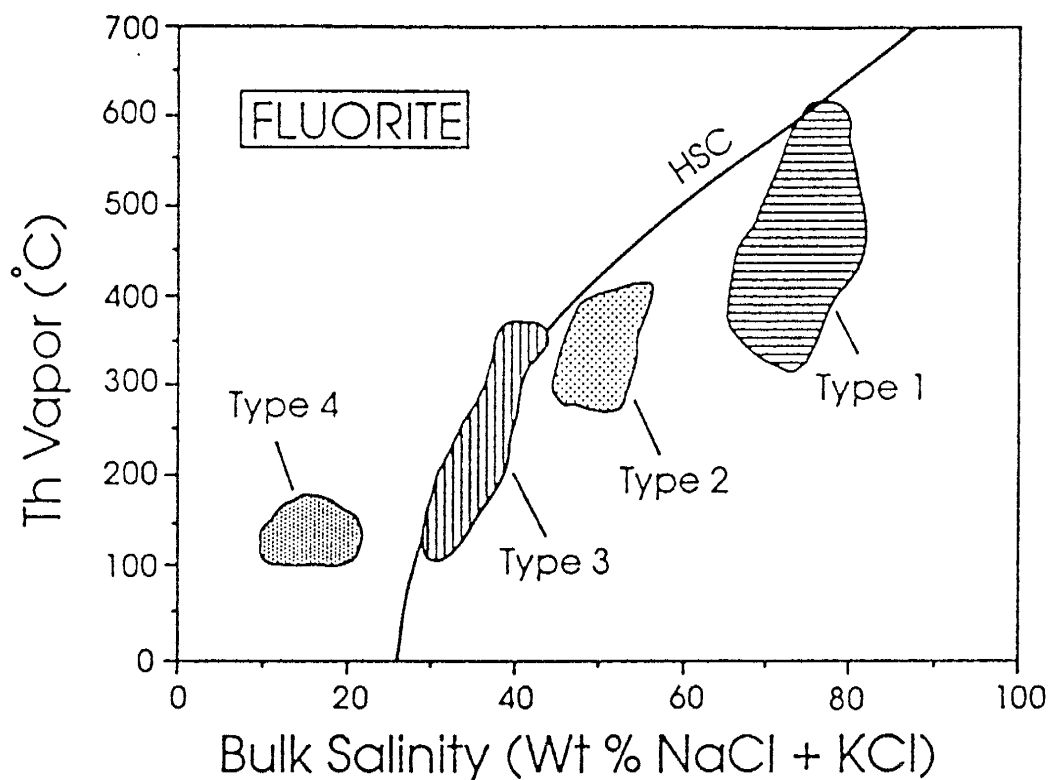


FIG. 27. Plot of combined vapor homogenization temperature versus bulk salinity for types 1, 2, 3 and 4 inclusions in vein fluorite from all of the prospects looked at in this study. Salinities for type 1 and 2 inclusions are expressed as eq wt% NaCl + KCl. Salinities for type 3 and 4 inclusions are expressed as eq wt% NaCl. Type 1 inclusions represent 53 measurements, type 2 inclusions represent 92 measurements, type 3 inclusions represent 92 measurements and type 4 inclusions represent 12 measurements. HSC is the halite saturation curve (from Sterner et al., 1988). All four types of inclusions plot in separate fields. Type 1 and 2 inclusions plot off the HSC because  $T_m$  NaCl is greater than  $T_h$  and/or the HSC is not a good representation of the NaCl-KCl-H<sub>2</sub>O system. Type 3 inclusions plot on or near the HSC. Type 4 inclusions plot off the HSC, suggesting some type of mixing trend.

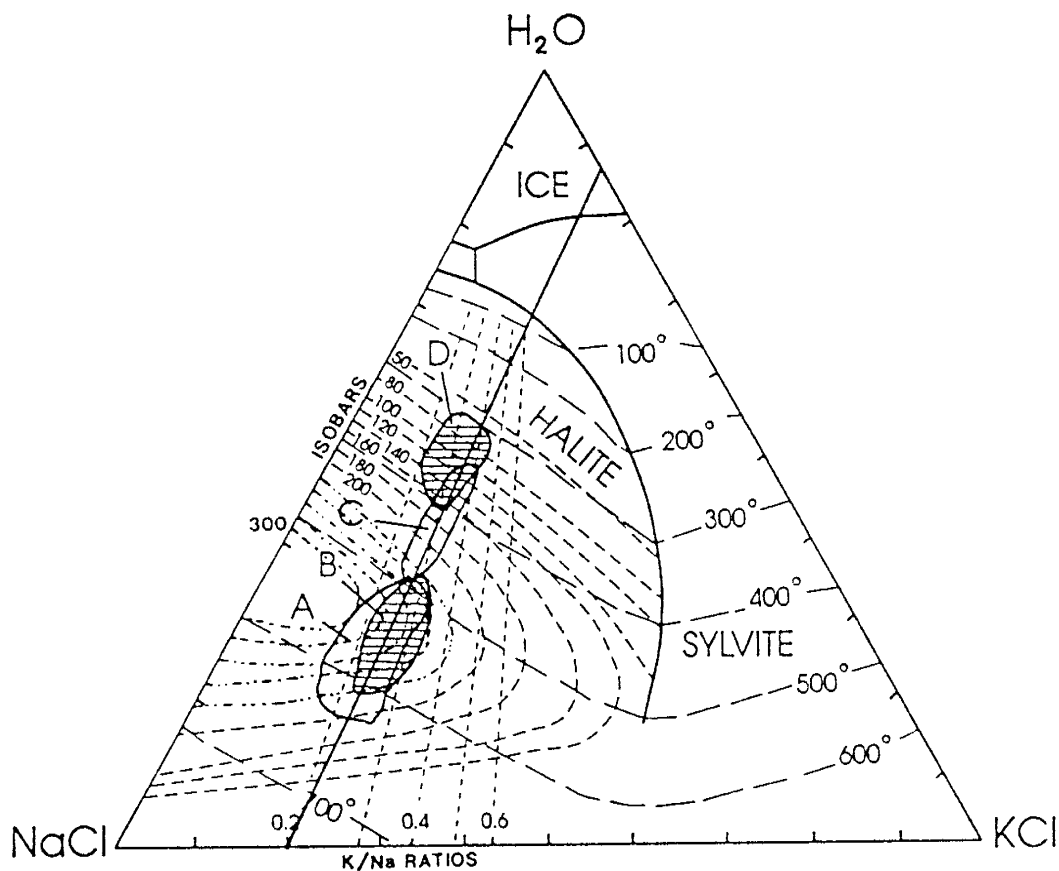


FIG. 28. NaCl-KCl-H<sub>2</sub>O ternary system (in wt%) showing compositional fields under vapor-saturated conditions for type 1 and 2 inclusions in quartz and fluorite from all the prospects. Figure is modified from Cloke and Kesler (1979). Field A shows the composition of type 1 inclusions in quartz and represents 186 measurements. Field B shows the composition of type 1 inclusions in fluorite and represents 53 measurements. Field C shows the composition of type 2 inclusions in quartz and represents 6 measurements. Field D shows the composition of type 2 inclusions in fluorite and represents 92 measurements. Heavy solid lines are cotectics, long dashed lines are isotherms (in °C), medium dashed lines are isobars (in bars), and short dashed lines projecting to the water apex are lines of constant K/Na ratios. Dot-dash lines are extrapolated isobars from 200 to 300 bars (see text). The solid straight line passing through the four fields is used to calculate a pressure-temperature diagram for the Capitan fluid inclusions (see main text and Appendix F for discussion). Fields A, B, C and D fall on a linear trend. This trend is similar to what Erwood et al. (1979) and Cloke and Kesler (1979) have referred to as a "halite trend", which has been interpreted to result from the separation and crystallization of KCl-bearing halite from the parent fluid prior to being entrapped as an inclusion.



## PRESSURE-DEPTH ESTIMATES

Minimum pressures can be estimated for type 1 and 2 inclusions in quartz and fluorite based on halite and sylvite dissolution temperatures and referring to the NaCl-KCl-H<sub>2</sub>O system of Cloke and Kesler (1979). Extrapolating the isobars in Figure 28 yields minimum pressure estimates for type 1 inclusions (Fields A and B, Fig. 28) of 190 to 300 bars. Assuming a lithostatic load and a rock density of 2.6 g/cm<sup>3</sup>, minimum depths for these pressures correspond from 0.74 to less than 1.18 km. According to Roedder and Bodnar (1980), the minimum pressures estimated above may actually be lower due to the additional ions (Ca, Fe, Mn, Mg) present in the fluid inclusions. Type 2 inclusions in quartz and fluorite (Fields C and D, Fig. 28) yield minimum pressure estimates of 60 to 240 bars. Assuming a lithostatic load, minimum depths corresponding to pressures in type 2 inclusions are 0.24 to 0.94 km. At present, no experimental data exist for the complex system of the type 1 and 2 inclusions which would allow for a true depth estimate.

A paleoreconstruction of the sedimentary thicknesses overlying the Capitan pluton during mid-Tertiary times can be approximated (B. Colpitts, pers. comm., 1990) by using oil well log data and data from Kelley (1971) and Bodine (1956). Well log data south of the Capitan Mountains indicates approximately 2100 feet of Permian Yeso Formation above the Precambrian basement rock (B. Colpitts, written comm., 1990). Estimated thicknesses of sedimentary strata from Kelley (1971) and Bodine (1956) which may have been present above the Capitan pluton during mid-Tertiary times are: 550 feet of Permian San Andres plus Glorieta Formations (200 feet of Four Mile Draw Member, 50 feet of Bonney Canyon Member and 300 feet of Rio Bonito Member), 350 feet of Permian Grayburg Formation, 100 feet of Permian Queen Formation, 600 feet of Triassic Chinle Shale and Santa Rosa Sandstone, 130 feet of Cretaceous Dakota Sandstone, 390 feet of

Cretaceous Mancos Shale, 490 feet of Cretaceous Mesaverde Formation and 500 feet of Paleocene Cub Mountain Formation. A total estimated thickness is 5210 feet (1.6 km), corresponding to a lithostatic load of 400 bars.

The fine-grained nature of the alkali granite pluton, the presence of miarolitic cavities within the pluton and the presence of a limestone-sandstone roof pendant on the west end of the pluton, suggest that the pluton was emplaced at shallow crustal levels. From the fluid inclusion evidence and geologic evidence mentioned above, the depth of pluton emplacement and vein formation was estimated to occur between 1.2 km and 1.6 km.

## FLUID INCLUSION LEACHATE ANALYSIS

Bulk crush-leach analysis was performed in order to establish a semi-quantitative estimate on the chemical composition of the mineral-forming fluids, represented by type 1 inclusions, on samples of vein quartz from the MTE, Hot Hill, Wee Three (W3-3), CPU-2, Fuzzy Nut and CMX prospects. Major elements were analyzed by atomic absorption spectrophotometry and anion chromatography. REE's were analyzed by inductively coupled plasma spectrophotometry on leachate solutions from MTE quartz. Samples from the MTE, Wee Three and CMX prospects contain greater than 90% type 1 inclusions. Samples from the CPU-2, Hot Hill and Fuzzy Nut prospects contain greater than 75% type 1 inclusions. A dilution effect caused by the greater abundance of type 3 and 4 inclusions in quartz from the Hot Hill, CPU-2 and Fuzzy Nut prospects may be apparent. Sample descriptions, detailed cleaning procedures, experimental procedures and experimental data (concentrations and calibration data for samples and blanks) are given in

## Appendix D.

**EXPERIMENTAL PROCEDURES**

Preliminary studies on MTE vein quartz were performed to determine the appropriate amount of quartz needed for crush-leaching and to find a suitable leaching solution. Room temperature deionized/distilled water, hot (80°C) deionized/distilled water, 0.13 N nitric acid and a 200 ppm  $\text{LaCl}_3$  solution in 0.13 N nitric acid (as prescribed by Bottrell et al., 1988) were used as leaching solutions. Sodium, K, Ca, Mg, Mn, Fe, Zn, Ba, Ag, Cu and Pb were analyzed by atomic absorption spectrophotometry using a Instrumentation Laboratory IL Video 12 AA/AE spectrophotometer. Chloride, sulphate, fluoride and nitrate were analyzed by anion chromatography using a Dionex ion chromatograph series 4000i with a sulfuric acid ion suppressor and a  $\text{NaHCO}_3$  eluant. Approximately 5 to 25 gram samples of clean MTE quartz was crushed as a slurry with a specific leach solution in an alumina mortar and pestle. The slurry was quantitatively transferred to a 0.2 micron pore-size Nalgene millipore disposable filter unit. The quartz in the filter unit was rinsed several times with the leaching solution until a leachate volume of 40 to 50 mL was obtained. For some samples, after collection of the first leachate solution, a second leachate solution (samples MTE-201, 203, 206) on the same sample was obtained by rinsing the crushed quartz residue with the appropriate leaching solution. This was done to ensure all ions were released from the crushed quartz and collected in the first leachate solution. Leaching solutions were "crushed" without quartz in the mortar and pestle and filtered through the millipore filter unit to serve as blanks. Solutions were stored in 60 ml polypropylene bottles.

To avoid the problems of adsorption of +2 and +3 cations onto the surfaces of freshly crushed quartz and to avoid the problems of contamination using the bulk

crush-leach technique described previously, a hydrofluoric acid dissolution of electrolytically cleaned MTE quartz was attempted. The purity of MTE quartz and the abundance of primary/pseudosecondary inclusions allowed this type of technique to be employed. The idea behind this method was that it should be possible to chemically dissolve the quartz, liberate the fluid inclusion contents, dissolve all daughter mineral phases (including barite) and hence obtain a complete chemical analysis of all major cations and anions within the inclusion fluids. Samples consist of one quartz blank (MTE-100), three MTE quartz samples containing abundant type 1 inclusions (MTE-101, 102, 103) and a hydrofluoric acid blank (MTE-104). The samples were analyzed for major elements by atomic absorption spectrophotometry and anion chromatography.

In order to achieve a complete bulk analysis on a single sample, the LaCl<sub>3</sub> leach solution (which caused Cl contamination of the sample) was replaced by a similar leach solution which employs a +3 cation to act as an inhibitor for adsorption of desirable ions onto the crushed quartz. A 250 ppm Sc in 0.25 wt% nitric acid solution was used for all subsequent studies. A total of 17 quartz samples were crushed and leached using the Sc leach solution in a similar manner described above. Leachate solution volumes of  $40 \pm 5$  mL were obtained. Na, K, Ca, Mn, Mg, Fe and Zn were analyzed by atomic absorption spectrophotometry and Cl and SO<sub>4</sub> were analyzed by anion chromatography. Sulphate was nondetectable by anion chromatography due to interferences from the nitrate of the leaching solution.

A single sample of previously electrolytically cleaned quartz from the MTE prospect was analyzed for La, Ce and Hf by a Perkin Elmer Model 1000 Inductively Coupled Plasma spectrometer. No REE's were detected by ICP (B. Popp, pers. comm., 1990).

## RESULTS OF CRUSH-LEACH ANALYSES

### Preliminary Crush-Leach Analyses

MTE fluid inclusion leachates were found to contain significant amounts of Na, K, Ca and Cl and minor amounts of Fe, Mn, Mg, Zn, and SO<sub>4</sub> (Table 4A, B). Ag, Cu, Pb, Ba, F and NO<sub>3</sub> were either below detection limit or not present in the leachate solutions. In order to compare leachate samples for a given leaching solution, the analyses are normalized with respect to a total concentration of 10 ppm. Duplicate and triplicate values for MTE leachate solutions are shown in Table 4A. In most cases, reproducibility for the duplicate and triplicate samples are generally good. K and Ca are ratioed with respect to one mole of Na in order to compare leaching efficiencies between the various leaching solutions. All leaching solutions removed the Na, K, and Cl from the crushed quartz. The water and 0.13 N nitric acid leaching solutions did not release all of the + 2 (Ca, Mn, Mg) and + 3 (Fe) cations from the crushed quartz, as evidenced by the higher concentrations of divalent and trivalent cations in the LaCl<sub>3</sub> leach solution. Bottrell et al. (1988) also noticed that simple water leaches were insufficient to remove all divalent ions from crushed quartz. For duplicate and triplicate samples, the K/Na and Ca/Na ratios reproduced well for a given leach solution (Table 4C). Barium may not have been detected because it may not have been released into the leach solution due to the insoluble nature of BaSO<sub>4</sub> (a potential daughter mineral in type 1 inclusions). Iron appears to be low in the crush-leach analyses for all leaching solutions. Based on phase volume estimates from a previous section for a type 1 inclusion, Fe<sub>2</sub>O<sub>3</sub> accounts for 3 %, NaCl accounts for 30%, and the liquid phase accounts for 39% (saturated with 26.3 wt% NaCl) of the total volume. Assuming a 1 cm<sup>3</sup> total volume, 3 vol% Fe<sub>2</sub>O<sub>3</sub> (density of 5.26g/cm<sup>3</sup>) corresponds to 0.1578 g Fe<sub>2</sub>O<sub>3</sub>

(0.0019725 moles Fe), 30 vol% NaCl (density of 2.16 g/cm<sup>3</sup>) corresponds to 0.648 g NaCl (0.011077 moles Na), and 39 vol% liquid (density of 1.2g/cm<sup>3</sup>; containing 10.3 wt% NaCl) corresponds to 0.0482 g NaCl (0.000824 moles Na; Na contains a total of 0.011901 moles). The expected Fe/Na molar ratio should be 0.166. Fe/Na ratios for the preliminary leaching solutions range from 0.015 to 0.028, which are very low compared to phase volume estimates. The low Fe concentrations are attributed to the fact that the hematite did not completely dissolve in any of the leach solutions. Charge balances for the different leach solutions are given in Table 4B. All leaching solutions show an apparent net deficiency in anions. The equivalent amount of Cl or SO<sub>4</sub> necessary to attain neutrality is listed in Table 4B. An accurate charge balance for the different leach solutions was hard to establish because: 1) the water leaches did not remove all of the divalent ions; and 2) the nitric acid and LaCl<sub>3</sub> leach solutions did not allow for all of the anions (Cl, SO<sub>4</sub>) to be determined; hence, a true anion charge balance could not be determined.

#### HF Acid - Quartz Dissolution Analyses

Experimental data, normalized concentrations, molar ratios and charge balances for the HF acid-quartz dissolution analyses are shown in Table 5. The HF acid technique indicates major amounts of Na, K and Fe and minor amounts of Ca, Mn, Mg, Zn, Ba and SO<sub>4</sub>. The low Ca values (as compared to the Ca values from the LaCl<sub>3</sub> leach solution analyses) from the HF acid technique may be caused by precipitation of an insoluble residue, CaF<sub>2</sub>. Barium was detected by this method, indicating the possibility of BaSO<sub>4</sub> as a daughter mineral in the type 1 fluid inclusions. Iron concentrations are much higher as compared to the Fe concentrations obtained from the crush-leach analyses. In the preceding section, an Fe/Na ratio of 0.166 was calculated based on phase volume estimates. Fe/Na

ratios for the HF method range from 0.077 to 0.081. The higher Fe/Na ratios, as compared to the previous section, indicates that about half of the Fe in hematite was dissolved and detected in the HF acid sample solutions. A major problem with this method was that fluoride from the HF acid was retained in the salty residue and carried over into the solution which was analyzed. The large amounts of fluoride interfered with the chloride peak in the anion chromatography analyses; thus, chloride could not be detected. Accurate charge balances were unable to be calculated due to the nondetectability of chloride.

#### Sc(NO<sub>3</sub>)<sub>3</sub> Crush-Leach Analyses

Leachate solution concentrations, normalized concentrations, mean values, standard deviations, molar ratios and charge balances for the Sc leachate analyses are shown in Table 6A,B. Significant amounts of Na, K, Ca, and Cl and minor amounts of Fe, Mn, Mg and Zn were detected in the fluid inclusion leachate solutions. Reproducibility on duplicate and triplicate samples for a given vein is good. Standard deviations are generally low for the elements which were detected. As a check for the efficiency of the Sc leach solution, the K/Na ratios obtained from the crush-leach procedure (Table 6D) were checked against the K/Na ratios obtained by heating measurements on type 1 inclusions in quartz. K/Na ratios, 0.22 to 0.27, of samples from MTE, Fuzzy Nut, Wee Three and CMX agree well with K/Na ratios obtained from fluid inclusion microthermometry. K/Na ratios, 0.19 to 0.20, of samples from Hot Hill and CPU-2 are slightly lower than K/Na ratios obtained from fluid inclusion microthermometry. This is probably due to a dilution effect caused by the higher percentage of type 3 and 4 inclusions in the samples. Fe/Na ratios for the vein quartz leachate solutions range from 0.009 to 0.031. These values are much lower than the expected Fe/Na (0.166) ratio, which is based on

phase volume estimates. The hematite daughter minerals in the crushed quartz was probably not adequately dissolved by the Sc leach solution. Charge balances show a large net deficiency in anions. The anion deficiency is attributed to the fact that some of the anions were either nondetectable (nitrate from the leach solution interfered with sulphate) or were not analyzed for. The presence of anhydrite and possibly calcite as daughter minerals in type 1 inclusions indicates that  $\text{SO}_4$  and  $\text{HCO}_3/\text{CO}_3$  are present in the inclusion fluids. Sulphate was detected in preliminary distilled water leaches (Table 4A). Since the inclusions were leached at atmospheric conditions,  $\text{HCO}_3/\text{CO}_3$  was unable to be determined. The equivalent amount of chloride or sulphate needed to achieve neutrality in the charge balances are given in Table 6C.

It was determined that no single leach solution can be used to obtain a complete analyses on fluid inclusion leachates. It is suggested for future studies that two leach solutions be employed - a hot water leach and a  $\text{LaCl}_3$  leach. The hot water leach will effectively remove all Na, K and Cl. The  $\text{LaCl}_3$  leach will effectively remove most of the desirable +2 and +3 cations (excluding Fe, which appears to be completely released into solution only by the HF acid technique) and  $\text{SO}_4$ . Bulk crush-leach analysis of inclusion fluids in quartz show that the fluids responsible for mineralization are best represented by the complex Na-K-Ca-Fe-Mn-Mg-Zn-Cl- $\text{SO}_4$ - $\text{H}_2\text{O}$  system. Based on the chemistry of the leachate solutions on quartz from the six vein systems, the fluids responsible for the mineralized zones appear to be similar in composition for all of the prospects looked at in this study.



Table 4A. Concentrations of Fluid Inclusion Leachate Solutions  
Normalized to 10 ppm Total Concentration for Vein Quartz  
Using Various Leaching Solutions

Sample	Leach Solution	Normalized concentrations in ppm (after blank subtraction)								
		Na	K	Ca	Fe	Mn	Mg	Zn	Cl	SO <sub>4</sub>
MTE-200	A	2.51	1.03	0.54	0.09	0.13	BD	BD	5.56	0.13
MTE-202	B	4.58	1.96	0.23	0.28	0.19	BD	0.05	2.71	(1)
MTE-204	B	3.52	1.50	0.32	0.16	0.12	0.08	0.05	4.25	(1)
Average		4.05	1.73	0.28	0.22	0.16		0.05	3.48	
Std Dev		0.75	0.33	0.06	0.08	0.05		0.00	1.09	
MTE-205	C	4.80	2.01	2.57	0.22	0.22	0.15	0.04	(2)	(1)
MTE-207	C	4.84	2.02	2.45	0.21	0.27	0.16	0.05	(2)	(1)
Average		4.82	2.02	2.51	0.22	0.24	0.16	0.04		
Std Dev		0.03	0.01	0.08	0.01	0.04	0.01	0.01		
MTE-208	D	2.38	1.06	0.40	0.13	0.13	BD	0.04	5.37	0.48
MTE-209	D	2.58	1.09	0.52	0.17	0.17	BD	0.02	5.15	0.31
MTE-210	D	2.68	1.12	0.50	0.15	0.15	0.02	0.02	5.14	0.22
Average		2.55	1.09	0.47	0.15	0.15	0.02	0.03	5.22	0.34
Std Dev		0.15	0.03	0.06	0.02	0.02		0.02	0.13	0.13

See Appendix D, Table D5 for actual concentrations (in ppm) and blanks

#### Leaching Solutions

A Distilled/Deionized Water

B 0.13 N HNO<sub>3</sub>

C 200 ppm LaCl<sub>3</sub> solution in 0.13 N HNO<sub>3</sub>

D Hot Distilled/Deionized Water

(1) Sulphate nondetectable due to interference with nitrate from leach solution

(2) Chloride nondetectable due to contamination from chloride in leach solution

BD = below detection limit

Table 4B. Molalities, Charge Balances and Anion Deficiencies for Fluid Inclusion Leachate Solutions of Vein Quartz Using Various Leaching Solutions Concentrations Normalized to 10 ppm Total Concentration

Sample	Leach Solution	Molalities ( $\times 10^{-5}$ ) for normalized ppm concentrations								
		Na	K	Ca	Fe	Mn	Mg	Zn	Cl	SO <sub>4</sub>
MTE-200	A	10.91	2.63	1.35	0.16	0.24	-----	-----	15.68	0.14
MTE-202	B	19.91	5.01	0.57	0.50	0.35	-----	0.08	7.64	-----
MTE-204	B	15.30	3.84	0.80	0.29	0.22	0.33	0.08	11.99	-----
MTE-205	C	20.87	5.14	6.41	0.39	0.40	0.62	0.06	-----	-----
MTE-207	C	21.04	5.17	6.11	0.38	0.49	0.66	0.08	-----	-----
MTE-208	D	10.35	2.71	1.00	0.23	0.24	-----	0.06	15.15	0.50
MTE-209	D	11.22	2.79	1.30	0.30	0.31	-----	0.03	14.53	0.32
MTE-210	D	11.65	2.86	1.25	0.27	0.27	0.08	0.03	14.50	0.23

See Appendix D, Table D5 for actual concentrations in ppm and blanks

#### Leaching Solutions

A Distilled/Deionized Water  
B 0.13 N HNO<sub>3</sub>

C 200 ppm LaCl<sub>3</sub> in 0.13 N HNO<sub>3</sub>  
D Hot distilled/deionized water

#### Charge Balance and Anion Deficiencies

Sample	$\sum m_i z_i^2$ cations	$\sum m_i z_i^2$ anions	Charge Balance	Anion Deficiency (ppm)	
	[ $\times 10^{-5}$ ]	[ $\times 10^{-5}$ ]		Cl equiv	SO <sub>4</sub> equiv
MTE-200	21.34	16.24	5.10	1.81	1.22
MTE-202	33.42	7.64	25.78	9.14	6.19
MTE-204	27.47	11.99	15.48	5.49	3.72
MTE-205	59.48	-----	59.48	21.09	14.28
MTE-207	58.99	-----	58.99	20.91	14.16
MTE-208	20.33	17.15	3.18	1.13	0.76
MTE-209	23.27	15.81	7.46	2.64	1.79
MTE-210	23.46	15.42	8.04	2.85	1.93

Column 4 represents the overall charge balance ( Column 2 - Column 3)

Column 5 and 6 represents the amount of Cl or SO<sub>4</sub> needed to achieve neutrality

m = molality of species i, z = charge of species i

Table 4C. Molar Ratios of Cations and Anions Analyzed for Preliminary Crush-Leach Data Using MTE Quartz and Various Leaching Solutions

Sample	Leach Sol'n	Molar Ratio (with respect to one mole of sodium)							
		K/Na	Ca/Na	Fe/Na	Mn/Na	Mg/Na	Zn/Na	Cl/Na	SO <sub>4</sub> /Na
MTE-200	A	0.241	0.123	0.015	0.022	--	--	1.436	0.013
MTE-202	B	0.252	0.029	0.025	0.017	--	0.004	0.384	--
MTE-204	B	0.250	0.053	0.019	0.014	0.022	0.004	0.783	--
Average		0.251	0.041	0.022	0.016	--	0.004	0.584	--
MTE-205	C	0.246	0.307	0.019	0.019	0.029	0.003	--	--
MTE-207	C	0.246	0.240	0.018	0.023	0.031	0.004	--	--
Average		0.246	0.274	0.018	0.021	0.030	0.004	--	--
MTE-208	D	0.261	0.096	0.023	0.023	--	0.006	1.466	0.048
MTE-209	D	0.249	0.117	0.028	0.025	--	0.003	1.297	0.028
MTE-210	D	0.245	0.107	0.024	0.024	0.006	0.002	1.243	0.020
Average		0.252	0.107	0.025	0.024	--	0.004	1.335	0.032

See Table 4B for molalities used to calculate molar ratios

#### Leaching Solutions

A = Distilled/Deionized Water

B = 0.13 N HNO<sub>3</sub>

C = 200 ppm LaCl<sub>3</sub> in 0.13 N HNO<sub>3</sub>

D = Hot (80°C) Distilled/Deionized Water

Table 5. Concentrations Normalized to 10 ppm Total Concentration, Molalities, Charge Balances and Anion Deficiencies for Fluid Inclusion Chemical Analyses Using the Hydrofluoric Acid-Quartz Dissolution Technique

Normalized concentrations (in ppm) normalized to 10 ppm total concentration										
Sample	Na	K	Ca	Fe	Mn	Mg	Zn	Ba	Cl	SO <sub>4</sub>
MTE-101	5.55	2.99	0.11	1.10	0.19	BD	0.05	BD	(1)	BD
MTE-102	4.97	2.56	0.18	0.98	0.27	0.04	0.04	0.20	(1)	0.77
MTE-103	5.19	2.68	0.07	0.97	0.22	0.01	0.04	0.18	(1)	0.63
Average	5.08	2.62	0.12	0.98	0.24	0.02	0.04	0.19		0.70
Std Dev	0.16	0.08	0.08	0.01	0.04	0.02	0.00	0.01		0.10

Only MTE-102 and 103 were used for average and std dev calculations

See Table D 7 for actual concentrations (in ppm) and blanks

BD = below detection limit

(1) = chloride nondetectable due to peak interference with fluoride

Molalities ( $\times 10^{-5}$ ) for concentrations listed above										
Sample	Na	K	Ca	Fe	Mn	Mg	Zn	Ba	Cl	SO <sub>4</sub>
MTE-101	24.13	7.65	0.27	1.97	0.35	-----	0.08	-----	-----	-----
MTE-102	21.61	6.55	0.45	1.75	0.49	0.16	0.06	0.15	-----	0.80
MTE-103	22.57	6.85	0.17	1.74	0.40	0.04	0.06	0.13	-----	0.66

Molar Ratios								
Sample	K/Na	Ca/Na	Fe/Na	Mn/Na	Mg/Na	Zn/Na	Ba/Na	SO <sub>4</sub> /Na
MTE-101	0.317	0.011	0.082	0.014		0.003		
MTE-102	0.303	0.021	0.081	0.023	0.007	0.003	0.007	0.037
MTE-103	0.304	0.008	0.077	0.018	0.002	0.003	0.006	0.029
Average	0.308	0.013	0.080	0.018	0.004	0.003	0.006	0.033

Charge Balance and Anion Deficiencies					
Sample	$\sum m_i z_i^2$ cations	$\sum m_i z_i^2$ anions	Charge Balance	Anion Deficiency (ppm)	
	[ $\times 10(-5)$ ]	[ $\times 10(-5)$ ]	[ $\times 10(-5)$ ]	Cl equiv	SO <sub>4</sub> equiv
MTE-101	52.31	-----	52.31	18.55	12.55
MTE-102	49.15	3.20	45.95	16.29	11.03
MTE-103	48.28	2.64	45.64	16.18	10.95

Columns 2 and 3 represent the sum of the cations and anions, respectively;

m=molality, z=charge

Column 4 represents the charge balance (Column 2 - Column 3)

Columns 5 and 6 represent the amount of Cl or SO<sub>4</sub> needed to achieve neutrality

Table 6A. Concentrations of Fluid Inclusion Leachate Solutions  
Normalized to 10 ppm Total Concentration for Vein Quartz  
(Sc Leaching Solution)

Sample	Normalized concentrations in ppm (after blank subtraction)							
	Na	K	Ca	Fe	Mn	Mg	Zn	Cl
MTE-500	3.48	1.42	1.03	0.20	0.20	BD	0.03	3.65
MTE-501	3.65	1.47	0.85	0.20	0.20	BD	0.03	3.58
MTE-502	3.31	1.36	0.97	0.21	0.16	BD	0.03	3.96
MTE-503	3.26	1.50	0.88	0.22	0.18	BD	BD	3.96
MTE-504	3.28	1.45	0.90	0.20	0.20	BD	BD	3.98
Average	3.40	1.44	0.93	0.21	0.19		0.03	3.83
Stand Dev	0.17	0.05	0.07	0.01	0.02		0.00	0.19
W3-3A	3.53	1.37	0.86	0.09	0.20	0.02	0.04	3.90
W3-3B	3.51	1.34	0.78	0.07	0.21	0.02	0.02	4.05
W3-3C	3.48	1.32	1.03	0.07	0.20	0.05	0.02	3.82
Average	3.51	1.34	0.89	0.08	0.20	0.03	0.03	3.92
Stand Dev	0.03	0.02	0.13	0.01	0.01	0.02	0.01	0.12
HH-100	3.40	1.14	0.98	0.20	0.26	0.06	0.04	3.93
HH-101	3.64	1.23	1.05	0.25	0.27	0.07	0.03	3.46
Average	3.52	1.18	1.02	0.22	0.26	0.06	0.04	3.70
Stand Dev	0.17	0.06	0.05	0.04	0.01	0.01	0.01	0.33
CMX-1	3.61	1.42	0.86	0.09	0.18	BD	0.03	3.75
CMX-2	3.63	1.47	0.84	0.09	0.21	BD	0.03	3.72
CMX-3	3.54	1.57	0.87	0.08	0.20	BD	0.04	3.70
Average	3.59	1.49	0.86	0.09	0.20		0.03	3.75
Stand Dev	0.05	0.08	0.02	0.01	0.02		0.01	0.06
FN-1	3.48	1.37	0.85	0.26	0.22	0.04	0.03	3.76
CPU-2A	3.45	1.03	1.03	0.21	0.21	0.05	0.05	3.97
CPU-2B	3.93	1.36	1.14	0.21	0.21	BD	0.07	3.07
CPU-2C	3.85	1.36	1.24	0.24	0.24	0.06	0.06	2.96
Average	3.74	1.25	1.14	0.22	0.22	0.06	0.06	3.33
Stand Dev	0.26	0.19	0.10	0.02	0.02	0.07	0.01	0.55

See Appendix D, Table D6 for actual concentrations (in ppm) and blanks  
 Samples W3-3A,B,C are from the Wee Three (W3-3) prospect  
 Samples HH-100, 101 are from the Hot Hill prospect  
 Sample FN-1 is from the Fuzzy Nut prospect

BD = below detection limit

Table 6B. Molalities for Fluid Inclusion Leachate Solutions of Vein Quartz Using a 250 ppm Sc Leachate Solution in 0.25wt% HNO<sub>3</sub> Values Normalized to 10 ppm Total Concentration

Sample	Concentrations in molalities ( $\times 10^{-5}$ ) after blank subtraction							
	Na	K	Ca	Fe	Mn	Mg	Zn	Cl
MTE-500	15.13	3.63	2.57	0.36	0.36	BD	0.05	10.29
MTE-501	15.87	3.76	2.12	0.36	0.36	BD	0.05	10.10
MTE-502	14.39	3.48	2.42	0.38	0.29	BD	0.05	11.17
MTE-503	14.17	3.84	2.20	0.39	0.33	BD	BD	11.17
MTE-504	14.26	3.71	2.25	0.36	0.36	BD	BD	11.23
W3-3A	15.35	3.50	2.16	0.16	0.36	0.08	0.06	11.00
W3-3B	15.26	3.43	1.95	0.13	0.38	0.08	0.03	11.42
W3-3C	15.13	3.38	2.57	0.13	0.36	0.21	0.03	10.77
HH-100	14.78	2.92	2.45	0.36	0.47	0.25	0.06	11.09
HH-101	15.83	3.15	2.62	0.45	0.49	0.29	0.05	9.76
CMX-1A	15.70	3.63	2.15	0.16	0.33	BD	0.05	10.77
CMX-1B	15.78	3.76	2.10	0.16	0.38	BD	0.05	10.49
CMX-1C	15.39	4.02	2.17	0.14	0.36	BD	0.06	10.44
FN-1	15.13	3.50	2.12	0.47	0.40	0.16	0.05	10.61
CPU-2A	15.00	2.63	2.57	0.38	0.38	0.21	0.08	11.20
CPU-2B	17.09	3.48	2.84	0.38	0.38	BD	0.11	8.66
CPU-2C	16.74	3.48	3.09	0.43	0.44	0.25	0.09	8.35

See Appendix D, Table D6 for actual concentrations in ppm and blanks

See Table 6A for concentration values in ppm which have been normalized to 10 ppm

BD = below detection limit

Samples W3-3A, B, C are from the Wee Three (W3-3) prospect

Samples HH-100,101 are from the Hot Hill prospect

Sample FN-1 is from the Fuzzy Nut prospect

Table 6C. Charge Balances and Charge Deficiencies for Fluid Inclusion Leachate Solutions of Vein Quartz Using a 250 ppm Sc Leach Solution Values Normalized to 10 ppm Total Concentration

Sample	$\sum m_i z_i^2$ cations	$\sum m_i z_i^2$ anions	Charge Balance	Anion Deficiencies (ppm)	
	[x 10(-5)]	[x 10(-5)]		[x 10(-5)]	Cl equiv
MTE-500	33.90	10.29	23.61	8.37	5.67
MTE-501	32.97	10.10	22.87	8.11	5.49
MTE-502	32.31	11.17	21.14	7.49	5.07
MTE-503	31.64	11.17	20.47	7.26	4.91
MTE-504	31.65	11.23	20.42	7.24	4.90
W3-3A	30.93	11.00	19.93	7.07	4.78
W3-3B	29.62	11.42	18.20	6.45	4.37
W3-3C	32.36	10.77	21.59	7.65	5.18
HH-100	33.86	11.09	22.77	8.07	5.46
HH-101	36.83	9.76	27.07	9.60	6.50
CMX-1	30.89	10.77	20.12	7.13	4.83
CMX-2	31.10	10.49	20.61	7.31	4.95
CMX-3	31.03	10.44	20.59	7.30	4.94
FN-1	33.78	10.61	23.17	8.21	5.56
CPU-2A	34.10	11.20	22.90	8.12	5.50
CPU-2B	37.31	8.66	28.65	10.16	6.88
CPU-2C	39.57	8.35	31.22	11.07	7.49

Column 2 represents the cation charge balance; m = molality, z = charge

Column 3 represents the anion charge balance

Column 4 represents the net charge balance ( Column 2 - Column 3)

Column 5 represents the amount of Cl needed to establish a neutral charge balance

Column 6 represents the amount of SO4 needed to establish a neutral charge balance

See Table 6B for molalities used to obtain charge balances

See Appendix D, Table D6 for actual concentrations (in ppm) and blanks

Samples W3-3A,B,C are from the Wee Three (W3-3) prospect

Samples HH-100,101 are from the Hot Hill prospect

Sample FN-1 is from the Fuzzy Nut prospect

Table 6D. Molar Ratios of Cations and Chloride on Fluid Inclusion Crush-Leach Analyses of Vein Quartz Using a 250 ppm Sc Solution in 0.25 wt% HNO<sub>3</sub>

Sample	Molar Ratio (with respect to one mole of sodium)						
	K/Na	Ca/Na	Fe/Na	Mn/Na	Mg/Na	Zn/Na	Cl/Na
MTE-500	0.241	0.169	0.024	0.024	--	0.003	0.681
MTE-501	0.236	0.134	0.023	0.023	--	0.003	0.637
MTE-502	0.243	0.168	0.026	0.020	--	0.003	0.777
MTE-503	0.271	0.155	0.028	0.024	--	--	0.787
MTE-504	0.259	0.157	0.025	0.025	--	--	0.788
Average	0.250	0.157	0.025	0.023	--	0.003	0.734
W3-3A	0.227	0.139	0.011	0.024	0.005	0.004	0.716
W3-3B	0.225	0.128	0.009	0.024	0.005	0.002	0.749
W3-3C	0.224	0.170	0.009	0.024	0.013	0.002	0.713
Average	0.225	0.146	0.010	0.024	0.008	0.003	0.726
HH-100	0.197	0.166	0.024	0.031	0.016	0.004	0.750
HH-101	0.198	0.165	0.029	0.031	0.019	0.003	0.617
Average	0.198	0.166	0.026	0.031	0.018	0.004	0.684
CMX-1A	0.231	0.136	0.010	0.021	--	0.003	0.686
CMX-1B	0.238	0.133	0.010	0.024	--	0.003	0.665
CMX-1C	0.261	0.140	0.009	0.023	--	0.004	0.678
Average	0.243	0.136	0.010	0.023	--	0.003	0.676
FN-1	0.231	0.140	0.031	0.026	0.011	0.003	0.702
CPU-2A	0.176	0.171	0.025	0.025	0.014	0.005	0.746
CPU-2B	0.203	0.167	0.022	0.023	--	0.006	0.507
CPU-2C	0.208	0.185	0.025	0.026	0.015	0.005	0.499
Average	0.201	0.174	0.024	0.025	0.014	0.005	0.584

See Table 6B for molalities used to calculate molar ratios.



## STABLE ISOTOPE STUDIES

Oxygen isotope ratios for vein quartz, adularia and calcite; hydrogen isotope ratios for inclusion fluids from quartz; and carbon isotope ratios for calcite were measured to indicate the source of the mineral-forming fluids. Oxygen isotope ratios for whole rock samples on the Capitan pluton were measured to determine the variation in  $\delta^{18}\text{O}$  values across the length of the pluton. Oxygen isotope ratios for plutonic rocks adjacent to mineralized zones and clasts of plutonic rocks within the brecciated mineralized zones were measured to determine if any alteration (ie., deuteritic alteration) of the host rock adjacent to and within the veins was present. Sample descriptions, detailed experimental procedures and all experimental data (oxygen isotope data on quartz, adularia, calcite and whole rocks, carbon isotope data on calcites and limestones, and hydrogen isotope data on fluid inclusion waters) are reported in Appendix E.

## EXPERIMENTAL PROCEDURES

A silicate extraction line employing a  $\text{ClF}_3$  reagent in the stable isotope lab at New Mexico Institute of Mining and Technology was used for extracting oxygen samples from quartz, adularia and whole rock samples (technique from Borthwick and Harmon, 1982; modified from Taylor and Epstein, 1962). Samples for  $\delta^{18}\text{O}$  analysis were crushed to a -80 mesh powder in an agate mortar and pestle and oven-dried at  $120^\circ\text{C}$  for six to eight hours prior to use. Ten to fifteen mg samples were placed in nickel reaction vessels on the silicate line and reacted at  $450^\circ\text{C}$  for 8 hours with the  $\text{ClF}_3$  reagent. Oxygen samples were converted to  $\text{CO}_2$  with a heated carbon rod. Carbon dioxide pressures were measured and the gases were stored in

sample collection vessels. Carbon dioxide yields from the extraction process gave product yields ranging from 93 to 112% for quartz, with the majority at  $100 \pm 4\%$ , and 107 to 128% for adularia. Oxygen isotope ratios with respect to SMOW were measured on the CO<sub>2</sub> samples using a Finnigan Mat Delta E mass spectrometer. Precision for silicate samples using a National Bureau of Standards sample (NBS-28,  $\delta^{18}\text{O} = 9.64\text{o/oo}$  vs SMOW) was  $\pm 0.07$  o/oo (actual values range from 9.59 to 9.84 o/oo, averaging 9.71 o/oo).

Calcite and limestone samples were reacted with 105% phosphoric acid at a temperature of 25°C for 10 hours to liberate CO<sub>2</sub> (technique modified from McCrea, 1950). Carbon and oxygen isotope ratios on the liberated CO<sub>2</sub> were determined on a Finnigan Mat delta E mass spectrometer. An isotope fractionation factor for the reaction of phosphoric acid with the carbonates was determined using NBS standards (NBS-18, 19, 20). A value of -10.62 o/oo was added to all vein carbonates and -10.32 o/oo was added to all limestones on the liberated CO<sub>2</sub> to obtain the true  $\delta^{18}\text{O}$  values for the carbonates.

Hydrogen samples on inclusion fluids of vein quartz were determined by using 10 to 25 grams of 0.2 to 1.0 cm sized pieces of material, crushing the sample under vacuum in a steel tube, transferring the evolved water in a vacuum line to a hydrogen reaction vessel containing 0.3 g Zn and reacting the water plus Zn under vacuum at 500°C for 30 minutes (technique modified from Coleman et al., 1982). The hydrogen formed by this technique was measured to obtain the hydrogen isotope ratio of the inclusion fluids on a Finnigan Mat Delta E mass spectrometer. Hydrogen isotope values were corrected with respect to NBS water standards SMOW (Standard Mean Ocean Water,  $\delta\text{D} = 0\text{o/oo}$ ), GISP (Greenland Ice and Snow Precipitation,  $\delta\text{D} = -189.7$  vs SMOW) and SLAP (Standard Light Antarctic Precipitation,  $\delta\text{D} = -428$  vs SMOW).

### Results of Oxygen Isotopes for Quartz, Adularia and Whole Rocks

Thirty-two samples of vein quartz were measured for  $\delta^{18}\text{O}$  (Table 7).  $\delta^{18}\text{O}$  of quartz ranges from 8.73 o/oo to 10.16 o/oo with respect to SMOW (Fig. 29). The isotopic composition of the waters in equilibrium with the quartz were calculated by using the highest halite dissolution temperature for a type 1 inclusion in quartz for a given prospect and referring to the fractionation equation given by Matsuhisa et al. (1979):  $10^3 \ln \alpha = (2.05 \times 10^6)/T^2 - 1.14$ . The  $\delta^{18}\text{O}$  of the corresponding water values range from 7.08 o/oo to 8.09 o/oo. Nine samples of vein adularia were measured for  $\delta^{18}\text{O}$  (Table 8).  $\delta^{18}\text{O}$  of adularia range from 7.94 o/oo to 10.09 o/oo. The isotopic composition of the waters in equilibrium with adularia were calculated using the highest halite dissolution temperature for a type 1 inclusion in quartz for a given prospect and referring to the fractionation equation given by Friedman and O'Neil (1977):  $10^3 \ln \alpha = (3.13 \times 10^6)/T^2 - 3.70$ . The  $\delta^{18}\text{O}$  of the corresponding water value ranges from 7.24 o/oo to 9.74 o/oo. There was no variation in the  $\delta^{18}\text{O}$  values between smoky quartz and clear quartz from the same vein, indicating the two types of quartz formed from the same fluid.  $\delta^{18}\text{O}$  values on massive quartz, vuggy quartz and Japanese-law twinned quartz from the MTE prospect are approximately the same, suggesting that all three forms of quartz originated from the same fluid. The  $\delta^{18}\text{O}$  water values for quartz and adularia are similar, which suggests that only one type of fluid was responsible for the quartz and adularia mineralization.

$\delta^{18}\text{O}$  measurements on whole rock samples of the Capitan pluton range from 7.64 o/oo to 9.22 o/oo (Table 8; see Fig.1 for sample localities).  $\delta^{18}\text{O}$  measurements on whole rock samples of plutonic rock adjacent to selected veins and pluton clasts within brecciated mineralized zones range from 8.23 o/oo to 10.84

o/oo (Table 8). The  $\delta^{18}\text{O}$  values are similar to fresh plutonic rock values, which implies that there was no significant late-stage alteration (ie deuteritic alteration) associated with the mineralized zones.

### Results of Carbon and Oxygen Isotope Analyses on Vein Calcites

Five late-stage, fine-grained white calcites from three veins (Fuzzy Nut, Hot Hill and HC prospects), four brownish-black carbonates from two veins, one pink carbonate sample from the Fuzzy Nut prospect and four unaltered limestone samples from the Permian San Andres formation (two samples from the limestone roof pendant and two samples from a roadcut two miles west of the Capitan pluton) were analyzed for carbon and oxygen isotope ratios (Table 9).  $\delta^{18}\text{O}$  values are with respect to SMOW and  $\delta^{13}\text{C}$  values are with respect to PDB.  $\delta^{13}\text{C}$  values range from -7.76 to -7.13o/oo for the white vein calcites, -8.02o/oo for the pink carbonate, -4.89 to -2.24o/oo for the brown carbonates, and 1.48 to 2.32o/oo for the limestone samples.  $\delta^{18}\text{O}$  values range from 21.96 to 23.17o/oo for the white vein calcites, 21.87o/oo for the pink carbonate, 21.10 to 22.84o/oo for the brown carbonates and 20.12 to 27.14o/oo for the limestone samples. The oxygen isotope ratios for waters in equilibrium with the white vein calcites were calculated by using the highest halite dissolution temperature (237°C) from a type 3 inclusion and referring to the fractionation equation given by Friedman and O'Neil (1977):  $10^3 \ln \alpha = 2.78 \times 10^6 / T^2 - 2.89$ .  $\delta^{18}\text{O}$  water values calculated this way are summarized in Table 9.

Table 7. Oxygen Isotopic values on Quartz and Hydrogen Isotopic Values on Fluid Inclusion Waters in Quartz (Values vs SMOW)

Prospect	Description	$\delta^{18}\text{O}_{\text{Qtz}}$	FI Temp	$\delta^{18}\text{OH}_2\text{O}$	$\delta\text{DH}_2\text{O}$
BS	clear qtz vein	9.12	549	7.23	
CM 104	clear qtz xls	8.86	577	7.16	
CM 235	clear qtz breccia	9.04, 9.46	559	7.22, 7.64	
CM 242	clear qtz vein	9.08, 9.62	n/m		
CM 301	clear qtz veinlet	9.07	n/m		
CMX-1	clear qtz xl	9.17, 9.14	610	7.68, 7.65	-50, -66, -67,
CMX-1	clear qtz xl				-73, -79, -80
CMX-2	smoky qtz xl	9.04, 8.82	610	7.55, 7.33	-86
CPU-2	clear vug qtz	9.11	568	7.35	
CPU-2	clear qtz vein	9.39	568	7.63	
CPU-2	smoky vug qtz	9.54	568	7.78	
CPU-2	smoky qtz xl	9.62	568	7.86	
Fuzzy Nut	clear vug qtz	8.82	570	7.08	67, -75
Fuzzy Nut	clear qtz vein	9.42	570	7.68	
Hot Hill-8	smoky qtz xl	8.99	610	7.50	
Hot Hill-1	smoky qtz xl	8.73	610	7.24	
Hot Hill-2	clear qtz xl	9.43	610	7.94	
Kopm Spgs	clear qtz xl	9.22	541	7.27	
McCory	smoky qtz xl	9.59	610	8.09	
MTE-1	clear vein qtz	9.10, 8.99	620	7.67, 7.56	
MTE-2	clear qtz xl	8.81, 8.94	620	7.38, 7.51	
MTE-3	Jap-law qtz xl	9.21, 8.85	620	7.78, 7.42	-22, -25, -34
MTE-3	Jap-law qtz xl				-36, -49, -50
Piney	smoky qtz xl	9.05	n/m		
W3-2	smoky qtz vein	9.15, 8.78	n/m		
W3-3	smoky qtz xl	9.34	610	7.85	
W3-3A	smoky qtz xl	9.06	610	7.57	-46
W3-3B	smoky qtz xl	9.01	610	7.52	-48
W3-3C	clear qtz xl	9.05	610	7.56	
W3-4	smoky qtz xl	9.16	595	8.58	
W3-5	smoky qtz breccia	9.37	n/m		
W3-7	clear qtz xl	9.58	n/m		

See Appendix E for sample descriptions, experimental procedures and a detailed data section.

Samples W3-2,3,4,5,7 are from the Wee Three claims.

Oxygen and hydrogen isotopic values were determined on different pieces of similar quartz and are not "true" paired values. n/m = not measured

See Appendix E for explanation of corrected hydrogen isotope values.

$\delta$  notation = a measure of the isotope ratio of sample with respect to the isotope ratio of a standard.

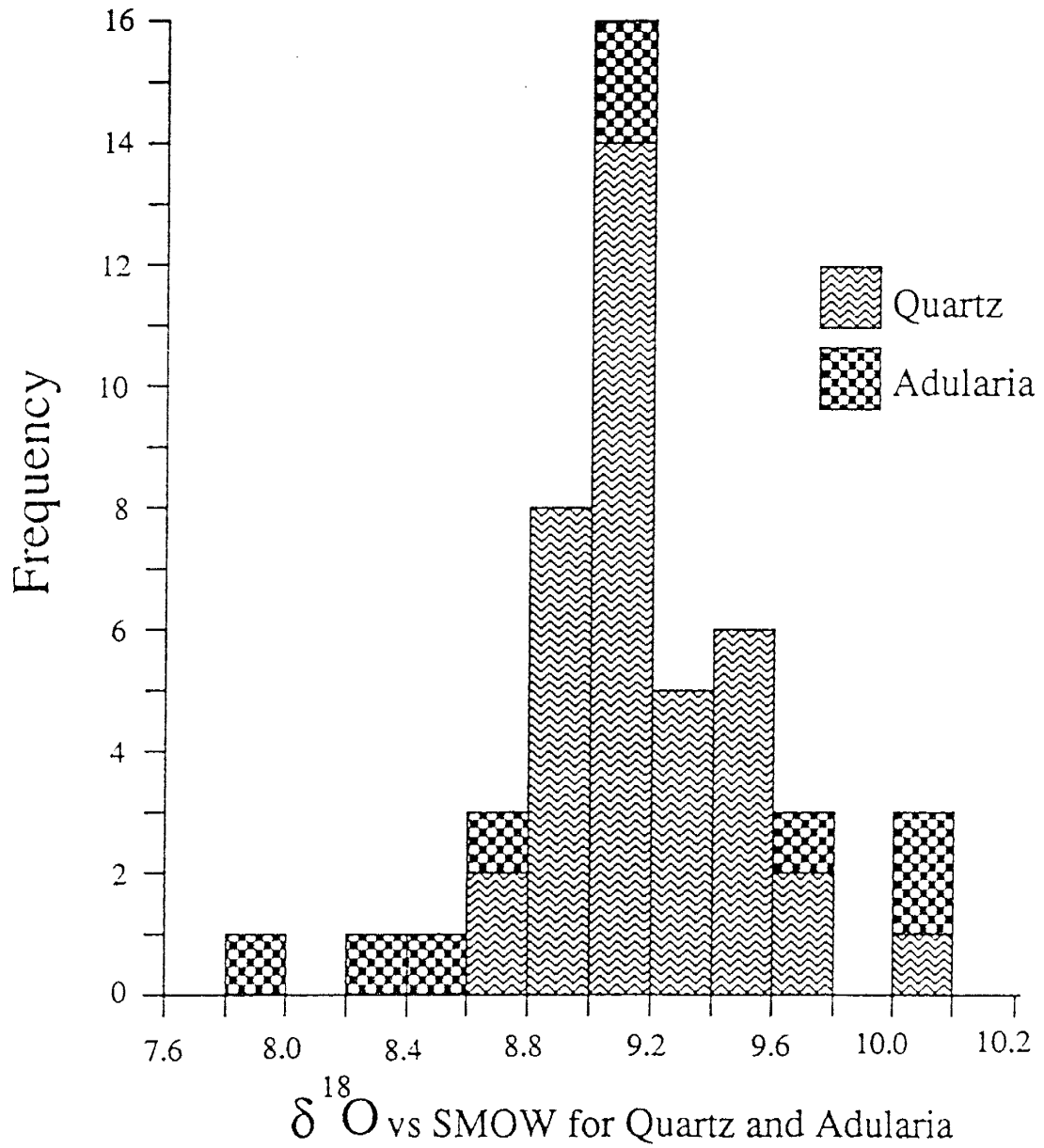


FIG. 29. Plot of  $\delta^{18}\text{O}$  versus frequency for quartz and adularia samples which were analyzed for oxygen isotope ratios.  $\delta^{18}\text{O}$  values are mineral values in permil and are with respect to SMOW.

Table 8. Oxygen Isotopic Ratios (vs SMOW) for Vein Adularia, Whole Rock Pluton, Pluton Vein Clasts and Pluton Rock Adjacent to Veins

$\delta^{18}\text{O}$  Values for Vein Adularia Samples

Prospect	Description	$\delta^{18}\text{O}$ (o/oo)	FI Temp	$\delta^{18}\text{O}_{\text{H}_2\text{O}}$
CPU-2	pink adularia xl	9.19	568	8.46
CPU-2	pink adularia xl	8.76	568	8.03
Fuzzy Nut	pink adularia xl	7.94	570	7.24
Hot Hill	pink adularia xl	10.05	610	9.74
Koprn Springs	white adularia xl	8.47	541	7.45
McCory	pink adularia xl	8.29	608	7.96
MTE	pink adularia xl	9.05	620	8.83
W3-3	white adularia xl	9.63	600	9.22
W3-4	pink adularia xl	10.09	595	9.64

Samples W3-3.4 are from the Wee Three prospects

$\delta^{18}\text{O}$  Values for Capitan Pluton Whole Rocks

Sample	Description	Alteration	$\delta^{18}\text{O}$ (o/oo)
CM 100	granophyric granite	unaltered	9.12
CM 103	aplitic granite	slightly altered	9.02
CM 211	porphyritic granite	unaltered	9.22
CM 225	granophyric granite	unaltered	8.86
CM 228	granophyric granite	slightly altered	7.96
CM 241	granophyric granite	unaltered	8.73
CM 243	aplitic granite	unaltered	7.64
CM 246	porphyritic granite	unaltered	7.85
CM 249	porphyritic granite	slightly altered	8.97

$\delta^{18}\text{O}$  Values for Whole Rocks Adjacent to Veins and Breccia Clasts

Prospect	Description	$\delta^{18}\text{O}$ (o/oo)
CPU-2	pluton clast in vein	8.23
Fuzzy Nut	pluton clast in vein	8.97
Hot Hill	plutonic rock near vein	8.49
Hot Hill	pluton clast in vein	8.61
Hot Hill	pluton clast in vein	9.68
McCory	pluton clast in vein	8.77
MTE	plutonic rock near vein	11.14
MTE	plutonic rock near vein	10.84

See Figure 1 for sample and prospect localities.

See Appendix E for sample descriptions and a detailed data section.  
MTE samples are dump/float samples and may be altered

Table 9. Carbon and Oxygen Isotopic Composition of Vein Carbonates and Limestone

Prospect	Description	$\delta^{13}\text{C}$ (o/oo)	$\delta^{18}\text{O}$	FI Temp (C)	$\delta^{18}\text{O}$ (H <sub>2</sub> O)
Fuzzy Nut	white calcite	-7.74	22.43	237	14.63
Fuzzy Nut	white calcite	-7.76	22.15	237	14.35
Fuzzy Nut	brown carbonate	-4.80	21.16		
Fuzzy Nut	brown carbonate	-4.89	21.10		
Fuzzy Nut	pink carbonate	-8.02	21.87		
Hopeful(HC)	white calcite	-7.68	21.96	237	14.16
Hot Hill	white calcite	-7.16	23.04	237	15.24
Hot Hill	white calcite	-7.13	23.17	237	15.37
Hot Hill	brown carbonate	-2.31	22.84		
Hot Hill	brown carbonate	-2.24	22.62		
LS-2A	limestone	2.32	26.13		
LS-2B	limestone	2.20	27.14		
LS-3A	limestone	2.00	21.01		
LS-3B	limestone	1.48	20.12		

LS-2A, B: unaltered limestone from San Andres formation; roadcut, mile marker 6, highway 48

LS-3A, B: unaltered (?) limestone roof pendant on west side of Capitan Mountains

Carbon isotope values with respect to PDB

Oxygen isotope values with respect to SMOW

See Appendix E for sample descriptions, detailed experimental procedures and detailed data section

See Figure 1 for prospect localities



### **Results of Hydrogen Isotope Analyses from Fluid Inclusion Waters**

Data for 17 hydrogen isotope ratio measurements on fluid inclusion waters in vein quartz from the MTE, Wee Three and CMX prospects are summarized in Table 7.  $\delta D$  values show a large range, from -22 ‰ to -86 ‰. A plot of  $\delta^{18}O$  water values versus the corresponding  $\delta D$  values from quartz samples is shown in Figure 30. Samples from the MTE, CMX, Fuzzy Nut and Wee Three prospects fall within, above and slightly below the magmatic water box. A smoky quartz sample from the CMX prospect plots near the magmatic water boundary.

## **DISCUSSION OF FLUID INCLUSION DATA**

Microthermometric and petrographic studies of 638 fluid inclusions in quartz, fluorite, calcite and titanite from the Th-U-REE deposits in the Capitan Mountains indicate that there are four main types of fluid inclusions (Figs. 26 and 27). The origin of all four inclusion types will be explained in the following sections.

### **Origin of Type 1 and 2 Inclusions (Halite Trend)**

When type 1 and 2 inclusions are plotted on a NaCl-KCl-H<sub>2</sub>O diagram (Fig. 28), the observed fields for both quartz and fluorite define a linear trend. This linear relationship implies that type 1 and 2 fluids are part of the same parent fluid which may have undergone some type of fluid evolution. This linear trend has previously been referred to as the "halite trend" (Erwood et al., 1979; Cloke and Kesler, 1979), because the trend extends from (or near) the halite apex.

Possible models which might explain the observed halite trend are (Cloke and Kesler, 1979; Quan et al., 1987): 1) boiling, 2) dilution or mixing with a meteoric

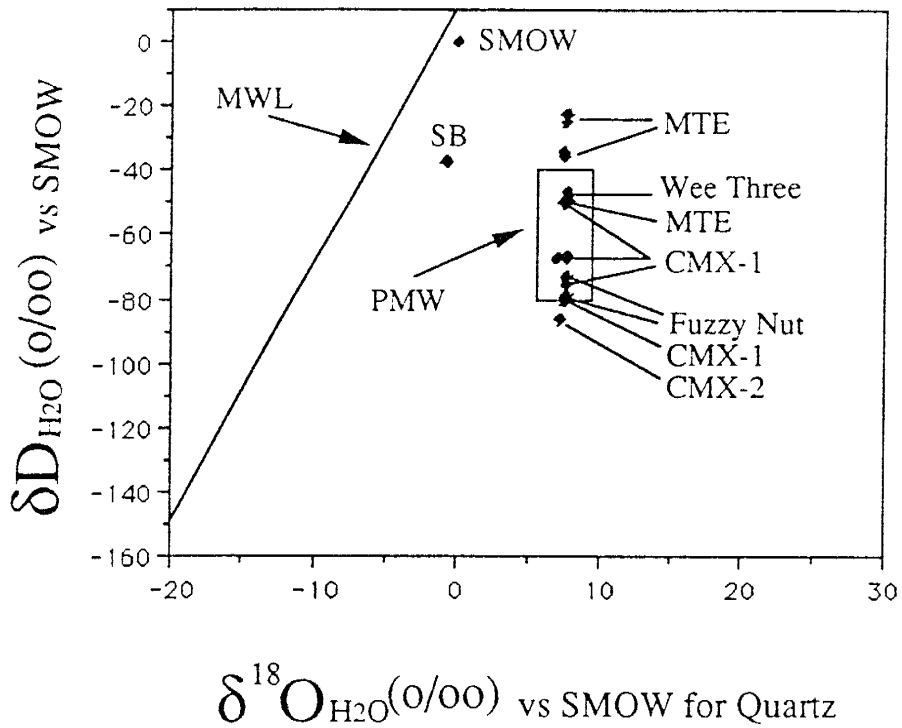


FIG. 30. Plot of hydrogen isotope values of fluid inclusion waters in quartz versus oxygen isotope values of water in equilibrium with quartz at 600°C for samples from four prospects. MWL is the meteoric water line, PMW is the primary magmatic water box (Sheppard, 1977). SMOW is Standard Mean Ocean Water. SB is a sample of Sierra Blanca smoky vein quartz - a suspected mid-Tertiary meteoric water (see text). Samples CMX-1 is clear vein quartz and CMX-2 is smoky vein quartz. Most quartz samples plot in the PMW box and are interpreted to have formed from magmatic fluids.

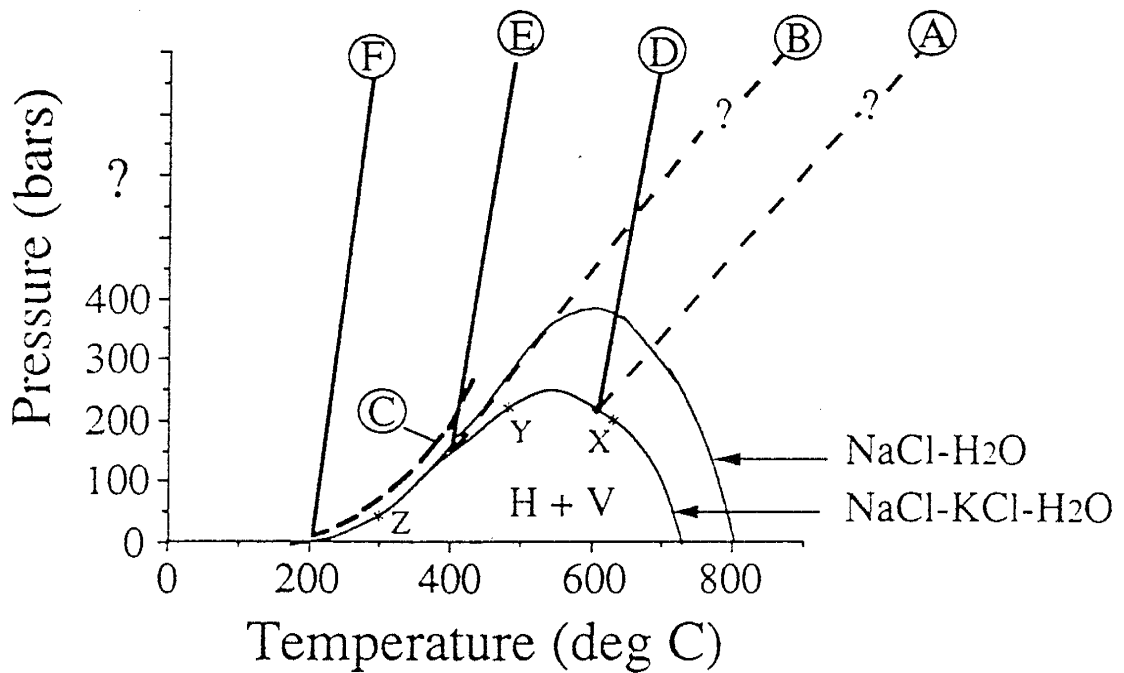
water, 3) water-rock interactions, and 4) subtraction of KCl-bearing halite from a fluid prior to entrapment.

Boiling is interpreted to be minor or non-existent for the Th-U-REE deposits - because of the lack of vapor-rich inclusions for most deposits (with the exception of the Wee Three prospects), classic textures associated with boiling are not present and interpreted depths of vein formation are too deep to allow boiling at the temperatures observed. The halite trend illustrated in Figure 28 does not converge to the water apex, which suggests that mixing with a meteoric water is not responsible for the observed halite trend. Mixing/dilution by a meteoric water would also tend to pull the fluid inclusion data off of the halite saturation curve (Figs. 26 and 27). From Figure 28, the K/Na ratio along the halite trend is observed to increase with decreasing temperature. Quan et al. (1987) have suggested that water-rock interactions could not account for the observed changes in the K/Na ratio along the halite trend. Thus models 1, 2 and 3 are not likely possibilities to explain the halite trend.

The fourth model appears to be the most likely model to explain the halite trend - a mineralizing fluid is saturated with respect to halite and subtraction (precipitation) of a KCl-bearing halite-rich solid from the high temperature-high salinity hydrothermal fluid occurs prior to entrapment as an inclusion. When a line is drawn through the type 1 and 2 populations (Fig. 28), it intersects the NaCl-KCl solid binary at NaCl<sub>80</sub>KCl<sub>20</sub> and not the NaCl apex. This can be explained as follows. The initial fluid may have been saturated with respect to halite, crystallizes out a KCl-bearing halite of composition NaCl<sub>80</sub>KCl<sub>20</sub> and evolves away from the NaCl<sub>80</sub>KCl<sub>20</sub> binary and along a linear trend towards the NaCl-KCl cotectic boundary. This halite trend would imply that solid halite should be in solution and hence found as solid inclusions in the host mineral. A serious problem with the

fourth model, as mentioned in Quan et al. (1987), is the lack of evidence for solid halite inclusions in minerals. Erwood et al. (1979) have mentioned that the early-formed solid halite may have been dissolved by later fluids. If this is true, casts of halite cubes would be expected to be observed in some minerals. No solid inclusions or casts of solid halite inclusions have been observed in the quartz or fluorite which delineate the halite trend. However, due to a lack of a better model to explain the halite trend inclusions, the fourth model appears to be the most likely process to explain the halite trend. It should be remembered that this interpretation is based on the NaCl-KCl-H<sub>2</sub>O system; additional ions (Ca, Fe, Mn, SO<sub>4</sub>) probably suggests a more complex situation.

Cloke and Kesler (1979) have proposed four reaction paths which could account for the halite trend inclusions. For the halite trend inclusions (type 1 and 2 inclusions) observed in quartz and fluorite from the Capitan Mountains Th-U-REE deposits, the "EL" path ("equilibrium-separation-of-halite-from-liquid") is the most likely of the four paths. In order to explain the origin of the type 1 and 2 inclusions using the "EL" path of Cloke and Kesler (1979), a pressure-temperature diagram for the NaCl-KCl-H<sub>2</sub>O system must be derived for the Capitan Mountain halite trend shown in Figure 28. The method for constructing the P-T diagram is given in Appendix F. The more adventurous reader is referred to the original article (Cloke and Kesler, 1979). The constructed P-T diagram is shown in Figure 31. Salinity contours (L/L + H) for 80 eq wt% NaCl + KCl (typical type 1 inclusion salinity), 55 eq wt% NaCl + KCl (typical type 2 inclusion salinity) and 35 eq wt% (typical type 3 inclusion salinity) and salinity contours (L + V/L) for 80 eq wt% NaCl + KCl, 55 eq wt% NaCl + KCl and 35 eq wt% are illustrated. Due to a lack of experimental data, the L/L + H and L + V/L solubility contours can only be schematically represented. The slopes and shapes of the L/L + H and L + V/L contours are oriented in a similar



- Ⓐ L + V/L 80% Liquid-Vapor Curve
- Ⓑ L + V/L 55% Liquid-Vapor Curve
- Ⓒ L + V/L 35% Liquid-Vapor Curve
- Ⓓ 80% L/L + H Liquid-Solid Line
- Ⓔ 55% L/L + H Liquid-Solid Line
- Ⓕ 35% L/L + H Liquid-Solid Line

FIG. 31. Pressure-temperature projection for the Capitan halite trend in the NaCl-KCl-H<sub>2</sub>O system (modified from Cloke and Kesler, 1979). Liquid-solid and liquid-vapor contours are shown for 80 and 55 eq wt% NaCl + KCl and 35 eq wt% NaCl. The NaCl-KCl-H<sub>2</sub>O solubility is constructed from Figure 28 (see main text and Appendix F for more details). The NaCl-H<sub>2</sub>O curve is shown for reference (data from Sourirajan and Kennedy, 1962; Keevil, 1942). Segment X-Y represents the range for type 1 fluids along the halite trend and segment Y-Z represents the range for type 2 fluids along the halite trend.

position as shown by Cloke and Kesler (1979; their Figs. 4 and 5) and are used only to illustrate the origin of the inclusions. The NaCl-H<sub>2</sub>O solubility curve (data from Sourirajan and Kennedy, 1962; and Keevil, 1942) is shown for reference.

Comparison of the NaCl-KCl-H<sub>2</sub>O and NaCl-H<sub>2</sub>O solubility curves show that the addition of KCl significantly lowers the NaCl-KCl-H<sub>2</sub>O curve downwards from the NaCl-H<sub>2</sub>O curve. It should be mentioned that the pressures used to calculate the P-T diagram are "minimum pressures" as determined from Figure 28. The reader is referred to Figures 32 and 33 for the following discussion concerning the origins of type 1 and 2 inclusions. Due to a lack of experimental data for the NaCl-KCl-H<sub>2</sub>O system, isochores for Figures 32 and 33 can only be represented schematically. The position (slopes) of the isochores are similar to the isochores found in the pressure-temperature diagrams of Roedder and Bodnar (1980; their Fig. 5) and Bloom (1981; his Fig. 7).

About 70% of the type 1 inclusions found in quartz and fluorite from the Capitan Th-U-REE deposits homogenize by halite dissolution. Depending on the location where a type 1 fluid becomes trapped as an inclusion along the L + H/L solubility line, the difference between  $T_m$  NaCl and  $T_h$  can be small (< 50, but > 10°C) or large (> 50, but < 150°C). Several paths exist on the P-T diagram (Fig. 32) which might explain the origin for these types of inclusions. The following discussion assumes a type 1 inclusion with 80 eq wt% NaCl + KCl.

Path A) The original saline parent fluid (1) undergoes isobaric cooling until it intersects the 80 eq wt% L + H/L solubility line (2). At (2) the fluid is saturated with respect to halite. If a fluid becomes trapped at (2), solid KCl-bearing halite will begin to crystallize. At (2), the path will follow a constant volume liquid-solid curve downwards with a drop in pressure and temperature until it intersects the solubility curve (3). At (3) a vapor bubble will form. From (3) the entrapped fluid will

continue to cool and other solid phases will begin to crystallize. The bulk salinity of this inclusion will be 80 eq wt% NaCl + KCl and the difference between  $T_m$  NaCl and  $T_h$  will be large.

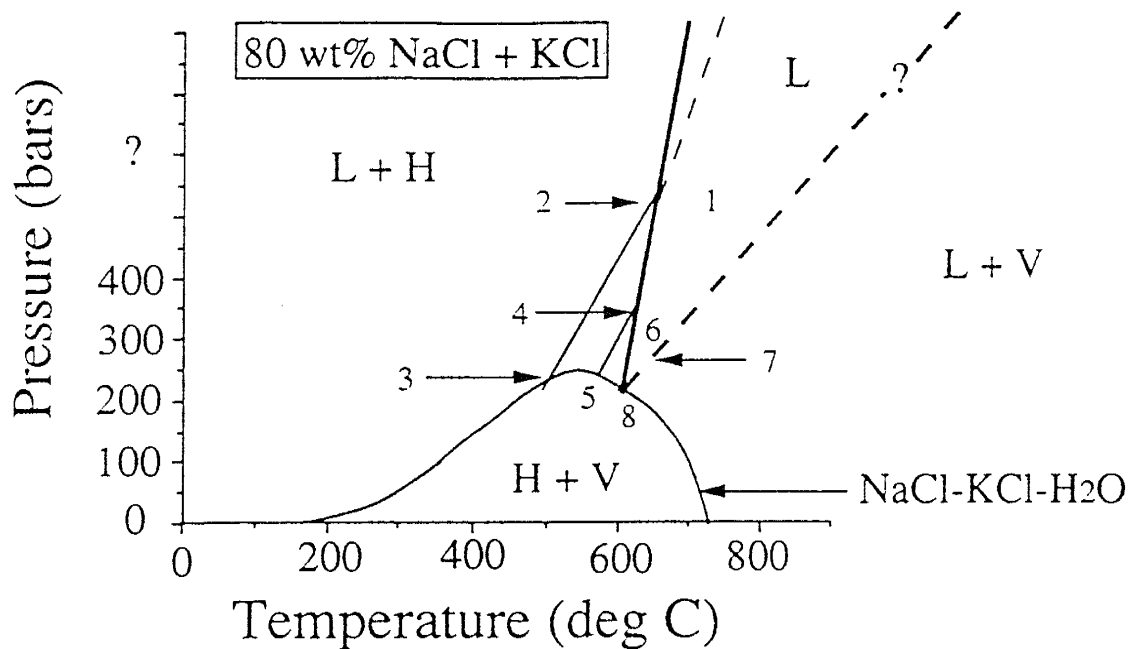
Path B) The original saline fluid (1) undergoes cooling and a pressure drop to (4). At (4) the fluid may become trapped, halite will begin to crystallize and the path will follow a constant volume liquid-solid curve downwards to (5). At (5) a vapor bubble will form. An inclusion will be similar to a path A inclusion, except the difference between  $T_m$  NaCl and  $T_h$  will be small.

For the 15% of type 1 inclusions which homogenize by vapor homogenization, Cloke and Kesler (1979) have discussed a possible path to explain these types of inclusions.

Path C) At (2) or (4), the fluid may drop in pressure to point (6). At (6) the fluid may become trapped and evolve along an isochore (not shown) towards (7), the L/L + V 80% isopleth. At (7) a vapor bubble will form. As the fluid cools, the cooling path will intersect the solubility curve (8) and halite will form. With further cooling along the solubility curve, other solid phases will form. This type of inclusion will have  $T_h$  greater than  $T_m$  NaCl.

About 15% of type 1 inclusions in quartz and fluorite have  $T_m$  NaCl about equal or equal to  $T_h$  ( $\pm 10^\circ\text{C}$ ).

Path D) The original saline fluid (1) may evolve towards the point (not shown) where the L/L + H and L + V/L solubility curves intersect the NaCl-KCl-H<sub>2</sub>O solubility curve. If a fluid becomes trapped at this point, halite and vapor will form and  $T_h$  is near or equal to  $T_m$  NaCl. Further cooling along the solubility curve will cause other solid phases to crystallize.



### Origin of Type 1 Fluid Inclusions

FIG. 32. Pressure-temperature diagram used to explain the possible origins for type 1 inclusions in quartz and fluorite. See text for explanation of different paths. Thick solid line is the L + H/L liquid-solid solubility line for 80 eq wt% NaCl + KCl, thick dashed line is the V + L/L liquid-vapor solubility curve for 80 eq wt% NaCl + KCl, thin solid lines are schematic representations of constant volume solubility curves (not an isochore), thin dashed line is a schematic isochore. Pressures are uncertain above 400 bars and are thus not shown.



The origin of type 2 inclusions can be explained in a similar manner. 25% of type 2 inclusions homogenize by halite dissolution. Two paths exist which may explain this behaviour, see Figure 33, are as follows.

Paths E and F) If a fluid does not become trapped at (2), the fluid may continue to cool isobarically to (9) or cool with a pressure drop to (10). At (9) or (10) the fluid may become trapped, halite will precipitate, and the inclusion will follow a constant volume liquid-solid curve towards the NaCl-KCl-H<sub>2</sub>O solubility curve (point 11 or 12) where vapor will form. Further cooling along the solubility curve will crystallize sylvite. This fluid is a lower salinity fluid, a type 2 inclusion fluid, and will consist of halite, sylvite, vapor and liquid with  $T_h$  less than  $T_m$  NaCl and a bulk salinity of 55 eq wt% NaCl + KCl.

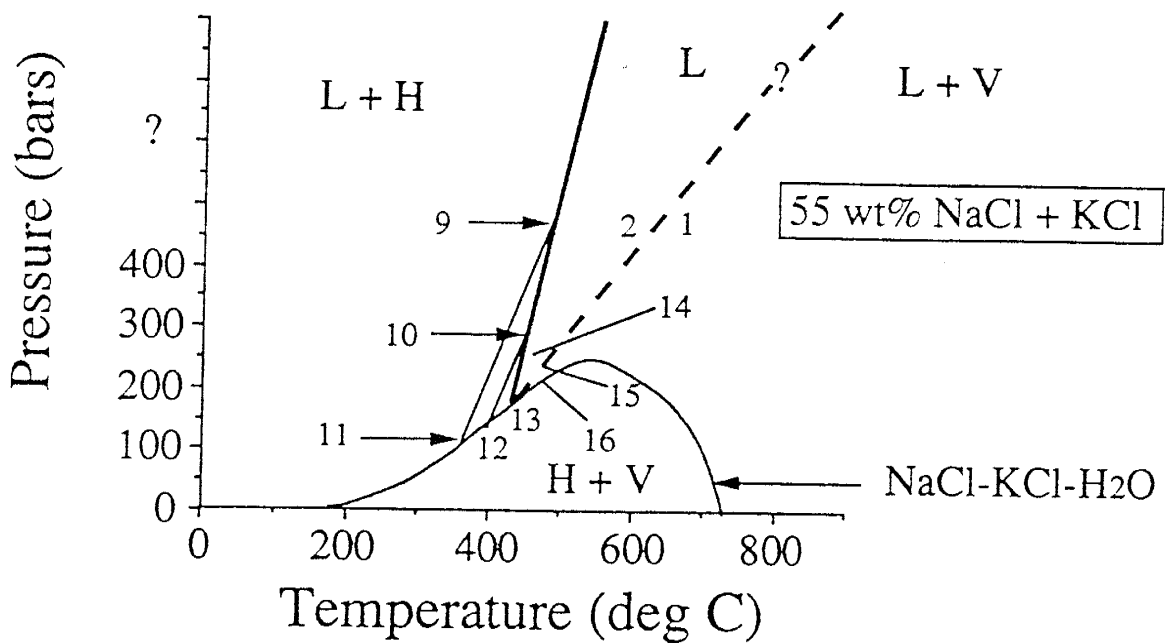
About 72% of type 2 inclusions have  $T_h$  nearly equal to or equal to  $T_m$  NaCl. A path which might explain this is (Fig. 33):

Path G) A fluid may become trapped at the intersection of the L + H/L and L/L + V solubility curves (13), in which case a vapor bubble and halite cube will form. Further cooling along the solubility curve will crystallize sylvite.

About 3% of the type 2 inclusions have  $T_h$  greater than  $T_m$  NaCl. This can be explained by the following path (Fig. 33):

Path H) A fluid at (9) or (10) may not become trapped and a pressure drop will cause this fluid to fall. At some point (14), the fluid may become trapped. Upon further cooling or a pressure drop or both, the fluid at (14) will move along an isochore and intersect the L 55%/L + V solubility curve (15) and a vapor bubble will form. Further cooling and intersection with the solubility curve (16) will cause halite to precipitate.

For type 2 inclusions, only halite and sylvite daughter minerals are present. The other daughter minerals (anhydrite, other chloride salts ...) are no longer



### Origin of Type 2 Fluid Inclusions

FIG. 33. Pressure-temperature diagram used to explain the possible origins for type 2 inclusions in quartz and fluorite. See text for explanation of different paths. Thick solid line is the L + H/L liquid-solid solubility line for 55 eq wt% NaCl + KCl, thick dashed line is the V + L/L liquid-vapor solubility curve for 55 eq wt% NaCl + KCl, thin solid lines are schematic representations of constant volume solubility curves (not an isochore). Pressures are uncertain above 400 bars and are thus not shown.

saturated in the type 2 fluids and therefore cannot form solid phases. As an example, for anhydrite [ reaction:  $\text{Ca}^{(+2)} + \text{SO}_4^{(-2)} \rightleftharpoons \text{CaSO}_4$  ] all or most of the  $\text{SO}_4$  or Ca may have been tied up as a daughter mineral in the type 1 fluid inclusions. By the time a type 2 fluid evolves, the deficient Ca or  $\text{SO}_4$  will cause the reaction to shift to the left (LeChatelier's Principle) and no anhydrite will form in a type 2 inclusion. Similar arguments can be applied to explain the lack of other daughter minerals in type 2 inclusions which were found in the type 1 inclusions.

The paths presented here represent inclusions with bulk compositions of 80 eq wt% NaCl + KCl ( typical type 1 inclusion) and 55 eq wt% NaCl + KCl (typical type 2 inclusion). Type 1 and 2 inclusions with different salinities have evolved by similar paths.

### **Origin of Type 3 Fluid Inclusions**

Although type 3 inclusions do not fall along the halite trend (they would plot in a field on Figure 28 represented by less than 12% KCl and between 30 to 55 wt% NaCl), they are believed to have originated in a similar manner to type 2 inclusions - by cooling and small pressure drops. As the original fluid continues along its fluid evolution path, a point will eventually be reached where the evolved fluid can no longer be saturated with respect to sylvite (see previous argument related to LeChatelier's Principle). At this point and beyond, inclusions will be represented by type 3 inclusions. Observed type 3 inclusions in quartz and fluorite have  $T_m$  NaCl greater than, equal to and less than  $T_h$ . Several possible paths can be explained to account for these behaviours. These paths would be similar to paths discussed for type 2 inclusions, except that the fluid can no longer be saturated with respect to

sylvite. Only one case will be discussed here, the case for  $T_m \text{ NaCl}$  greater than  $T_h$ . Refer to Figure 34.

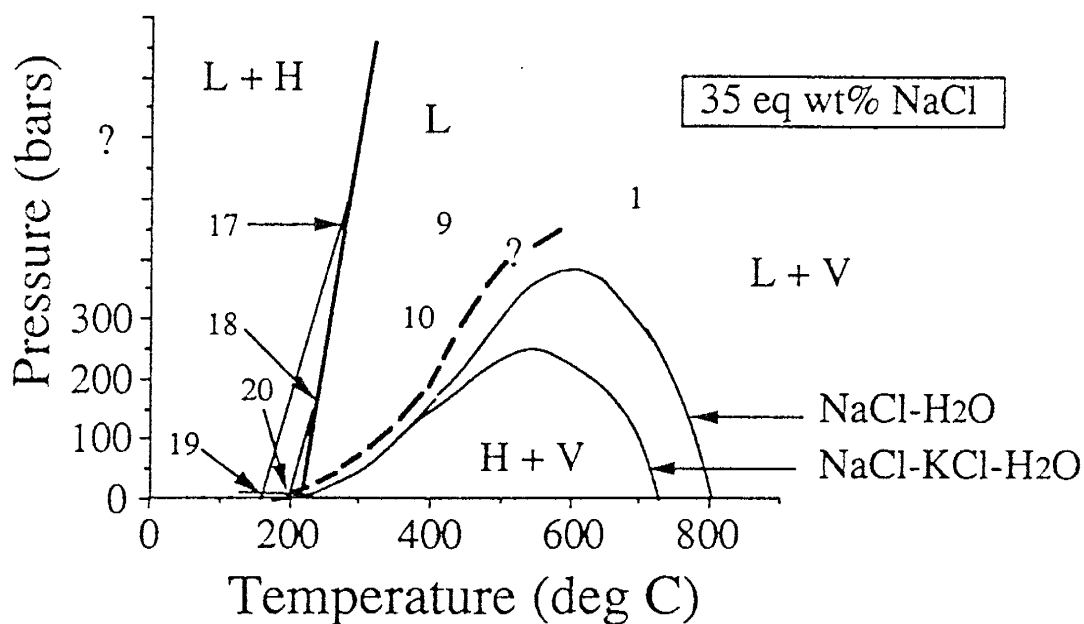
Paths I and J) If a fluid at (9) or (10) does not become entrapped, the fluid may evolve to (17) or (18) and become trapped. The trapped fluid will begin to crystallize halite, follow an imaginary constant volume liquid-solid curve in the NaCl-H<sub>2</sub>O system downward until it intersects with the NaCl-H<sub>2</sub>O solubility curve (19) or (20), where a vapor bubble will form. This inclusion will have a bulk salinity of 35 eq wt% NaCl and contain only halite, vapor and liquid.

#### **Origin of Type 4 Fluid Inclusions**

Type 4 inclusions plot away from the cooling trend observed by types 1, 2 and 3 inclusions for both quartz and fluorite (Figs. 26 and 27). It is believed that type 4 inclusions represent the influx of a meteoric water (which may be slightly saline from percolating through Permian sediments which contain evaporite sequences) into the cooling pluton and mixing with some of the evolved type 2 or 3 fluids. The amount of meteoric water influx into the Capitan pluton is assumed to be small compared to that of a typical porphyry copper deposit. The altered feldspars in the apex of the Capitan pluton also supports the presence of a meteoric water (V. McLemore, written comm., 1990).

#### **Summary of Fluid Inclusion Origins**

Based on the preceding discussion and the observed trends in Figures 26 and 27 : type 1 inclusions represent high-salinity, high-temperature brines exsolved from a crystallizing granitic melt; type 2 inclusions represent a cooling and evolved fluid from the original type 1 fluids; type 3 inclusions represent fluids from an even



### Origin of Type 3 Fluid Inclusions

FIG. 34. Pressure-temperature diagram used to explain the possible origins for type 3 inclusions in quartz and fluorite. See text for explanation of different paths. Thick solid line is the L + H/L liquid-solid solubility line for 35 eq wt% NaCl, thick dashed line is the V + L/L liquid-vapor solubility curve for 35 eq wt% NaCl, thin solid lines are schematic representations of constant volume solubility curves (not an isochore). Pressures are uncertain above 400 bars and are thus not shown.

further evolved and cooling fluid from the original type 1 fluids and; type 4 inclusions represent a mixture between a meteoric fluid and an evolved type 2 or 3 fluid.

## CHEMICAL COMPOSITION OF THE MINERALIZING FLUIDS

Analysis of daughter minerals in type 1 inclusions indicate the presence of titanite - a host mineral for REE's. The presence of titanite as a daughter phase in type 1 inclusions of quartz from the MTE prospect suggest that the fluids, represented by type 1 inclusions, carried at least some of the REE's. Also, type 1 inclusions in titanite are similar to those in the associated quartz. This is further evidence that REE's were transported in type 1 fluids. The actual means of REE transport in the type 1 fluids is beyond the scope of this paper and will be addressed only briefly. The high chlorinity of the type 1 inclusion fluids may indicate that chloride complexes with REE's could have been the means of hydrothermal transport in a high temperature - high salinity fluid. Fluoride has been known to form strong complexes with REE's (Bandorkin, 1961). Fluorite is present at most of the Th-U-REE deposits looked at in this study. It is possible that the REE's were transported from their source to the site of deposition as fluoride and possibly chloride complexes in fluids which are best represented by the type 1 inclusion fluids. Other unknown complexes could be involved in the transportation of the Th-U-REE's.

Fluid inclusion leachate solutions were found to contain significant amounts of Na, K, Ca, and Cl and lesser amounts of Fe, Mn, Mg, Zn, Ba and SO<sub>4</sub>. K/Na ratios from bulk analyses of inclusion fluids were found to range from 0.19 to 0.27. The lower K/Na ratios are interpreted to arise as a result of dilution of the type 1 fluids

with lower salinity type 4 inclusions. The actual K/Na ratios for the mineralizing fluids, 0.24 to 0.27 (Tables 4, 6), are therefore best represented by the crush-leach analyses from the MTE prospect. This prospect contains > 95% type 1 inclusions and thus dilution problems are at a minimum. In order to see if the mineralizing fluids were in equilibrium with the granitic rocks, the K/Na ratios for the MTE fluids were plotted (dashed lines) on a diagram, Figure 35, which illustrates the temperature dependence of K/Na ratios of fluids in equilibrium with granitic rocks (thick solid line). As mentioned in Rye and Haffty (1969), this curve shows only a generalized relation between K/Na in the fluid and temperature. The K/Na ratios for the MTE fluids plot along or near the curve, illustrating that the hydrothermal type 1 fluids were in contact with and at or near equilibrium with granitic rocks, hence showing further evidence that the fluids were magmatic fluids. From Figure 28, the K/Na ratios along the halite trend are plotted versus temperature (thin solid line) onto Figure 35. The segment X-Y represents the compositional field for type 1 fluids and segment Y-Z represents type 2 fluids. Based on microthermometry, type 1 fluids plot along or near the thick solid line, showing that the type 1 fluids are at or near equilibrium with granitic rocks at temperatures of 550°C ( $\pm 50^\circ\text{C}$ ). As temperature decreases along the thin solid line, the K/Na ratio increases showing that type 2 fluids are not in equilibrium with granitic rocks at lower temperatures. This non-equilibrium may be a kinetic effect - lowering the temperature decreases the rate of fluid-rock equilibration.

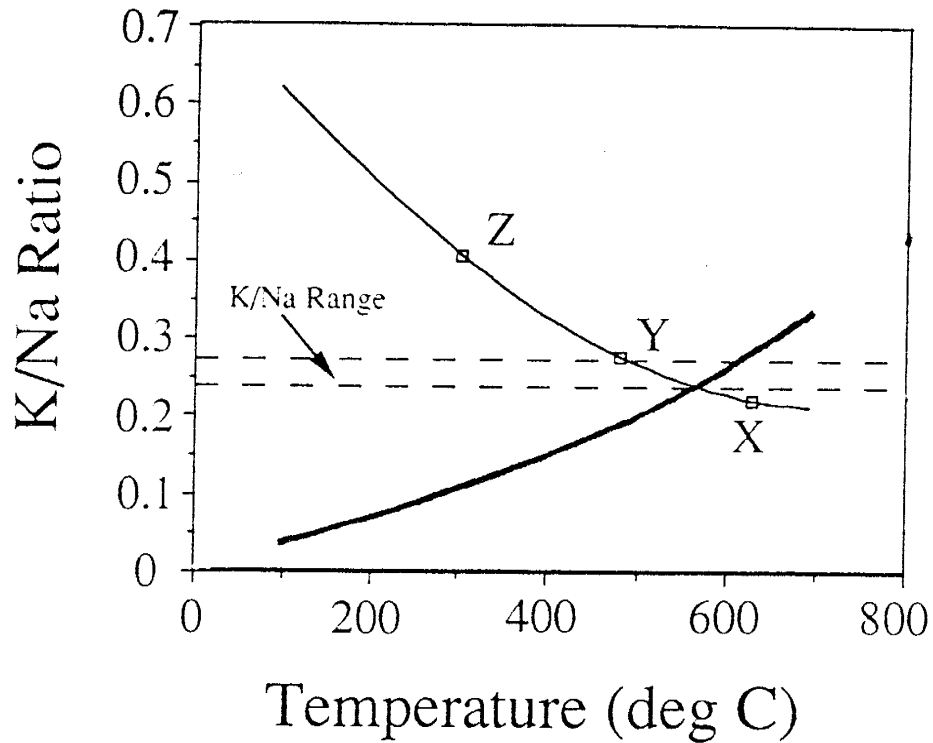


FIG. 35. Diagram showing range for K/Na ratios from MTE fluid inclusion leachates (dashed lines represent a K/Na range of 0.24 to 0.27). Thick solid curve shows the temperature dependence of K/Na ratios of fluids in equilibrium with granitic rocks [data from Rye and Haffty (1969), White (1968), and Ellis and Mahon (1967)]. Thin solid line shows K/Na ratios from the halite trend line of Figure 28. X-Y is the range for type 1 fluids along the halite trend. Y-Z is the range for type 2 fluids along the halite trend. See text for further discussion.



## DISCUSSION OF STABLE ISOTOPE DATA

### $\delta^{18}\text{O}$ of Quartz and Adularia and $\delta\text{D}$ of Inclusion Fluids in Vein Quartz

The observed fluid  $\delta^{18}\text{O}$  values of 7.08 to 8.09 o/oo for vein quartz fall within the range of accepted values for magmatic fluids ( $\delta^{18}\text{O}$  values of 5.5 to 9.5 o/oo; Sheppard, 1977). The  $\delta\text{D}$  values on inclusion fluids in quartz, -22 to -86 o/oo, also fall within and near the accepted values of magmatic fluids ( $\delta\text{D}$  values of -40 to -80 o/oo; Sheppard, 1977).

The isotopic compositions of the fluids responsible for the Th-U-REE deposits are depicted in Figure 30. The data for the MTE, Wee Three, Fuzzy Nut and CMX prospects plot within, slightly above and slightly below the magmatic water box. The isotopic data strongly imply that the vein quartz was deposited from fluids of magmatic origin. Similar  $\delta^{18}\text{O}$  values on vein quartz (Table 7), high temperatures (Figs. 7 to 23) and high salinities for the other Th-U-REE deposits looked at in this study suggest that the fluids responsible for the mineralized zones were of magmatic origin.

Other possible fluids which may account for the observed  $\delta\text{D}$  values of the inclusion fluids are meteoric waters. A study was undertaken to determine hydrogen isotope values of a suspected mid-Tertiary meteoric water from smoky quartz vein occurrences in the Sierra Blanca igneous complex, 30 km south-southwest of the Capitan Mountains. The quartz veins occur within a brecciated zone in a mid-Tertiary (25.8 Ma; Thompson, 1972) syenite porphyry. The mineralized zones are interpreted to have formed from heated meteoric waters which have circulated through the cooling syenite porphyry (Phillips et al., in prep.). Liquid plus vapor inclusions in the quartz indicate the fluids were 290 to 340°C

(vapor homogenization temperatures) and low in salinity (0.5 to 4 equiv wt% NaCl; D. Mitcheltree, written comm., 1990).  $\delta^{18}\text{O}$  values on the quartz are 3.50/00, corresponding to water values of -0.80/00.  $\delta\text{D}$  values of the inclusion fluids are near -370/00. The  $\delta\text{D}$  values are close to published data on clays from late-stage fluids (meteoric fluids) of the Santa Rita porphyry copper deposit in southwestern New Mexico ( $\delta\text{D}$  values are -500/00; Sheppard et al., 1969).

The  $\delta\text{D}$  values of the suspected meteoric waters and some of the more enriched  $\delta\text{D}$  values obtained from inclusion fluids in quartz from the Capitan deposits clearly overlap, Figure 30. Based on the high salinities and high temperatures of the Capitan inclusion fluids in quartz,  $\delta^{18}\text{O}$  water values from quartz and field relations, a meteoric fluid is not likely to be the source for the associated quartz mineralization.

The large variation observed in the  $\delta\text{D}$  values of inclusion fluids is presently poorly understood. Possible causes for the variation are: 1) contamination of type 1 fluids by dilution/mixing with a meteoric water, 2) isotopic fractionation of inclusion fluids by formation of hydrated daughter minerals. Contamination by mixing/dilution with a meteoric water ( $\delta\text{D} = -370/00$ , see previous section) would not produce  $\delta\text{D}$  values which plot in the lower portion of the magmatic water box. Isotopic fractionation in inclusion fluids by hydrated daughter minerals (ie.,  $\text{CaCl}_2 \cdot x\text{H}_2\text{O}$ ) may cause the  $\delta\text{D}$  values to plot out of the magmatic water box; however, it is thought that hydration effects would not cause the large variations observed in Figure 30 - the values should be effected by the same amount and thus plot together. Further studies on inclusion fluids [decrepitation of inclusions at high temperatures (which will theoretically release the hydrated water as well as free water) versus crushing only (which will theoretically release only free water)] may determine if hydration effects are in fact the cause of the variation.

The fluid  $\delta^{18}\text{O}$  values for adularia, 7.24 to 9.74 o/oo, fall within the accepted range of values for magmatic fluids. The close association of adularia and quartz (quartz and adularia commonly occur as intergrowths with one another) in the Th-U-REE deposits and the similar  $\delta^{18}\text{O}$  values that both minerals exhibit, suggests that the adularia has formed from the same fluid type that the quartz was deposited from.

### $\delta^{18}\text{O}$ of Pluton Whole Rocks and Vein Clasts

The observed  $\delta^{18}\text{O}$  values on whole rock Capitan pluton samples, 7.64 to 9.22 o/oo, fall within the range of normal igneous rock values ( $\delta^{18}\text{O}$  values of 6 to 10 o/oo; Taylor, 1978). No significant trend was seen traversing west to east across the Capitan pluton. Future studies will focus more closely on the meaning of the variation in the oxygen isotope data.

The observed  $\delta^{18}\text{O}$  values on whole rock samples of plutonic rock adjacent to selected veins, 8.49 o/oo for the Hot Hill prospect and 10.84 to 11.14 o/oo for the MTE prospect, and pluton clasts within the brecciated vein material, 8.23 to 9.68 o/oo, are similar to fresh Capitan pluton whole rock values. This implies that there was no significant late-stage alteration (ie., a large influx of meteoric water into the vein system as the hydrothermal system collapsed, as is common for the end stages of porphyry copper deposits ) associated with the mineralized zones.

### $\delta^{18}\text{O}$ and $\delta^{13}\text{C}$ of Vein Calcites

Observed  $\delta^{13}\text{C}$  values on white vein calcites range from -7.76 to -7.13 o/oo. The brown carbonates may be iron-stained calcites or possibly a mixture of calcite and siderite, their  $\delta^{13}\text{C}$  values range from -4.89 to -2.31 o/oo. The  $\delta^{13}\text{C}$  value for the pink calcite is -8.02 o/oo. These  $\delta^{13}\text{C}$  values fall within the range of a deep-

seated igneous carbon source (Barnes, 1979;  $\delta^{13}\text{C}$  values for most diamonds range from -2 to -9; Deines, 1980). Other possible sources for carbon could be one of the limestone members of the San Andreas Formation.  $\delta^{13}\text{C}$  values for one limestone member ranges from 1.48 to 2.32 o/oo. The large gap between the  $\delta^{13}\text{C}$  values of the limestone and the vein carbonates clearly indicates that the carbon of the vein carbonates was not directly derived from the limestone. It is therefore suggested that the carbon for the vein carbonates was derived from a magmatic fluid. The fluid  $\delta^{18}\text{O}$  values for vein calcites range from 14.16 to 15.37o/oo. The fluid  $\delta^{18}\text{O}$  values may indicate a mixture of two fluid types, a magmatic fluid and a meteoric fluid which has passed through Permian sedimentary rocks. At present, the meaning of the fluid  $\delta^{18}\text{O}$  values for the vein carbonates is poorly understood.

## SUMMARY AND CONCLUSIONS

This fluid inclusion and stable isotope study on REE and Th-U-REE deposits in the Capitan Mountains has shown that:

1. Four main types of fluids were evident, as determined by optical and microthermometric studies in quartz, fluorite, calcite and titanite. Type 1 inclusions are the most important of the four types and represent high temperature - high salinity fluids, Th and Tm NaCl > 600°C, bulk salinities up to 84 wt% NaCl + KCl; type 2 inclusions represent high to moderate temperature - high salinity fluids; type 3 inclusions represent moderate temperature - moderate salinity fluids and; type 4 inclusions represent lower temperature - lower salinity fluids.

2. All 4 types of inclusions can be explained by P-T phase equilibria, Th vs. salinity plots and NaCl-KCl-H<sub>2</sub>O ternary plots. Type 1 inclusions can best be

explained as being a high salinity fluid which has exsolved from a crystallizing granitic melt. Cooling of this highly saline fluid, followed by crystallization and subtraction of KCl-bearing halite from solution, will lead to the formation of the observed halite trend. Type 2 inclusions represent a cooling and evolved fluid from the original type 1 fluid. Type 2 inclusions also define the halite trend. Type 3 inclusions represent an even further evolved fluid from the original type 1 fluid. Type 4 inclusions represent the influx of a meteoric water into the cooling pluton and mixing with some of the evolved type 2 or 3 fluids.

3. For a given prospect, both quartz and fluorite contain type 1 inclusions. This suggests that the two minerals are cogenetic. For the MTE prospect, quartz and titanite contain type 1 inclusions and hence these two minerals must be cogenetic. This implies that quartz deposition was simultaneous with REE deposition.

4. Bulk crush-leach analyses on fluid inclusion leachates indicates that the fluid inclusion chemistry is complex. The fluids were found to contain significant amounts of Na, K, Ca and Cl and lesser amounts of Fe, Mg, Mn, Zn, Ba and SO<sub>4</sub>. The fluid inclusion chemistry may indicate that chloride complexes may be important for transporting REE's.

5. Pressures and depths of pluton emplacement and vein formation are estimated to occur between 300 to 400 bars and 1.2 to 1.6 km, respectively.

6. Oxygen isotopes on vein quartz and adularia and hydrogen isotopes on fluid inclusion waters in quartz suggest that the fluids responsible for the associated Th-U-REE deposits were derived from magmatic fluids.

7. Carbon isotopes on vein calcites suggest that the carbon was derived from a deep-seated igneous source.

In conclusion, field relations, petrologic, fluid inclusion microthermometry, fluid inclusion chemistry and stable isotope data indicate that the REE and Th-U-REE deposits in the Capitan Mountains were formed as a result of cracking of the outer carapace of the Capitan pluton during cooling, followed by the injection of exsolved high temperature - high salinity fluids from a crystallizing granitic melt into the brecciated and cracked zones. Type 1 inclusion fluids represent the main-stage, mineral-forming fluids. Type 2 and 3 inclusion fluids represent an evolved and cooling type 1 fluid. Type 4 inclusions represent a mixture of a meteoric water with an evolved type 2 or 3 fluid. These late-stage type 4 fluids contribute little, if any, to the mineralization events. A cartoon to help summarize the process of the Th-U-REE vein formation is shown in Figure 36.

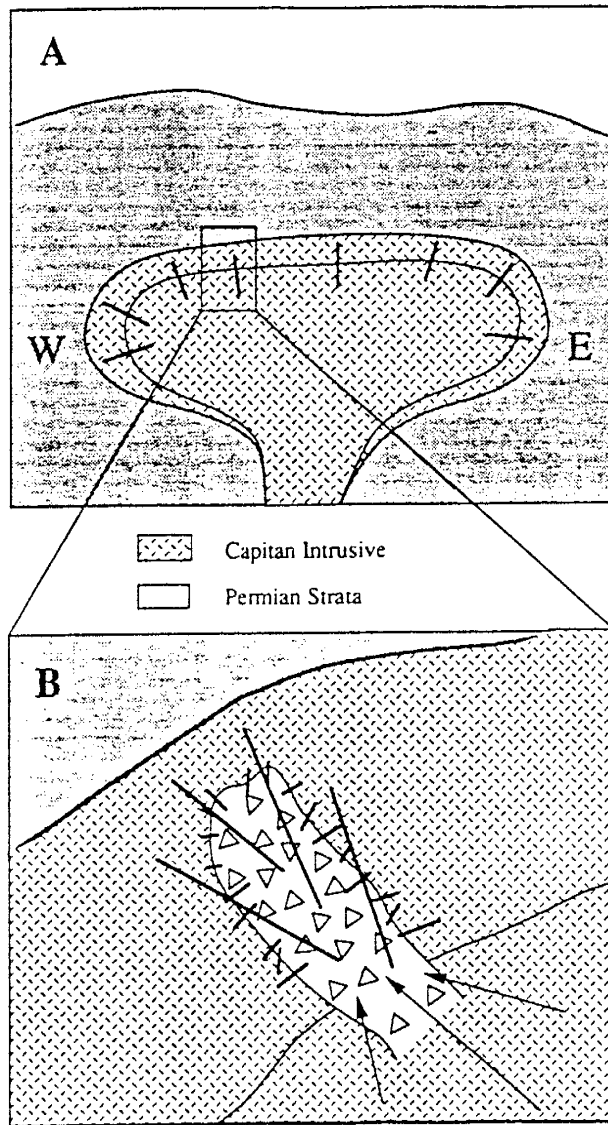


FIG. 36. Summary cartoon illustrating vein formation in the Capitan Mountains. Cross sections are oriented east-west. A) Illustration showing intrusion and emplacement of Capitan pluton in Permian sedimentary strata. The outer portion of the pluton illustrates the crystallization of the outer carapace. Brecciation and fracturing of the outer carapace occurs due to continued cooling and contraction of the pluton. Thick solid lines represent fracture/brecciated zones in the outer carapace of the pluton. B) Enlargement of A, showing brecciated/fractured zone. Solid lines represent fracture zones. As the outer carapace is brecciated, magmatic fluids from the inner magma chamber are exsolved into the newly created brecciated/fracture zones. These fluids are responsible for the associated mineralization and are best represented by type 1 fluid inclusions. As the mineralizing fluids cool, fluid evolution occurs which results in the formation of type 2 and 3 fluids.

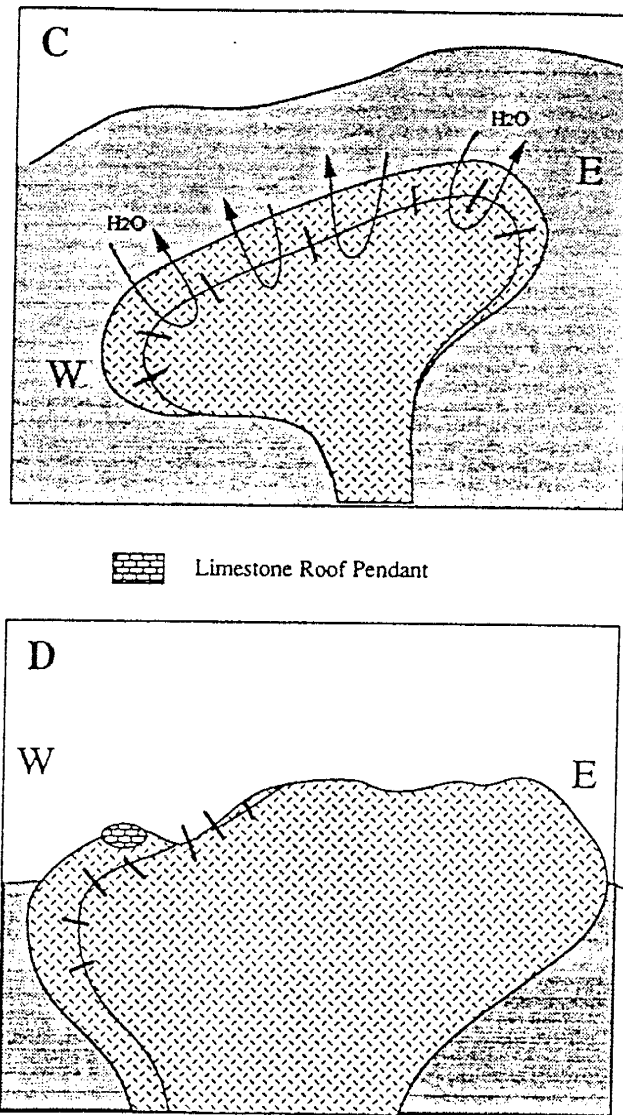


FIG. 36 (continued). C) As the pluton cools, the hydrothermal system collapses and late-stage meteoric fluids percolate through the Permian strata and infiltrate the brecciated/fractured zones. Type 4 fluids represent the mixing of these late-stage meteoric fluids with an evolved type 2 or 3 fluid. Tilting of the pluton occurs. D) Tilting of the surrounding region followed by erosion exposes the Capitan pluton and associated mineralized zones to its present day appearance. From the illustration, the east end has been eroded away more than the west end. It is believed that Th-U-REE mineralized zones similar to the west end occurrences were once present within the east end of the pluton, but have since been eroded away. Limestone roof pendant on west end of pluton.



**REFERENCES**

- Allen, M. S., 1988, The Capitan Pluton, New Mexico: An example of a zoned granitic magma chamber: *GSA Abstr. w. Prog.*, v. 20, no. 7, p. A 313.
- Allen, M. S. and McLemore, V. T., 1991, The geology and petrogenesis of the Capitan pluton, New Mexico: *New Mexico Geological Society Guidebook to the 42nd field conference*, in preparation.
- Altshuler, H. I., 1959, Capitan and Pedernal Prospects, New Mexico: A private consulting mining engineering report, 18p.
- Bandurkin, G. A., 1961, Behaviour of the rare earths in fluorine-bearing media: *Geochem. Intl.*, v. 2, p. 159-167.
- Barnes, H. L., ed., 1979, *Geochemistry of Hydrothermal Ore Deposits*: Wiley and Sons, New York, NY, 798 p.
- Bethke, P. M., and Rye, R. O., 1979, Environment of ore deposition in the Creede mining district, San Juan Mountains, Colorado: Part IV, Source of fluids from oxygen, hydrogen, and carbon isotope studies: *ECON. GEOL.*, v. 74, p. 1832-1851.
- Bloom, M. S., 1981, Chemistry of inclusion fluids: stockwork molybdenum deposits from Questa, New Mexico, and Hudson Bay Mountain and Endako, British Columbia: *ECON. GEOL.*, v. 76, pp. 1906 - 1920
- Bodine, M. W., 1956, Geology of Capitan coal field, Lincoln County, New Mexico: *N. Mex. State Bur. Mines Mineral Resources, Circ. 35*, 27p.
- Bodnar, R. J., Sterner, S. M., and Hall, D. L., 1989, SALTY: A FORTRAN program to calculate compositions of fluid inclusions in the system NaCl-KCl-H<sub>2</sub>O: *Comp. and Geoscience*, v. 15, p. 19-41.
- Borthwick, J. and Harmon, R. S., 1982, A note regarding ClF<sub>3</sub> as an alternative to BrF<sub>5</sub> for oxygen isotope analysis: *Geochim. et Cosmochim. Acta*, v. 46, p. 1665-1668.
- Bottrell, S. H., Yardley, B., and Buckley, F., 1988, A modified crush-leach method for the analysis of fluid inclusion electrolytes: *Bull. Mineral.*, v. 111, p. 279-290.
- Brown, P. E., 1989, FLINCOR: A microcomputer program for the reduction and investigation of fluid-inclusion data: *Am Mineral.*, v. 74, p. 1390-1393.

- Brown, P. E., and Lamb, W. M., 1989: P-V-T properties of fluids in the system  $H_2O \pm CO_2 \pm NaCl$ : New graphical presentations and implications for fluid inclusion studies: *Geochim. et Cosmochim. Acta*, v. 53, p. 1209-1221.
- Burrows, D. R., and Spooner, E. T. C., 1987, Generation of a magmatic  $H_2O - CO_2$  fluid enriched in Mo, Au, and W within an Archean sodic granodiorite stock, Mink Lake, Northwestern Ontario: *ECON. GEOL.*, v. 82, p. 1931-1957.
- Chapin, C. E., Chamberlin, R. M., Osburn, G. R., White, D. W., and Sanford, A. R., 1978, Exploration framework of the Socorro geothermal area, New Mexico: New Mexico Geological Society, Special Publication no. 7, p. 115-129.
- Cloke, P. L., and Kesler, S. E., 1979, The halite trend in hydrothermal solutions: *ECON. GEOL.*, v. 74, p. 1823-1831.
- Coleman, M. L., Shepherd, T. J., Durham, J. J., Rouse, J. E., and Moore, G. R., 1982. Reduction of water with zinc for hydrogen isotope analysis: *Anal. Chem.* v. 54, p. 993-995.
- Collins, G., 1956, Thorium occurrences in the Capitan Mountains area, Lincoln County, New Mexico: Technical Memorandum Report DA0-4-TM-1, U.S. Atomic Energy Commission, Division of Raw Materials, Albuquerque Branch Office, 11p.
- Deines, P., 1980, The carbon isotopic composition of diamonds, relationship to diamond shape, color, occurrence and vapor composition: *Geochim. et Cosmochim. Acta*, v. 37, p. 1707-1733.
- Ellis, A. J., and Mahon, W. A., 1967, Natural hydrothermal systems and experimental hot water/rock interactions (Pt. 2): *Geochim. et Cosmochim. Acta*, v. 31, p. 519-538.
- Erwood, R. J., Kesler, S. E., and Cloke, P. L., 1979, Compositionally distinct, saline hydrothermal solutions, Naica Mine, Chihuahua, Mexico: *ECON. GEOL.*, v. 74, p. 95-108.
- Friedman, I., and O'Neil, F. R., 1977, Compilation of stable isotope fractionation factors of geochemical interest: U. S. Geol. Survey Prof. Paper 440-KK, 12 p.
- Griswold, G. B., 1964, Mineral resources of Lincoln County: New Mexico Geological Society Guidebook, Fifteenth Field Conference, Ruidoso Country, p. 148-151.
- Hall, W. E., Friedman, I., and Nash, J. T., 1974, Fluid inclusion and light stable isotope study of the Climax Molybdenum deposits, Colorado: *ECON. GEOL.*, v. 69, p. 884-901.
- Hanson, T., 1989, Mina Tiro Estrella: *Mineralogical Record*, v. 20, p. 51-53.

- Harner, C. M., and Kelley, V. C., 1963, Reconnaissance of iron resources in New Mexico: U. S. Bureau of Mines, Info. Circ. 8190, 112p.
- Keevil, N. B., 1942, Vapor pressures of aqueous solutions at high temperatures: *Am. Chem. Soc. J.*, v. 64, p. 841-850.
- Kelley, V. C., 1952, Origin and pyrometamorphic zoning of the Capitan iron deposits, Lincoln County, New Mexico: *ECON. GEOL.* v. 47, p. 64-83.
- Kelley, V. C., 1971, Geology of the Pecos country, southeastern New Mexico: New Mexico Bureau of Mines and Mineral Resources Memoir 24, 75pp.
- Kelly, W. C., and Rye, R. O., 1979, Geologic, fluid inclusion, and stable isotope studies of the tin-tungsten deposits of Panasqueira, Portugal: *ECON. GEOL.*, v. 74, p. 1721-1819.
- Klein, C. and Hurlbut, C. S., 1985, *Manual of Mineralogy*: Wiley and Sons, New York, NY, 596pp.
- Landis, G. P., and Rye, R. O., 1974, Geologic, fluid inclusion, and stable isotope studies of the Pasto Bueno tungsten-base metal ore deposit, northern Peru: *ECON. GEOL.*, v. 69, p. 1025-1059.
- Larson, P. B., 1987, Stable isotope and fluid inclusion investigations of epithermal vein and porphyry molybdenum mineralization in the Rico mining district, Colorado: *ECON. GEOL.*, v. 82, p. 2141-2157.
- Matsuhisa, Y., Goldsmith, J. R., and Clayton, R. N., 1979, Oxygen isotope fractionation in the system quartz-albite-anorthite-water: *Geochim. et Cosmochim. Acta*, v. 43, p. 1131-1140.
- McCrea, J. M., 1950, The isotopic chemistry of carbonates and a paleotemperature scale: *J. Chem. Phys.*, v. 18, p. 849 - 857.
- McLemore, V. T., 1983, Uranium and Thorium occurrences in New Mexico: New Mexico Bureau of Mines and Mineral Resources Open-File Report 183.
- McLemore, V. T., and Phillips, R. S., (in press), Mineral Resources of the Capitan Mountains: New Mexico Geological Society, Guidebook to the 42nd Field Conference, in preparation.
- Paterson, C. J., Uzunlar, N., Groff, J., and Longstaffe, F. J., 1989, A view through an epithermal-mesothermal precious metal system in the northern Black Hills, South Dakota: A magmatic origin for the ore-forming fluids: *ECON. GEOL. Monograph* 6, *The Geology of Gold Deposits: The Perspective in 1988*, p. 564- 570.

- Phillips, R. S., Mitchell, D. B., Campbell, A. R. and Hanson, T., in prep, Geochemistry of smoky quartz veins from the Sierra Blanca igneous complex, New Mexico: New Mexico Geological Society, Guidebook to the 42nd Field Conference, in preparation.
- Quan, R. A., Cloke, P. L., and Kesler, S. E., 1987, Chemical analysis of halite trend inclusions from the Granisle porphyry copper deposit, British Columbia: ECON.GEOL., v. 82, p. 1912-1930.
- Ravich, M., and Borovaya, F., 1949, Phase equilibria in ternary water-salt systems at elevated temperatures: *Izvest. Sektora. Fiz. Khim. Anal., Inst. Obshch. i Neorg. Khim., Akad. Nauk SSSR*, v. 19, p. 68-81. ( in Russian; translated in *Fluid Inclusion Res.*, 1977, -- *Proc. of COFFI*, v. 10, p. 330-340.)
- Richards, J. P., and Spooner, E. T. C., 1989, Evidence for Cu-(Ag) mineralization by magmatic- meteoric fluid mixing in Keweenawan fissure veins, Mamainse Point, Ontario: ECON. GEOL., v. 84, p. 360-385.
- Roedder, E., 1971, Fluid inclusion studies on the porphyry-type ore deposits at Bingham, Utah, Butte, Montana, and Climax, Colorado: ECON. GEOL., v. 66, p. 98-120.
- Roedder, E., 1984, ed., *Fluid Inclusions: Reviews in Mineralogy* volume 12, Mineralogical Society of America, 646 p.
- Roedder, E., and Bodnar, R. J., 1980, Geologic pressure determinations from fluid inclusion studies: *Ann. Rev. Earth Planet. Sci.*, v. 8, p. 263-301.
- Rye, R. O., 1966, The carbon, hydrogen, and oxygen isotopic composition of the hydrothermal fluids responsible for the lead-zinc deposits at Providencia, Zacatecas, Mexico: ECON. GEOL., v. 61, p. 1399-1427.
- Rye, R., O., and Haffty, J., 1969, Chemical composition of the hydrothermal fluids responsible for the lead-zinc deposits at Providencia, Zacatecas, Mexico: ECON. GEOL., v. 64, p. 629-643.
- Rye, R. O., and Sawkins, F. J., 1974, Fluid inclusion and stable isotope studies on the Casapalca Ag-Pb-Zn-Cu deposit, Central Andes, Peru: ECON. GEOL., v. 69, p. 181-205.
- Sheppard, S. M. F., 1977, The identification of the origin of ore-forming solutions by the use of stable isotopes: *Volcanic Processes in Ore Genesis*, Inst. of Mining and Metallurgy and the Geol. Soc. of London, p. 25-41.
- Sheppard, S. M. F., and Gustafson, L. B., 1976, Oxygen and hydrogen isotopes in the porphyry copper deposit at El Salvador, Chile: ECON. GEOL., v. 71, p. 1549-1559.

- Sheppard, S. M. F., and Taylor, H. P., Jr., 1974, Hydrogen and oxygen isotope evidence for the origins of water in the Boulder Batholith and the Butte ore deposits, Montana: *ECON. GEOL.*, v. 69, p. 926-946.
- Sheppard, S. M. F., Nielsen, R. L., and Taylor, H. P., Jr., 1969, Oxygen and hydrogen isotope ratios of clay minerals from porphyry copper deposits: *ECON. GEOL.*, v. 64, p. 755-777.
- Sheppard, S. M. F., Nielsen, R. L., and Taylor, H. P., Jr., 1971, Hydrogen and oxygen isotope ratios in minerals from porphyry copper deposits: *ECON. GEOL.*, v. 66, p. 515-542.
- Sourirajan, S., and Kennedy, G. C., 1962, The system H<sub>2</sub>O-NaCl at elevated temperatures and pressures: *Am J. Sci.*, v. 260, p. 115-141.
- Sterner, S. M., Hall, D. L., and Bodnar, R. J., 1988, Synthetic fluid inclusions: V. Solubility relations in the system NaCl-KCl-H<sub>2</sub>O under vapor-saturated conditions: *Geochim. et Cosmochim. Acta*, v. 52, p. 989-1005.
- Taylor, H. P., Jr., 1978, Oxygen and hydrogen isotope studies of plutonic granitic rocks: *E. Planet. Sci. Lett.*, v. 38, p. 177-210.
- Taylor, H. P. and Epstein, S., 1962, Relationship between  $\frac{^{18}\text{O}}{^{16}\text{O}}$  ratios in coexisting minerals of igneous and metamorphic rocks, Part 1: Principles and experimental results: *Bull. Geol. Soc. Am.*, v. 73, p. 461 - 480.
- Thompson, T. B., 1972, Sierra Blanca Igneous Complex, New Mexico: *GSA Bull.*, v. 83, p. 2341-2356.
- Thom, P. G., 1988, Fluid inclusion and stable isotope studies at the Chicote tungsten deposit, Bolivia: *ECON. GEOL.*, v. 83, p. 62-68.
- Tuftin, S., 1984, Mineral investigation of the Capitan Mountains Wilderness Area, Lincoln County, New Mexico: United States Department of the Interior, Bureau of Mines, Open-File Report MLA 20-84, 20 p.
- White, D. E., 1968, Environments of generation of some base-metal ore deposits: *ECON. GEOL.*, v. 63, p. 301-335.
- Willis, M., Campbell, A., and Phillips, R., 1989, High salinity fluids associated with allanite mineralization, Capitan Mountains, New Mexico: *GSA Abstr. w. Prog.*, v. 21, p. A 287.
- Wilson, J. W. J., Kesler, S. E., Cloke, P. L., and Kelly, W. C., 1980, Fluid inclusion geochemistry of the Granisle and Bell porphyry copper deposits, British Columbia: *ECON. GEOL.*, v. 75, p. 45-61.

**APPENDIX A****CHEMICAL, TEXTURAL AND MINERALOGICAL  
DESCRIPTIONS FOR REPRESENTATIVE SAMPLES OF THE  
CAPITAN PLUTON**

Textural and mineralogical descriptions based on the work of V. T. McLemore (written comm., Nov. 1990) are given for the three textural zones (granophyre, aplite and porphyry) of the Capitan pluton. Representative chemical analyses for several Capitan pluton samples (V. T. McLemore, written comm., Nov. 1990) are listed in Table A 1. Samples were analyzed at the New Mexico Bureau of Mines and Mineral Resources X-ray lab.

**Granophyric Granite**

The following descriptions are based on point count samples of 3 samples (V. T. McLemore, written comm., 1990). The mineralogy consists of quartz 22-28%, Kspar 20-25%, grains with graphic texture (1/2 quartz, 1/2 feldspar) 25-28%, plagioclase 10-24%, biotite <2%, zircon <3%, apatite <1%, also <1% titanite, magnetite, hematite (alteration). The granophyric granites are fine-grained, equigranular to slightly porphyritic, contain micromiarolites and consist of feldspars which are typically altered to sericite/clay/chlorite.

**Aplitic Granite**

Based on point counts of 2 samples (V. T. McLemore, written comm., 1990). Mineralogy consists of quartz 23-26%, Kspar 43-48%, graphic textures <5%, plagioclase 10-15%, biotite 2-4%, zircon <3%, <1% apatite, titanite, magnetite, hematite, hornblende. The aplitic granites are fine-grained, equigranular and contain fresher feldspars.

Porphyritic Granite (not a porphyry)

Based on estimates (V. T. McLemore, written comm., 1990). Mineralogy consists of quartz 20-25%, Kspar 40-50%, plagioclase 10-20%, biotite <5%, zircon <3%, <2% apatite, titanite, magnetite, hornblende, monazite, allanite. Samples exhibit crystal aggregates of biotite, albite phenocrysts often rimmed by Kspar, feldspar and quartz phenocrysts forming a porphyritic texture.

TABLE A 1

## Representative Chemical Analyses for Capitan Pluton Samples

	<u>CM 228</u>	<u>CM 225</u>	<u>CM 103</u>	<u>CM 100</u>	<u>CM 249</u>	<u>CM 293</u>	<u>CM 289</u>	<u>CM 241</u>
SiO <sub>2</sub>	75.3	75.4	75.7	73.7	73.2	72.3	69.0	73.4
TiO <sub>2</sub>	0.16	0.18	0.18	0.25	0.27	0.30	0.38	0.23
Al <sub>2</sub> O <sub>3</sub>	13.2	13.5	13.3	13.9	14.2	14.5	14.9	13.7
Fe <sub>2</sub> O <sub>3</sub>	1.20	1.14	1.31	1.81	1.94	1.99	2.24	1.83
MgO	0.01	0.00	0.03	0.37	0.04	0.13	0.28	0.06
CaO	0.27	0.15	0.18	0.30	0.49	0.56	0.88	0.15
Na <sub>2</sub> O	4.55	6.40	5.63	4.86	4.90	4.67	4.25	4.97
K <sub>2</sub> O	4.94	2.21	3.79	5.05	5.48	5.70	5.81	5.20
MnO	0.01	0.01	0.03	0.05	0.06	0.03	0.07	0.05
P <sub>2</sub> O <sub>5</sub>	0.01	0.01	0.01	0.02	0.01	0.02	0.05	0.02
LOI	0.32	0.39	0.34	0.34	0.35	0.38	0.88	0.22
Totals	99.97	99.38	100.50	100.65	100.94	100.58	98.74	99.83
Texture	(1)	(1)	(2)	(1)	(3)	(3a)	(3)	(1)

	<u>CM 243</u>	<u>CM 246</u>	<u>CM 280</u>	<u>CM 211</u>	<u>CM 221</u>	<u>CM 104</u>	<u>CM 242</u>	<u>CM 301</u>
SiO <sub>2</sub>	72.4	73.1	74.3	69.9	73.7	74.8	74.0	72.4
TiO <sub>2</sub>	0.29	0.26	0.38	0.44	0.27	0.29	0.24	0.28
Al <sub>2</sub> O <sub>3</sub>	14.0	14.0	15.8	14.9	14.3	13.9	13.9	14.5
Fe <sub>2</sub> O <sub>3</sub>	1.84	1.80	0.47	2.35	1.20	1.16	1.77	1.87
MgO	0.14	0.05	0.03	0.22	0.00	0.05	0.01	0.03
CaO	0.49	0.41	0.59	0.98	0.16	0.38	0.19	0.53
Na <sub>2</sub> O	5.01	4.95	6.60	4.43	4.91	6.34	5.06	4.57
K <sub>2</sub> O	5.37	5.23	3.46	5.59	5.25	2.89	5.00	5.31
MnO	0.03	0.04	0.00	0.07	0.01	0.05	0.01	0.03
P <sub>2</sub> O <sub>5</sub>	0.05	0.01	0.00	0.06	0.02	0.00	0.01	0.04
LOI	0.30	0.35	0.52	0.69	0.52	0.57	0.50	0.65
Totals	99.92	100.20	102.15	99.63	100.34	100.43	100.59	100.31
Texture	(2)	(3)	(3a)	(3)		(2b)	(1)	(3)

(1) granophyre (2) aplite (3) porphyry (a) slightly altered (b) near prospect

Total Fe calculated as Fe<sub>2</sub>O<sub>3</sub>

LOI = loss on ignition

Data from V. T. McLemore (written comm., 1990)



## APPENDIX B

### INDIVIDUAL PROSPECT DESCRIPTIONS

Individual REE and Th-U-REE prospects are described in the following section. The descriptions are based on field observations. Refer to Figure 1 for prospect localities. Textural descriptions (granophyre, aplite and porphyry) are from V. T. McLemore (pers. comm., 1990) and are noted in parantheses.

#### BS Prospect

Location: NE 1/4 SE 1/4, Section 21; T8S, R15E; Capitan Pass Quad, 7 1/2' topographic map.

Elevation: 2120 meters (6960 feet).

Description: A shallow pit, 15m x 5m, at the base of the Capitan Mountains. Pit appears to be filled in by overburden. All samples are dump/float material which consist of small, clear quartz veins up to 1.5 cm cutting through the alkali granite (aplite). No visible outcrop. Only other minerals noted in dump material are adularia and iron oxide stains on quartz.

#### CM 104 Prospect

Location: NE1/4 SE1/4, Section 6; T8S, R16E; Encinoso Quad, 7 1/2' topo map.

Elevation: 2225 to 2286 meters (7300 to 7500 feet).

Description: Series of bulldozer cuts in outcrop of alkali granite (aplite) exposing fractured material. Small quartz stringers with adularia cutting through the alkali granite. Samples consist of dump material containing quartz and adularia coating fractured surfaces and as veinlets cutting alkali granite.

CM 235 Prospect

Location: SE1/4 NE1/4, Section 31; T7S, R15E; Jacob Springs Quad, 7 1/2' topographic map.

Elevation: 2384 meters (7820 feet).

Description: A small pit, 5 x 5 x 1m, in fractured alkali granite (granophyre). Prospect occurs on top of northwestern Capitan Mountains. Visible vein minerals consist of clear quartz and purple fluorite. Quartz occurs as small, euhedral crystals lining fractures and filling vugs. Fluorite occurs as small cubes and as massive material filling vugs. Minor amounts of iron staining are associated with the brecciated vein material.

CMX Prospect

Location: SW1/4 SE1/4, Section 15; T8S, R15E; Capitan Pass Quad, 7 1/2' topographic map.

Elevation: 2500 meters (8200 feet).

Description: Veins cutting fractured alkali granite (granophyre). Prospect occurs within an outcrop on a ridge. Visible vein minerals consist of smoky and clear quartz, adularia, clay minerals and Fe-Mn oxides. Quartz occurs as massive material forming 0.5 to 2 cm veins and as euhedral crystals up to 1.5 cm lining open spaces in the massive vein quartz. Adularia occurs as euhedral crystals lining fractured surfaces along the vein-pluton contact and as massive material intergrown with the massive vein quartz. The vein trends roughly east-west and can be traced for up to 50 m.

CPU-1 Prospect

Location: SE1/4 SE1/4, Section 33; T7S, R15E; Encinoso Quad, 7 1/2' topographic map.

Elevation: 2210 meters (7250 feet).

Description: A 20 x 20 x 10 m outcrop block of brecciated alkali granite (granophyre) on the northwest flank of the Capitan Mountains. Visible minerals consist of green fluorite, adularia, Mn-Fe oxides and trace amounts of quartz. Fluorite is the dominant mineral and occurs as massive vein-filling material and as cubes up to 3 cm filling vugs. Adularia occurs as euhedral crystals lining fractured surfaces. Quartz occurs as small crystals lining fractures in the brecciated alkali granite. The Mn-Fe oxides occur as surface stains on the brecciated material.

CPU-2 Prospects

Location: E1/2 SW1/4, Section 33; T7S, R15E; Encinoso Quad, 7 1/2' topographic map.

Elevation: 2255 to 2316 meters (7400 to 7600 feet).

Description: Two brecciated fissure veins exposed by trenches cut into the alkali granite (granophyre), within a canyon on the northwest flank of the Capitan Mountains. Both trenches are roughly 15 m in length, 2 m in width and 5 m in depth. Both veins are oriented NNE-SSW and dip nearly vertical. A system of joints/fractures parallel the veins. The average width for the mineralized portion is about 0.5 m. The main parts of the veins are strongly hematized. Visible vein minerals consist of smoky and clear quartz, adularia, Fe-Mn oxides, fluorite and clay minerals. Quartz occurs as euhedral crystals lining the brecciated parts of the alkali granite and as massive vein-filling material. Adularia is found as euhedral crystals lining fractures in the brecciated material. Fluorite occurs as small, broken

cubes and as massive material lining fractures and filling vugs within the main part of the veins.

#### Fuzzy Nut Prospect

Location: SW1/4 NW1/4, Section3; T8S, R15E; Encinoso Quad, 7 1/2' topographic map.

Elevation: 2271 meters (7450 feet).

Description: A shallow pit, 15 x 5 m, cut into brecciated alkali granite (granophyre), near a saddle. Visible vein minerals consist of clear quartz, purple fluorite, goethite, maghemite/hematite, calcite, pyrolusite, garnet, apatite, unknown brown nodular masses and clay minerals. Quartz occurs as massive material filling fractures in brecciated alkali granite. Fluorite occurs as massive material filling open spaces. Maghemite/hematite occurs as massive vein filling material in brecciated alkali granite. Calcite occurs as a late-stage, white, crystalline material coating brown nodular masses. Goethite occurs as small masses filling vugs in the vein material. Garnet and apatite are found as euhedral crystals lining fractured surfaces in the brecciated material. Quartz and maghemite are the dominant minerals.

#### Hopeful (HC) Prospect

Location: SE1/4 SW1/4, Section 17; T8S, R15E; Capitan Pass Quad, 7 1/2' topographic map.

Elevation: 2255 meters (7400 feet).

Description: A small pit, 5 m long, 2 m wide and 1 m deep, exposed in highly fractured alkali granite (granophyre or aplite) near a small canyon on a southwest flank of the Capitan Mountains. East-west fractures (joints ?) are very abundant.

A clay-filled fracture striking roughly NW cuts the east-west trending fractures. Visible vein minerals in the fracture consist of hematite, purple fluorite, calcite, brown nodular masses and clay minerals. Hematite occurs as stains on the fractured surfaces. Fluorite occurs as small, broken cubes lining the fractured vein. Calcite occurs as a late-stage, white crystalline material coating brown nodular masses. The nodular masses may be the host for the REE's. No quartz was observed.

#### Hot Hill Prospect

Location: SW1/4 SW1/4, Section 23; T8S, R15E; Capitan Pass Quad, 7 1/2' topographic map.

Elevation: 2286 meters (7500 feet).

Description: The Hot Hill prospect consists of a main trench cut into the alkali granite (granophyre; near the granophyre-aplite transition zone) and several smaller cuts in the alkali granite just west of the main pit. The prospect occurs on a small knob, along a ridge. The main trench is oriented with the open face towards the east and the back of the trench oriented to the west. The vein in the main trench trends roughly east-west, dips nearly vertical and can be traced for about 50 m. The most intense part of the mineralization in the main trench consists of a strongly brecciated zone that is 0.2 to 0.6 m wide. The breccia consists of alkali granite clasts, ranging from 10 cm to < 1 cm, which are held together by red iron oxide cements. Visible minerals in the main trench are smoky and clear quartz, fluorite, calcite, brown "earthy" tabular masses, adularia, Fe oxides, siderite (?) and clay minerals. The quartz occurs as small, euhedral crystals in vugs. The fluorite occurs as broken cubes within open spaces along fractured zones and as massive material filling vugs. Adularia is found coating surfaces on fractured vein

material. Calcite is a late-stage, white crystalline mineral found as overgrowths on the brown nodular to tabular masses and as small veinlets within the most intensely brecciated part of the trench. The brown tabular masses are reactive with hydrochloric acid, suggesting the brown mass to be some type of iron-stained carbonate. The Fe oxides (hematite, goethite, limonite) occur as cementing material within the main trench. Trace amounts of gold were assayed from the main part of the breccia zone.

Directly west of the main trench are two smaller trench cuts in the alkali granite. The two cuts both contain smoky quartz veins/veinlets up to 2 cm cutting the fractured alkali granite. Adularia and Fe oxides are associated with the quartz veins. The veins in the smaller cuts trend roughly east-west and are probably part of the same vein system that the main trench is centered on.

#### Koprian Springs Prospect

Location: NW1/4 SW1/4, Section 11; T8S, R15E; Encinoso Quad, 7 1/2' topographic map.

Elevation: 2470 meters (8100 feet).

Description: A small pit in alkali granite (aplite), which is located on a ridge. The pit is 5m long, 2 m wide and 3 m deep. The fracture system containing the vein trends roughly east-west and dips nearly vertical. Brecciation of the alkali granite occurs on the backwall (south side) of the pit. Visible minerals in the brecciated zone are purple to clear fluorite, adularia, clear quartz, hematite and clay minerals. The fluorite occurs as small, broken cubes which are found within vuggy zones and along the fractures of the brecciated zone. Quartz and adularia occur as crystals along fractures. Hematite occurs as an oxide staining on the surfaces of the brecciated material.

### McCory Prospects

Location: NW1/4, Section 1; T8S, R15E; Encinos o Quad, 7 1/2' topographic map.

Elevation: 2255 to 2377 meters (7400 to 7800 feet).

Description: The McCory prospects consist of two groups ( East and West groups). Both groups are located on the west flanks of ridges. The East and West groups are separated by a small canyon. The vein system for both groups trend roughly east-west and dips steeply. The orientation of the vein implies that the East and West groups are located on the same vein system.

The East group consists of a series of bulldozer cuts and small trenches in the fractured alkali granite (aplite; close to aplite-porphyry gradational zone). The exposed vein system is strongly brecciated and hematized. The vein is up to 2 m in width in some places. Hematite is the dominant mineral and occurs as intense stains on the brecciated vein material and as specular hematite coating fractured surfaces. Two small, < 3mm, smoky quartz crystals and two unidentifiable, black tabular minerals (allanite ?) were found in vugs at the lower part of the East group prospects.

The West group consists of four small pits and bulldozer cuts in the fractured alkali granite. Parts of the vein system are strongly brecciated and hematized, similar to the East group. Vein widths vary from < 1 cm to 1.5 m. Visible minerals include fluorite, hematite, adularia and clay minerals. Fluorite occurs as broken cubes in the open spaces of the brecciated zones and as massive, vein-filling material. Adularia occurs as pink to white euhedral crystals coating fractured surfaces. Hematite occurs as intense stains and cements on the brecciated part of the vein system and as specular hematite plates coating fractured surfaces. Of all the prospects visited in the Capitan Mountains, the McCory prospects show the most intense hematization.

Mina Tiro Estrella (MTE) Prospect

Location: NE1/4, Section 35; T8S, R16E; Capitan Peak Quad, 7 1/2' topographic map.

Elevation: 2255 meters (7400 feet).

Description: The vein occurs in a weathered brecciated (fault ?) zone within the alkali granite (aplite ?) and is poorly exposed. The vein strikes N48<sup>o</sup> E, dips 52<sup>o</sup> SW and can be traced for about 275 m by noting the appearance of float material (Hanson, 1989). The samples are all dump material. The minerals of the vein are quartz, allanite, titanite, adularia, chlorite/epidote and clay minerals. Tourmaline (?) was found in nearby float material. Quartz is the most dominant mineral and occurs as massive, somewhat transparent vein-filling material, as clear to smoky crystals up to 2 cm filling open spaces in massive vuggy vein quartz, and as clear to smoky Japanese-law twinned crystals up to 3 cm in size. The allanites are black, tabular crystals as large as 3 cm, averaging 5mm. Allanite occurs within open spaces of the vuggy vein quartz. The titanite crystals are reddish-brown, wedge-shaped and range from less than 1mm to 5mm. The titanite is found as massive intergrowths with adularia and as single crystals on the associated vein quartz. The adularia is pink to white and commonly occurs as massive intergrowths with the vein quartz. Some of the adularia has been kaolinized. Chlorite/epidote has been observed as needle-like inclusions within single quartz crystals. Clay minerals are fairly abundant and occur as clay gouge coating most of the vein material.

Similar veins may occur upslope from the MTE vein, as evidenced by float material.



### Piney-Drunzer Prospects

Location: SE1/4 SE1/4, Section 16; SW1/4 SW1/4, Section 15; NE1/4 NE1/4, Section 21; NW1/4 NW1/4, Section 22; T8S, R15E; Capitan Pass Quad, 7 1/2' topographic map.

Elevation: 2255 to 2316 meters (7400 to 7600 feet).

Description: Two separate prospects which occur on the same ridge within alkali granite (aplite) on a southwestern flank of the Capitan Mountains.

The Piney prospects occur on a southward facing ridge and consist of a series of bulldozer cuts, small pits and trenches. The main trench is situated along a fracture which trends east-west and dips  $60^{\circ}$  to  $80^{\circ}$  to the north. The trench is 2 m wide and 10 m long. Mineralization within the fractured/brecciated zone occurs as a 0.1 to 1 m wide vein composed of limonite, hematite and minor amounts of small, 1 to 2 mm, smoky quartz crystals.

The Drunzer prospect is a small trench cut into the aplite. The trench is 6m long, 3 m wide and 5 m deep. The face of the trench opens to the south. The brecciated aplite contains hematite and limonite as the cementing material. No other minerals were observed. The Piney and Drunzer prospects may be situated along the same vein system.

### Wee Three Prospects

Location: SE1/4 SE1/4, Section 15; NE1/4 NE1/4, Section 22; T8S, R15E; Capitan Pass Quad, 7 1/2' topographic map.

Elevation: 2316 to 2438 meters (7600 to 8000 feet).

Description: The Wee Three prospects consist of a series of small prospects which are exposed as small pits, bulldozer cuts and outcrop within fractured and brecciated granite (aplite). The prospects occur within a small canyon, along the

sides of the small canyon and on top of ridges above the small canyon. Seven mineralized zones were observed in the Wee Three area and are briefly described below. Refer to the map at the end of this appendix for the prospect localities.

W3-1: A small pit/trench in the fractured granite, located near the top of a ridge. The pit is 2 x 2 x 2 m in dimension. Trace amounts of smoky quartz and minor amounts of limonite and hematite staining were observed.

W3-2: An outcrop of fractured granite with abundant smoky quartz veins/veinlets filling the fractures. The outcrop is roughly 2 x 2 m in extent.

W3-3: A bulldozer cut, within the small canyon, in fractured granite. The exposed vein is about 2 m wide and trends roughly due north. The brecciated/fractured zone contains smoky and clear quartz crystals up to 2 cm, adularia, specular hematite, moderate amounts of hematite/limonite staining and clay minerals.

W3-4: A small pit, 1 x 1 x 1 m, within a small canyon in fractured and brecciated granite. The brecciated aplite is filled by smoky quartz veins and veinlets. Purple to clear fluorite, specularite, limonite, adularia and calcite also occur within the brecciated aplite. Calcite occurs as overgrowths on brown tabular masses. The mineralized zone trends N20<sup>o</sup> W and dips 75<sup>o</sup> to 80<sup>o</sup> to the east. The W3-4 vein system may be a part of the W3-3 vein system, which would indicate that the vein is at least a three hundred meters in length. Abundant vein float material occurs in the immediate area.

W3-5: A small pit on top of a ridge, east of W3-4. Pit is 1.5 x 1.5 x 1 m in dimension and occurs within brecciated granite. Mineralization consists of small stringers of smoky quartz, adularia, minor biotite and minor amounts of iron staining.

W3-6: Float material on top of ridge above W3-1. Float material consists of brecciated granite with abundant fluorite filling the open spaces.

W3-7: Small smoky quartz veinlets in brecciated granite, just down the ridge from W3-6.

### Miscellaneous Prospects not Mentioned in Thesis

#### Pierce Canyon Fe/Mn Prospects

Location: W1/2 SW1/4, Section 30; T8S, R17E; Capitan Peak Quad, 7 1/2' topographic map.

Elevation: 2210 meters (7250 feet).

Description: Described in Tuftin (1984). Five, isolated magnetite lenses in granite (porphyry) are exposed as bulldozer cuts. The largest magnetite lense is a 10 m wide, northeast-trending lens, which averages 60% iron. Several smaller magnetite bodies occur in the immediate area and are exposed primarily as float material.

#### CM 230 Iron Skarn Prospect

Location: NW1/4 SE1/4, Section 31; T7S, R15E; Jacob Springs Quad, 7 1/2' topographic map.

Elevation: 2377 meters (7800 feet).

Description: Located 1 km west of CM 235 prospect. Prospect is a pit that is 1.5 m long, 1.5 m wide and 5 m deep. Minerals consist of green garnet (with type 1 inclusions), magnetite and actinolite/tremolite. The prospect is a skarn, situated at the granite-limestone contact. The underlying granite shows granophyre texture.

### Smokey Iron Mine

Location: SE1/4 SE1/4, Section 10; T8S, R14E; Capitan Quad, 7 1/2' topographic map.

Elevation: 2103 meters (6900 feet).

Description: The iron mine is described as a pyrometamorphic magnetite body replacing limestone. Minerals consist of magnetite, epidote, phlogopite and tremolite. Refer to Kelley (1949) for a detailed description of this deposit.

### Unnamed Iron Prospect

Location: SE1/4 NE1/4, Section 30; T7S, R15E; Jacob Springs Quad, 7 1/2' topographic map.

Elevation: 1996 meters (6550 feet).

Description: Occurs at the base of a flank, northwestern Capitan Mountains. Prospect consists of an area of about 20 square meters with abundant magnetite nodules as float material. No visible outcrop of magnetite was observed.

### Unnamed Quartz Prospects - Capitan Pass Road

Location: NW1/4, Section 16; T8S, R15E; Capitan Pass Quad, 7 1/2' topographic map.

Elevation: 2180, 2210 meters (7150, 7250 feet two pits).

Description: Two small shallow pits filled with overburden. Only small clear quartz crystals were observed in float material of alkali granite (aplite and granophyre).

Arabela Mn Mine

Location: N1/2, Section 12; T8S, R17E; Arabela Quad, 7 1/2' topographic map.

Elevation: 1920 meters (6300 feet).

Description: Described in Griswold (1959). The two foot wide vein is exposed by a trench/bulldozer cut, trends  $N60^{\circ}W$  and dips  $30^{\circ}NE$ . The vein consists of manganese ore (psilomelane) and is located in alkali granite (porphyry)

Peppin Canyon Prospect

Location: NE1/4, Section 26; T8S, R15E; Capitan Pass Quad, 7 1/2' topographic map.

Elevation: 2225 meters (7300 feet).

Description: A small prospect pit that is 5 m long, 2 m wide and 1 m deep. Located at the mouth of Peppin Canyon. Calcite was the only observed mineral. Deposit appears to be a low-temperature skarn-type deposit near the contact of the San Andres limestone with the granitic pluton (aplite).

**APPENDIX C**  
**FLUID INCLUSION SAMPLES USED FOR**  
**HEATING/FREEZING MEASUREMENTS**

BS

BS prospect, shallow pit/excavation, southwest Capitan Mountains. Float material. One doubly-polished thick section of a 1 cm wide, clear to gray quartz vein cutting through granite. Minor iron stain on contact of vein with alkali granite. Most inclusions are type 1 and generally less than 10 microns. Less than 1% of inclusions are vapor-rich (leaked?). Less than 5% of inclusions are types 3 and 4, which are less than 2-3 microns.

CM 235

CM 235 prospect pit, northwest Capitan Mountains. Brecciated vein material. Quartz samples consist of three doubly-polished thick sections of 1-2 mm wide, clear quartz veinlets in brecciated granophyric granite from the main part of the vein. Quartz in veinlets is very fine-grained. Types 1,3 and 4 inclusions are found in the quartz. Type 1 inclusions are generally 10-15 microns in size.

Fluorite samples obtained from vugs in brecciated vein material from main part of prospect pit. 0.2-1mm thick cleavage chips of clear to purple fluorite were used for heating measurements. Type 1 inclusions range in size from < 5 to 50 microns.

CM 104

Trenches and road cuts, north-central Capitan Mountains. One doubly-polished thick section of a clear, fine-grained, 1mm quartz veinlet cutting the granite. Quartz contains 95% type 1 inclusions.

CMX

Prospect pit and veins within the granite, southwestern Capitan Mountains. Three doubly-polished thick sections of 0.5-1 cm smoky quartz and white adularia veins within the granite. Type 1 inclusions account for about 90%. Types 2, 3 and 4 inclusions occur randomly throughout the sections.

CPU-1

Outcrop of fractured granophyric granite with abundant fluorite veins, northwestern Capitan Mountains. Samples consist of four doubly-polished thick sections of 2-3 cm pieces of green vein fluorite. Type 1 inclusions account for 90% of the inclusions and occur as isolated, primary inclusions up to 60 microns in size and as pseudosecondary inclusions within healed cracks. A few type 2 inclusions were noted in the thick sections.

CPU-2

Trench/open-pit in fractured granite, northwestern Capitan Mountains. Two doubly-polished thick sections of 0.5 to 1 cm wide clear quartz veins cutting through fractured granite. Type 1 inclusions in quartz account for > 75% of the total inclusions. Types 3 and 4 inclusions occur randomly throughout the quartz.

Fuzzy Nut

Shallow pit in alaskite, northeastern Capitan Mountains. Three doubly-polished thick sections of 0.2 to 1 cm clear quartz veins and veinlets cutting through brecciated granite. Type 1 inclusions are greater than 80% of the total inclusions. Type 2 and 3 inclusions also observed.

Several 0.1 to 0.5 mm purple fluorite cleavage fragments from small, < 0.5 cm, fluorite cubes and massive, open-space filling fluorite. Type 1 inclusions fairly abundant for fluorite, > 50% of total inclusions. Types 2 and 3 inclusions also observed. Type 3 inclusions very abundant, > 25% of total inclusions.

0.1 to 0.5 mm cleavage fragments of white crystalline calcite were looked at for inclusions, but none were observed.

0.1 to 0.3 mm plates of hematite/maghemite from 0.5 to 1 cm brecciated hematite veins in fractured granite were observed under transmitted infrared light, but no inclusions were observed.

#### Hopeful Claim (HC)

Small pit in fractured granite, southwestern Capitan Mountains. 0.2 to 1 mm purple fluorite cleavage fragments from vug-filling, subhedral fluorite cubes. Type 1 inclusions account for > 25% of the total inclusions. Type 4 inclusions > 50%, probably most dominant type. Cleavage chips blew up before Tm NaCl and Th measurements could be determined during heating runs - probably due to decrepitation of the type 4 inclusions.

#### Hot Hill

Trench and quartz vein outcrops in fractured granite, southern Capitan Mountains. Four doubly-polished thick sections of 0.5 to 1.5 cm smoky quartz veins in brecciated aplite. Type 1 inclusions account for > 85% of the total inclusions. Type 2 and 3 inclusions also observed.

Several 0.1 to 0.5 mm, purple to colorless fluorite cleavage fragments from vug-filling fluorite in main part of pit and some small, < 0.5 cm, fluorite cubes from the most intense part of the brecciated zone. Type 1 inclusions very rare, < 10% of



the total inclusions. Type 2 inclusions account for < 40%. Types 3 and 4 inclusions account for < 50% of the total inclusions.

Several 0.1 to 1 mm, white crystalline calcite cleavage fragments from overgrowths on brown nodular masses and < 5mm, white calcite veinlets from main part of brecciated zone in trench. Only a few type 3 inclusions were observed and measured. Type 4 inclusions were observed, but not measured due to their small size ( < 2 microns ).

#### Koprian Springs

Small pit, northern Capitan Mountains. Several 0.5 to 1 mm size, clear fluorite cleavage chips from fracture filling material in brecciated granite. Type 1 inclusions are < 5% of the total inclusions. Type 2 inclusions account for > 30%, type 3 inclusions account for > 25% and type 4 inclusions account for > 25%.

Type 1 inclusions observed in clear quartz crystals lining fractures, but not measured due to their small size.

#### McCory Claims

Pits and trenches in brecciated granite, northern Capitan Mountains. Several 0.5 to 1 mm purple to clear fluorite cleavage chips from fluorite cubes (< 0.5 cm) filling vugs and lining fractures. Type 1 inclusions account for < 5% of total inclusions. Type 2 inclusions account for > 25%, type 3 account for > 40% and type 4 account for > 25% of the total inclusions.

Type 1 inclusions were noted in small, < 3 mm, smoky quartz crystals.

Mina Tiro Estrella (MTE)

Small pit/trench in side of hill, mostly dump material, south-central Capitan Mountains. Two doubly-polished thick sections of massive clear quartz intergrown with massive pink adularia. Two doubly-polished thick sections of massive, vuggy clear quartz intergrown with euhedral to subhedral titanite crystals. Two doubly-polished thick sections of 2 to 3 cm, euhedral, clear quartz crystals. One doubly-polished thick section of a 2 cm, single, clear Japanese-law twinned quartz crystal. Single smoky quartz crystals and smoky Japanese-law twinned quartz crystals were looked at and contain similar types of inclusions as the clear quartz. Type 1 inclusions account for > 95% of the total inclusions in all quartz specimens. Types 2 and 3 inclusions account for < 5% of the total inclusions. No type 4 inclusions were observed.

Two doubly-polished thick sections of massive adularia vein material were looked at, but no inclusions were observed.

One doubly-polished thick section of a 1 x 1 cm, euhedral allanite crystal from an open-space in vuggy vein quartz was observed under transmitted infrared light, but no inclusions were observed.

Several ( at least 100) 0.1 to 1mm chips of titanite were observed under visible light, only three identifiable type 1 inclusions were observed and only one was measurable. Several inclusions were observed in some of the titanite chips, but were too small, < 1 micron, to be identifiable. Two doubly-polished thick sections of titanite intergrown with massive vein quartz were looked at, but no inclusions were observed in the titanite.

W3-3

Trench/roadcut in fractured granite, southern Capitan Mountains. Four doubly-polished thick sections of 1 to 2 cm, euhedral smoky quartz crystals. Type 1 inclusions account for > 90% of the total inclusions. No type 2 or 4 inclusions were observed. Type 3 inclusions account for < 10% of the total inclusions. A few vapor-rich inclusions were observed, they account for < 1% of the total inclusions.

W3-4

Small pit in brecciated granite, southern Capitan Mountains. Three doubly-polished thick sections of smoky quartz veins (< 1 cm) in brecciated aplite. Type 1 inclusions account for > 90% of the total inclusions. No type 2 or 4 inclusions were observed. Type 3 inclusions account for < 10% of the total inclusions.

Several 0.1 to 0.5 mm fluorite cleavage fragments from clear to purple fluorite cubes (< 1 cm in size). Type 1 inclusions account for < 15% of the total inclusions. Type 2 inclusions account for > 25%, type 3 inclusions account for > 40% of the total inclusions. Few type 4 inclusions were observed, none were measured due to their small size, < 2 microns.

### **Fluid Inclusion Samples Without Heating Measurements**

W3-2

Small outcrop of brecciated granite with smoky quartz veins, southern Capitan Mountains. One doubly-polished thick section of smoky quartz veins (< 0.5 cm) cutting through fractured/brecciated granite. Type 1 inclusions account for > 85% of the inclusions. A few planes of vapor-rich inclusions. No heating measurements, only optical observations.

W3-6

Float material on top of ridge above W3-3 prospect, southern Capitan Mountains. Several fluorite cleavage chips from massive fluorite and fluorite cubes in brecciated granite. Inclusions in fluorite are similar to W3-4 fluorite samples. No heating measurements, optical observations only.

W3-7

Smoky quartz float, down the ridge from W3-6, southern Capitan Mountains. One doubly-polished section of smoky quartz veinlets in brecciated granite. Inclusions similar to other Wee Three quartz samples. No heating measurements, optical observations only.

Piney Claim

Large trench in granite, southern Capitan Mountains. Several, 2 to 3 mm smoky quartz crystals protruding from fractures along mineralized zones in aplite. Type 1 inclusions most abundant. No heating measurements, optical observations only.

CM 301

Clear quartz vein in granite, southeastern Capitan Mountains. Not near a prospect. A 1 cm, clear vuggy quartz vein (crystalline mush) filling fracture in granite. Small quartz crystals (< 2mm) contain small, < 5 microns, type 1 inclusions similar to other quartz samples from other prospects. No heating measurements, optical observations only.

CM 224

Outcrop of granite, southwestern Capitan Mountains. Not near a prospect. One doubly-polished thick section of small (< 3 mm) igneous quartz blebs in granite. Inclusion types consist of types 1, 2, 4, vapor-rich and liquid only inclusions. Vapor inclusions and type 2 inclusions most common. Most inclusions very small, < 5 microns. No heating measurements, optical observations only.

CM 243

Outcrop of aplitic granite, near radio towers, central Capitan Mountains. Not near a prospect. One doubly-polished thick section of igneous quartz blebs/grains, < 2mm, in aplite. Inclusion types in quartz blebs consist of: vapor-rich inclusions (> 90% vapor), which occur within growth planes and are less than 15 microns; liquid only inclusions, less than 5 microns; type 4 inclusions, with 1 to 5% vapor and less than 3 microns in size; type 3 inclusions, which consist of 5% vapor and 5% halite and are commonly stretched; type 1 inclusions, which are less than 5 microns in size and account for less than 5% of the total inclusions. Dominant inclusion types are vapor-rich and liquid only. Most inclusions too small to analyze. No heating measurements, optical observations only.

CM 230

Pit in iron skarn, top of southern Capitan Mountains, 1 km west of CM 235 prospect. One doubly-polished thick section of magnetite and green garnet (andradite ?) from iron skarn. Type 1 inclusions, < 15 microns, were observed in garnet and are similar to type 1 inclusions in quartz from other prospects. No heating measurements, optical observations only.

CM 223

Outcrop of granophyric granite, top of southern Capitan Mountains. Not near a prospect. One doubly-polished thick section of a 0.5 cm vuggy clear quartz vein cutting through granophyric granite. All inclusion types are very small, < 10 microns. Less than 20% type 1 inclusions, most of which are stretched. Greater than 70% vapor-rich inclusions, most of which occur along growth planes and as trails healing cracks which do not cut across quartz grain boundaries. Some vapor-rich inclusions may have been leaked liquid plus vapor inclusions. Type 4 inclusions account for < 25% of total inclusions. Less than 5% type 3 inclusions and < 10% liquid only inclusions. No heating measurements, optical observations only.

CM 222

Prospect pit/skarn near mouth of Peppin Canyon, about 1 km east of Hot Hill prospect, southern Capitan Mountains. One doubly-polished thick section of vein material containing clear, crystalline calcite stringers and eyes. No inclusions were observed in the calcite.

See Figure 1 for sample localities.

See Appendix B for prospect descriptions.

## APPENDIX C

### Fluid Inclusion Data - Heating/Freezing Measurements

Appendix C summarizes all fluid inclusion data which was collected in the project. The column headings are briefly described as follows. Type refers to fluid inclusion type (1, 2, 3 or 4). Tm ice refers to type 4 inclusions and is the temperature at which the final melting of ice occurs. In some cases where Tm ice is greater than zero, it was unclear if ice, hydrohalite or metastable halite had formed upon freezing. High Tm ice values may be the temperature at which hydrohalite or metastable halite disappears. For calculation purposes (Th vs salinity plots), all Tm ice values greater than zero were discarded. Tm Sylv is the sylvite dissolution temperature. Tm Halite is the halite dissolution temperature. Th is the vapor homogenization temperature. All temperatures are in degrees celsius. Tm NaCl - Th is self-explanatory. Wt% KCl and Wt% NaCl are the weight percentages of sylvite and halite, respectively, in a given inclusion. Bulk salinity, expressed as a weight percent, is the sum of wt% KCl plus wt% NaCl. The K/Na ratio is the molar ratio calculated from the wt% KCl and wt% NaCl.

Salinities (wt% KCl, wt% NaCl) for type 1 and 2 inclusions were calculated from the program SALTY (Bodnar et al., 1989). Salinities for type 3 and 4 inclusions were calculated from the program FLINCOR (data from Brown and Lamb, 1989).

The Linkham TH 600 heating/freezing stage used for the fluid inclusion studies has an upper limit of 600°C; therefore, for those inclusions which do not homogenize by 600°C, the values are reported as > 600°C. Based on the size of the halite or vapor bubble still present at 600°C for some of the inclusions, it would appear that complete homogenization would occur by 650°C. For some inclusions, an estimate ( $\pm 10^\circ\text{C}$ ) could be made for when the halite or vapor bubble would homogenize.

## BS Prospect - Quartz Fluid Inclusion Data

Type	Tm Sylv	Tm Halite	Th	Tm NaCl - Th	Weight %		Bulk Salinity	K/Na Ratio
					NaCl	KCl		
1	197	502	461	41	50.2	19.5	69.7	0.305
1	191	522	525	-3	53.6	17.8	71.4	0.260
1	209	536	493	43	55.2	18.4	73.5	0.261
1	224	549	473	76	56.7	18.6	75.3	0.257
1	188	541	501	40	56.8	16.5	73.3	0.228
1	218	548	466	82	56.8	18.2	75.0	0.251
1	220	546	450	96	56.4	18.5	74.9	0.257
1	223	542	501	41	55.6	19.0	74.6	0.268
1	213	544	501	43	56.3	18.1	74.4	0.252
1	216	539	483	56	55.4	18.7	74.1	0.265
3		469	461	8	55.8		55.8	



## CM 104 Prospect - Quartz Fluid Inclusion Data

Type	Tm Sylv	Tm Halite	Th	Tm NaCl - Th	Weight %		Bulk Salinity	K/Na Ratio
					NaCl	KCl		
1	210		459	96	58.3	17.2	75.4	0.231
1	181	533	456	77	55.7	16.4	72.2	0.231
1	166	541	463	78	57.6	14.9	72.5	0.203
1	214	549	450	99	57.1	17.9	75.0	0.246
1	250	571	501	70	59.4	19.0	78.4	0.251
1	173	577	509	68	63.3	13.3	76.6	0.165
1	194	539	435	104	56.2	17.0	73.3	0.237
1	175	522	404	118	54.2	16.6	70.8	0.240
1	203	531	430	101	54.6	18.2	72.8	0.261
1	212	544	474	70	56.4	18.1	74.4	0.252
1	216	546	467	79	56.5	18.2	74.7	0.253
1	200	541	428	113	56.3	17.3	73.7	0.241

## CM 235 Prospect - Fluorite Fluid Inclusion Data

Type	Tm Ice	Tm Sylv	Tm Halite	Th	Tm NaCl-Th	Weight % NaCl	Weight % KCl	Bulk Salinity	K/Na Ratio
1		216	529	440	89	53.7	19.3	73.1	0.282
1		228	536	465	71	54.4	19.8	74.2	0.285
1		222	537	462	75	54.8	19.3	74.1	0.276
1		230	539	433	106	54.8	19.8	74.6	0.283
1		220	526	440	86	53.1	19.9	72.9	0.294
1		223	532	458	74	53.9	19.7	73.6	0.287
1		225	512	429	83	50.6	21.2	71.8	0.328
1		224	527	559	-32	53.1	20.1	73.2	0.297
1		221	539	571	-32	55.2	19.1	74.2	0.271
1		230	547	571	-24	56.1	19.2	75.4	0.268
1		242	547	484	63	55.6	20.2	75.8	0.285
3			289	259	30	37.5		37.5	
3			288	203	85	37.4		37.4	
3			288	273	15	37.4		37.4	
3			253	254	-1	35.0		35.0	
3			255	259	-4	35.2		35.2	
3			255	257	-2	35.2		35.2	
3			254	256	-2	35.1		35.1	
4	10.7			162					
4	10.7			162					
4	7.1			162					
4	10.7			163					
4	10.6			144					
4	-11.2			167		15.2		15.2	
4	-11.2			166		15.2		15.2	
4	12.0			162					
4	-8.3			156		12.1		12.1	
4	-8.2			157		15.2		15.2	
4	11.8			163					
4	11.7			163					
4	-11.0			169		15.0		15.0	
4	-11.2			166		15.2		15.2	

## CM 235 Prospect - Quartz Fluid Inclusion Data

Type	Tm Ice	Tm Sylv	Tm Halite	Th	Tm NaCl-Th	Weight%		Bulk	K/Na
						NaCl	KCl	Salinity	Ratio
1		206	545	445	100	56.8	17.5	74.3	0.242
1		205	541	429	112	56.1	17.7	73.9	0.247
1		210	538	417	121	55.4	18.3	73.7	0.259
1		212	534	438	96	54.7	18.7	73.4	0.268
1		207	542	425	117	56.2	17.8	74.0	0.248
1			529	398	131				
1			533	400	133				
1		209	532	424	108	54.5	18.6	73.1	0.268
1		207	539	407	132	55.7	18.0	73.7	0.253
1		207	535	409	126	55.1	18.3	73.3	0.260
1			527	421	106				
1		205	540	407	133	56.0	17.8	73.8	0.249
1		204	559	414	145	59.2	16.5	75.6	0.218
1		208	547	414	133	57.0	17.6	74.6	0.242
1			526	491	35				
1			513	427	86				
1		198	528	423	105	54.3	18.0	72.3	0.260
1			511	433	78				
1			535	443	92				
2		114	448	390	58	45.5	15.3	60.8	0.264
2			452	440	12				
2		152	466	436	30	46.6	17.7	64.3	0.298
2		130	464	434	30	47.2	16.0	63.1	0.266
2		130	465	443	22	47.3	15.9	63.2	0.264
2			465	415	50				
2			469	448	21				
2		151	484	439	45	49.3	16.8	66.0	0.267
3			385	364	21				
3			389	354	35	46.4		46.4	
3			382	385	-3	45.7		45.7	
3			376	361	15	45.1		45.1	
3			358	365	-7	43.3		43.3	
3			357	367	-10	43.2		43.2	
3			291	256	35	37.7		37.7	
3			377	379	-2	45.2		45.2	
3			377	384	-7	45.2		45.2	
3			378	402	-24	45.3		45.3	
4	-15.8			125		19.3		19.3	
4	-15.7			125		19.2		19.2	
4	-15.8			125		19.3		19.3	

## CMX Prospect - Smoky Quartz Fluid Inclusion Data

Type	Tm Sylv	Tm Halite	Th	Tm NaCl - Th	Weight%		Bulk Salinity	K/Na Ratio
					NaCl	KCl		
1	222	544	521	23	56.0	18.8	74.8	0.263
1	222	529	505	24	53.5	19.8	73.3	0.290
1		589	586	3				
1	257	582	569	13	61.0	18.6	79.7	0.239
1	226	545	515	30	56.0	19.1	75.0	0.267
1	229	541	563	-22	55.2	19.6	74.7	0.278
1		574	530	44				
1		576	538	38				
1		555	502	53				
1		547	505	42				
1		583	463	120				
1		584	518	66				
1		538	518	20				
1	252	590	528	62	62.6	17.6	80.3	0.220
1	237	599	548	51	64.8	15.9	80.7	0.192
1	236	586	527	59	62.6	16.8	79.4	0.210
1	234	585	519	66	62.5	16.8	79.2	0.211
1		571	>600					
1		590	533	57				
1		570	>600					
1		593	565	28				
1		581	572	9				
1	232	596	>600		64.5	15.8	80.3	0.192
1	232	595	589	6	64.3	15.9	80.2	0.194
1		595	575	20				
1	243	580	540	40	61.2	17.8	79.0	0.228
1		589	517	72				
1		586	509	77				
1	238	577	466	111	60.9	17.6	78.6	0.227
1		585	495	90				
1		595	515	80				
1	250	596	507	89	63.8	17.0	80.8	0.209
1		581	>600					
1	224	542	523	19	55.5	19.1	74.6	0.268
1	222	541	518	23	55.5	19.0	74.5	0.268
1	222	543	515	28	55.8	18.9	74.7	0.266
1	222	545	523	22	56.1	18.7	74.9	0.261
2		509	480	29				
2		509	462	47				
2	204	501	429	72	49.8	20.2	69.6	0.318
2		451	415	36				
3		287	301	-14	37.4		37.4	
3		286	297	-11	37.3		37.3	
4			142					
4			207					

## CPU-1 Prospect - Fluorite Fluid Inclusion Data

Type	Tm Sylv	Tm Halite	Th	Tm NaCl - Th	Weight%		Bulk Salinity	K/Na Ratio
					NaCl	KCl		
1	204	527	426	101	53.9	18.5	72.4	0.269
1	190	542	329	213	56.9	16.6	73.4	0.229
1	250	547	380	167	55.3	20.8	76.1	0.295
1	202	517	365	152	52.4	19.0	71.4	0.284
1	197	514	369	145	52.1	18.8	70.9	0.283
1	237	548	494	54	56.0	19.7	75.7	0.276
1	205	533	447	86	54.8	18.2	73.1	0.260
1	215	520	451	69	52.3	19.9	72.2	0.298
1	167	498	456	42	50.8	17.3	68.1	0.267
1	180	506	392	114	51.5	17.9	69.4	0.272
1	237	530	476	54	53.0	21.0	74.0	0.311
1	194	514	422	92	52.2	18.6	70.8	0.279
1	201	517	407	110	52.4	18.9	71.3	0.283
1	191	511	392	119	51.9	18.5	70.3	0.279
1	173	497	418	79	50.4	17.9	68.2	0.278
1	170	494	409	85	50.0	17.8	67.8	0.279
1	172	483	374	109	48.3	18.5	66.8	0.300
1	252	563	434	129	57.9	19.7	77.7	0.267
1	197	509	461	48	51.3	19.1	70.4	0.292
1	196	512	395	117	51.8	18.8	70.6	0.285
1	197	513	397	116	51.9	18.9	70.8	0.285
2	162	306	289	17	26.9	25.2	52.0	0.734
2	160	305	288	17	26.9	25.0	51.8	0.729
2	160	305	288	17	26.9	25.0	51.8	0.729

## CPU-2 Prospect - Quartz Fluid Inclusion Data

Type	Tm Ice	Tm Sylv	Tm Halite	Th	Tm NaCl-Th	Weight%		Bulk	K/Na
						NaCl	KCl	Salinity	Ratio
1		192	565	475	90	60.6	15.3	75.9	0.198
1		227	568	494	74	59.8	17.5	77.3	0.229
1		145	517	420	97	54.5	14.7	69.2	0.211
1		214	563	501	62	59.5	16.9	76.4	0.223
1		222	564	531	33	59.3	17.4	76.8	0.230
1		154	527	522	5	55.8	14.8	70.6	0.208
1		182	536	545	-9	56.2	16.3	72.5	0.227
1		221	551	467	84	57.2	18.3	75.4	0.251
1		210	552	467	85	57.8	17.4	75.1	0.236
1		219	554	473	81	57.7	17.9	75.7	0.243
1		214	554	467	87	57.9	17.5	75.5	0.237
1		217	556	493	63	58.2	17.6	75.8	0.237
1		181	529	435	94	55.1	16.7	71.8	0.238
1		177	527	426	101	54.9	16.5	71.4	0.236
1		226	551	481	70	57.0	18.6	75.6	0.256
1		223	555	524	31	57.8	18.1	75.9	0.245
1		204	533	451	82	54.9	18.2	73.0	0.260
1		215	541	520	21	55.7	18.5	74.2	0.260
1		211	528	535	-7	53.8	19.0	72.8	0.277
1		212	553	503	50	57.9	17.5	75.3	0.237
1		220	555	427	128	57.9	17.9	75.8	0.242
1		228	551	497	54	56.9	18.8	75.7	0.259
3			370	362	8	44.5		44.5	
3			368	353	15	44.3		44.3	
3			367	355	12	44.2		44.2	
3			139	119	20	29.4		29.4	
3			271	232	39	36.2		36.2	
3			268	256	12	36.0		36.0	
4	-15.4			122		18.9		18.9	
4	-15.3			119		18.9		18.9	
4	-15.3			113		18.9		18.9	
4	-15.2			116		18.8		18.8	
4	-15.4			127		18.9		18.9	
4				123					

## Fuzzy Nut Prospect - Fluorite Fluid Inclusion Data

Type	Tm Sylv	Tm Halite	Th	Tm NaCl - Th	Weight%		Bulk Salinity	K/Na Ratio
					NaCl	KCl		
1	260	544	573	-29	54.3	21.9	76.2	0.316
1	265	561	591	-30	57.0	20.9	77.9	0.287
1	256	551	553	-2	55.7	21.0	76.7	0.296
1	259	538	561	-23	53.4	22.2	75.6	0.326
1	262	559	565	-6	56.8	20.8	77.6	0.287
1	263	544	>600		54.2	22.1	76.3	0.320
1	260	544	>600		54.3	21.9	76.2	0.316
1	259	546	>600		54.7	21.6	76.3	0.310
1	263	550	>600		55.2	21.6	76.8	0.307
1	264	562	>600		57.2	20.8	78.0	0.285
2	97	374	364	10	36.9	16.2	53.0	0.344
2	89	371	349	22	36.9	15.4	52.3	0.327
2	104	376	355	21	36.8	16.8	53.6	0.358
2	104	374	369	5	36.6	16.9	53.5	0.362
2	102	375	364	11	36.8	16.6	53.4	0.354
2	61	310	304	6	32.1	13.6	45.7	0.332
2	60	310	307	3	32.1	13.5	45.6	0.330
2	63	309	302	7	31.9	13.8	45.7	0.339
2	61	309	297	12	32.0	13.6	45.6	0.333
3		310	304	6	39.1		39.1	
3		310	303	7	39.1		39.1	
3		244	236	8	34.5		34.5	
3		244	235	9	34.5		34.5	
3		245	236	9	34.5		34.5	
3		304	283	21	38.6		38.6	
3		307	284	23	38.9		38.9	
3		308	283	25	39.0		39.0	
3		294	282	12	37.9		37.9	
3		293	282	11	37.8		37.8	
3		292	286	6	37.7		37.7	
3		294	284	10	37.9		37.9	
3		274	271	3	36.4		36.4	
3		274	272	2	36.4		36.4	

Th Vapor > Tm NaCl may indicate inclusion in fluorite has stretched

Based on size of vapor bubble still present at 600°C, complete homogenization for inclusions with Th > 600°C would probably occur near 605°C.

## Fuzzy Nut Prospect - Quartz Fluid Inclusion Data

Type	Tm Sylv	Tm Halite	Th	Tm NaCl - Th	Weight%		Bulk Salinity	K/Na Ratio
					NaCl	KCl		
1	227	566	501	65	59.5	17.6	77.1	0.232
1	228	559	492	67	58.2	18.2	76.5	0.245
1	221	570	475	95	60.4	16.9	77.3	0.219
1	226	554	487	67	57.5	18.4	75.9	0.251
1	210	549	477	72	57.3	17.6	74.8	0.241
1	217	553	484	69	57.7	17.8	75.5	0.242
1	210	537	449	88	55.3	18.4	73.6	0.261
1	188	531	497	34	55.2	17.1	72.2	0.243
1	206	525	492	33	53.5	18.8	72.3	0.275
1	195	518	481	37	52.8	18.4	71.2	0.273
1	220	560	491	69	58.7	17.6	76.3	0.235
1	218	545	501	44	56.3	18.4	74.7	0.256
1	214	543	501	42	56.1	18.3	74.4	0.256
1	223	560	501	59	58.6	17.8	76.4	0.238
1	209	559	535	24	59.0	16.8	75.8	0.223
1	213	555	521	34	58.1	17.4	75.5	0.235
1	194	514	490	24	52.2	18.6	70.8	0.279
1	160	500	481	19	51.3	16.7	68.0	0.255
1	147	483	496	-13	49.3	16.5	65.8	0.262
2	96	370	356	14	36.5	16.2	52.6	0.348
2	102	363	354	9	35.4	17.0	52.4	0.376
2	108	381	343	38	37.2	17.1	54.3	0.360
3		262	253	9	35.6		35.6	
3		260	251	9	35.5		35.5	



### Hopeful (HC) Prospect - Fluorite Fluid Inclusion Data

Type	Tm Sylvite	Tm Halite	Th Vapor
1	231	> 485	chip blew
1	231	> 420	"
1	228	> 540	"
1	224	> 541	"
1	221	chip blew	"
1	224	"	"
1	225	"	"
1	224	"	"
1	219	"	"
1	232	"	"
1	234	"	"
1	229	"	"
1	223	"	"
1	218	"	"
1	217	"	"
1	234	"	"
4			172
4			173
4			173
4			132
4			132
4			152
4			150
4			158
4			206
4			180

No measurements on type 1 inclusions could be made because the cleavage chip kept blowing up. This was probably a result of the decrystallization of the type 4 inclusions at high temperatures.

## Hot Hill Prospect - Calcite Fluid Inclusion Data

Type	Tm Halite	Th	Tm NaCl-Th	Wt% NaCl	Bulk Salinity
3	231	230	1	33.7	33.7
3	233	225	8	33.8	33.8
3	233	231	2	33.8	33.8
3	237	233	4	34.1	34.1

## Hot Hill Prospect - Fluorite Fluid Inclusion Data

Type	Tm Sylv	Tm Halite	Th	Tm NaCl-Th	Weight%		Bulk Salinity	K/Na Ratio
					NaCl	KCl		
1	266	591	511	80	62.2	18.6	80.8	0.234
1	283	585	443	142	60.4	20.4	80.8	0.265
2		377	374	3				
2		377	374	3				
2	55	358	350	8	37.2	11.9	49.1	0.251
2	55	361	350	11	37.5	11.9	49.3	0.249
2	51	359	352	7	37.5	11.9	48.9	0.238
2		357	351	6				
2	53	332	333	-1	34.6	12.2	46.8	0.276
2	51	321	320	1	33.7	12.1	45.8	0.281
2	51	321	323	-2	33.7	12.1	45.8	0.281
2	51	321	320	1	33.7	12.1	45.8	0.281
2	51	323	321	2	33.9	12.1	46.0	0.280
2		323	302	21				
2		316	268	48				
2		300	293	7				
2		300	291	9				
2		314	307	7				
2	52	321	317	4	33.6	12.3	45.9	0.287
2	52	325	323	2	34.0	12.2	46.2	0.287
2		321	317	4				
2		294	289	5				
2		306	354	-48				
2		297	306	-9				
2		295	295	0				
2		294	287	7				
2	68	355	372	-17	36.2	13.5	49.7	0.292
2	62	363	348	15	37.3	12.6	50.0	0.265
2	63	364	361	3	37.4	12.7	50.1	0.266
2	62	362	354	8	37.2	12.7	49.9	0.268
2	61	362	359	3	37.3	12.5	49.8	0.263
2	63	362	354	8	37.2	12.8	50.0	0.270
2	70	363	357	6	36.9	13.5	50.5	0.287
2	107	407			40.4	16.1	56.5	0.312
2	85	399	397	2	40.4	14.2	54.6	0.276
2	88	399	394	5	40.3	14.5	54.8	0.282
2	84	401	400	1	40.7	14.0	54.7	0.270
2	87	401	399	2	40.5	14.3	54.9	0.277
2		288	293	-5				
2		288	288	0				
2		290	294	-4				
2		289	287	2				
2		356	354	2				

## Hot Hill Prospect - Fluorite Fluid Inclusion Data (continued)

Type	Tm Sylv	Tm Halite	Th	Tm NaCl - Th	Weight% NaCl KCl	Bulk Salinity	K/Na Ratio
2		298	281	17			
2		357	355	2			
3		263	263	0	35.7	35.7	
3		263	263	0	35.7	35.7	
3		263	265	-2	35.7	35.7	
3		264	268	-4	35.8	35.8	
3		263	262	1	35.7	35.7	
3		193	193	0	31.7	31.7	
3		167	119	48	30.5	30.5	
3		168	168	0	30.6	30.6	
3		173	173	0	30.8	30.8	
4			110				

## Hot Hill Prospect - Quartz Fluid Inclusion Data

Type	Tm Sylv	Tm Halite	Th	Tm NaCl - Th	Weight%		Bulk	K/Na
					NaCl	KCl	Salinity	Ratio
1		557	504	53				
1		551	540	11				
1	244	567	553	14	59.0	18.8	77.8	0.250
1		551	536	15				
1	241	564	>600		58.6	18.8	77.4	0.251
1		570	512	58				
1	219	558	572	-14	58.4	17.6	76.1	0.236
1	202	534	495	39	55.1	17.9	73.0	0.255
1	202	552	480	72	58.1	16.8	74.9	0.227
1		521	432	89				
1	222	558	437	121	58.3	17.9	76.2	0.241
1	191	551	562	-11	58.3	16.1	74.4	0.216
1	223	557	507	50	58.1	18.0	76.1	0.243
1	232	571	539	32	60.1	17.6	77.8	0.230
1	232	581	509	72	61.9	16.9	78.8	0.214
1		574	554	20				
1		> 600	>600					
1		555	528	27				
1		580	507	73				
1		> 600	>600					
1		579	480	99				
1		571	485	86				
1		559	433	126				
1		553	486	67				
1		580	531	49				
1		552	571	-19				
1		> 600	>600					
1		> 600	478					
1		564	508	56				
1		578	553	25				
1		596	587	9				
1		592	589	3				
1		567	482	85				
2		440	445	-5				
3		280	270	10			36.9	
					36.9			
3		277	269	8			36.6	
					36.6			

Based on the size of the vapor bubble and halite cube still present at 600°C,  
 > 600°C inclusions would probably homogenize by 610°C.

## Koprian Springs Prospect - Fluorite Fluid Inclusion Data

Type	Tm Ice	Tm Sylv	Tm Halite	Th	Tm NaCl-Th	Weight% NaCl	Weight% KCl	Bulk Salinity	K/Na Ratio
1		237	541	523	18	54.8	20.2	75.0	0.289
2		61	328	323	5	33.8	13.2	47.0	0.306
2		61	328	327	1	33.8	13.2	47.0	0.306
2		61	327	291	36	33.7	13.3	46.9	0.309
2		62	329	325	4	33.8	13.3	47.2	0.308
2		97	329	325	4	32.1	17.4	49.4	0.425
2		64	327	326	1	33.5	13.6	47.1	0.318
2		58	331	327	4	34.2	12.8	47.1	0.293
2		57	329	326	3	34.1	12.7	46.8	0.292
2		55	379	383	-4	39.5	11.5	51.0	0.228
2		78	354	351	3	35.6	14.7	50.2	0.324
2		78	354	353	1	35.6	14.7	50.2	0.324
2		75	352	351	1	35.5	14.4	49.9	0.318
2		77	356	350	6	35.8	14.5	50.3	0.318
2		79	337	358	-21	33.7	15.2	48.9	0.354
2		76	353	351	2	35.6	14.5	50.0	0.319
2		75	354	354	0	35.7	14.3	50.0	0.314
2		79	353	349	4	35.4	14.8	50.2	0.328
2		77	362	360	2	36.5	14.4	50.8	0.309
2		81	341	339	2	34.0	15.3	49.4	0.353
2		78	356	332	24	35.8	14.6	50.4	0.320
2		78	353	349	4	35.5	14.7	50.1	0.325
2		77	353	352	1	35.5	14.6	50.1	0.322
2		76	353	352	1	35.6	14.5	50.0	0.319
3			247	246	1	34.7		34.7	
3			247	245	2	34.7		34.7	
3			245	244	1	34.5		34.5	
3			246	244	2	34.6		34.6	
3			237	234	3	34.1		34.1	
3			236	235	1	34.0		34.0	
3			236	236	0	34.0		34.0	
3			225	227	-2	33.4		33.4	
3			226	224	2	33.4		33.4	
3			264	263	1	35.8		35.8	
3			265	264	1	35.8		35.8	
3			267	267	0	36.0		36.0	
3			267	266	1	36.0		36.0	
4	-7.3			124		10.9		10.9	
4	-7.1			119		10.6		10.6	
4	-7.4			130		11.0		11.0	
4	-7.3			126		10.9		10.9	
4	-16.2			116		19.6		19.6	
4	-17.7			146		20.7		20.7	

## McCory Prospect - Fluorite Fluid Inclusion Data

Type	Tm Sylv	Tm Halite	Th	Tm NaCl - Th	Weight% NaCl	Weight% KCl	Bulk Salinity	K/Na Ratio
1		600	590	10				
2	85	405	407	-2	41.1	14.0	55.1	0.267
2	76	382	375	7	38.8	13.7	52.5	0.277
2		313	313	0				
2		386	386	0				
2		389	394	-5				
2	58	339	326	13	35.0	12.7	47.7	0.284
2	58	339	286	53	35.0	12.7	47.7	0.284
2	59	358	330	28	37.0	12.4	49.4	0.263
2	57	338	333	5	35.0	12.6	47.6	0.282
2	58	337	323	14	34.8	12.7	47.5	0.286
2	58	338	331	7	34.9	12.7	47.6	0.285
2	58	338	333	5	34.9	12.7	47.6	0.285
2	76	337	388	-51	33.9	14.8	48.7	0.342
2	77	388	390	-2	39.4	13.7	53.1	0.273
2		387	390	-3				
2		385	388	-3				
2		387	388	-1				
3		312	305	7	39.3		39.3	
3		311	276	35	39.2		39.2	
3		311	305	6	39.2		39.2	
3		312	358	-46	39.3		39.3	
3		311	304	7	39.2		39.2	
3		311	305	6	39.2		39.2	
3		312	304	8	39.3		39.3	
3		331	332	-1	40.9		40.9	
3		331	328	3	40.9		40.9	
3		331	329	2	40.9		40.9	
3		351	356	-5	42.7		42.7	
3		311	305	6	39.2		39.2	
3		312	306	6	39.3		39.3	
3		311	304	7	39.2		39.2	
3		318	310	8	39.8		39.8	
3		317	303	14	39.7		39.7	
3		317	310	7	39.7		39.7	
3		317	313	4	39.7		39.7	
3		316	312	4	39.6		39.6	
3		316	298	18	39.6		39.6	
3		316	310	6	39.6		39.6	
3		329	328	1	40.7		40.7	
3		332	330	2	41.0		41.0	
3		329	329	0	40.7		40.7	
3		330	328	2	40.8		40.8	

## McCory Prospect - Fluorite Fluid Inclusion Data (continued)

Type	Tm Sylv	Tm Halite	Th	Tm NaCl - Th	Weight%		Bulk Salinity	K/Na Ratio
					NaCl	KCl		
3		332	331	1	41.0		41.0	
3		331	329	2	40.9		40.9	
3		188	180	8	31.5		31.5	
3		188	182	6	31.5		31.5	
3		188	181	7	31.5		31.5	
3		188	182	6	31.5		31.5	
3		188	182	6	31.5		31.5	
3		316	300	16	39.6		39.6	
3		315	285	30	39.5		39.5	
3		331	331	0	40.9		40.9	
3		331	333	-2	40.9		40.9	



## Mina Tiro Estrella (MTE) Prospect - Quartz Fluid Inclusion Data

Type	Tm Sylv	Tm Halite	Th	Tm NaCl - T	Weight%		Bulk Salinity	K/Na Ratio
					NaCl	KCl		
1	276	586	567	19	60.9	19.7	80.6	0.254
1	275	598	570	28	63.1	18.6	81.7	0.231
1	244	596	587	9	64.0	16.6	80.6	0.203
1	289	581	588	-7	59.4	21.2	80.6	0.280
1	298	591	581	10	60.9	20.9	81.8	0.269
1	263	589	587	2	62.0	18.5	80.5	0.234
1	266	604	593	11	64.6	17.5	82.1	0.212
1	287	587	567	20	60.6	20.5	81.1	0.265
1	275	586	583	3	61.0	19.7	80.6	0.253
1	265	492	480	12	49.9	17.5	67.4	0.275
1	273	499	489	10	50.7	17.8	68.4	0.275
1	276	584	570	14	60.6	19.9	80.5	0.257
1	272	589	568	21	61.6	19.2	80.8	0.244
1	278	590	586	4	61.5	19.5	81.1	0.249
1	252	614	580	34	66.9	15.7	82.6	0.184
1	240	580	555	25	61.4	17.6	78.9	0.225
1	244	577	557	2	60.7	18.1	78.8	0.234
1	148	538	538	0	57.7	13.8	71.5	0.187
1	233	562	548	14	58.5	18.4	76.9	0.247
1	226	588	567	21	63.3	16.0	79.3	0.198
1	232	564	497	67	58.9	18.2	77.1	0.242
1	253	563	489	74	57.9	19.8	77.7	0.268
1	259	569	514	55	58.7	19.8	78.5	0.264
1	169	490	483	7	49.5	17.9	67.4	0.283
<u>1</u>	<u>313</u>	<u>604</u>	<u>587</u>	<u>17</u>	<u>62.4</u>	<u>21.1</u>	<u>83.5</u>	<u>0.265</u>
1		>600	>600					
1		568	>600					
1		573	>600					
1		595	588	7				
1		>600	>600					
1		584	558	26				
1		>600	553					
1		>600	558					
1		593	574	19				
1		594	573	21				
1		>600	600					
1		>600	587					
1		>600	>600					
1		>600	595					
1		>600	602					
1		>600	597					
1		551	533	18				
1		601	592	9				
1		593	583	10				

## Mina Tiro Estrella Prospect - Quartz Fluid Inclusion Data (continued)

Type	Tm Sylv	Tm Halite	Th	Tm NaCl - Th	Weight% NaCl	Weight% KCl	Bulk Salinity	K/Na Ratio
1		>600	581					
1		598	582	16				
1		485	475	10				
1		578	536	42				
1		559	510	49				
1	287	>600	>600		64.8	18.5	83.2	0.224
1	185	506	500	6	51.3	18.3	69.6	0.280
1	187	509	491	18	51.7	18.3	70.0	0.277
1	300	>600	>600		64.2	19.4	83.6	0.237
1	275	594	575	19	62.4	19.0	81.4	0.239
1	251	574	564	10	59.9	18.8	78.7	0.246
1	255	576	573	3	60.1	19.0	79.0	0.248
1	262	>600	>600		65.8	16.7	82.5	0.199
1	265	>600	590		65.7	16.9	82.6	0.202
1		577	543	34				
1		579	558	21				
1		581	566	15				
1		580	561	19				
1		590	568	22				
1		>600	560					
1		>600	552					
1		587	570	17				
1		>600	598					
1		603	533	70				
1		>600	568					
1		>600	563					
1		>600	561					
1		>600	>600					
1		>600	>600					
1		588	554	34				
1		603	558	45				
1		604	>600					
1		593	564	29				
1		>600	>600					
1		590	543	47				
2		360	351	9				
3		201	203	-2	32.1		32.1	
3		230	225	5	33.7		33.7	
3		210	214	-4	32.6		32.6	

The first 25 inclusions are data from M. Willis (written comm., 1989).

Based on the size of the halite cube and vapor bubble still present at 600°, it is estimated that complete homogenization would occur by 610°.

## Wee Three (W3-3) Prospect - Smoky Quartz Fluid Inclusion Data

Type	Tm Sylv	Tm Halite	Th	Tm NaCl - Th	Weight%		Bulk Salinity	K/Na Ratio
					NaCl	KCl		
1	263	581	566	15	60.6	19.2	79.8	0.248
1	254	596	>600		63.6	17.3	80.9	0.213
1	272	580	580	0	60.0	19.9	80.0	0.260
1	273	588	>600		61.4	19.3	80.7	0.246
1	270	584	>600		60.8	19.4	80.3	0.250
1	260	578	578	0	60.2	19.2	79.4	0.250
1	255	591	584	7	62.7	17.8	80.5	0.223
1	268	596	>600		63.0	18.3	81.3	0.228
1	266	593	>600		62.6	18.4	81.0	0.230
1	264	592	>600		62.5	18.3	80.8	0.230
1	260	578	578	0	60.2	19.2	79.4	0.250
1	278	591	599	-8	61.7	19.5	81.2	0.248
1	271	592	>600		62.2	18.8	81.1	0.237
1	272	582	>600		60.4	19.8	80.1	0.257
1	276	588	599	-11	61.3	19.6	80.8	0.251
1	262	583	599	-16	61.0	18.9	79.9	0.243
1	280	592	595	-3	61.8	19.5	81.3	0.247
1	260	572	599	-27	59.1	19.7	78.8	0.261
1	295	586	>600		60.0	21.3	81.3	0.278
1	275	582	>600		60.2	20.0	80.2	0.260
1	269	576	>600		59.4	20.0	79.5	0.264
1	267	576	568	8	59.5	19.9	79.4	0.262
1	288	591	>600		61.3	20.2	81.5	0.258
1	271	571	>600		58.5	20.6	79.1	0.276
1	243	591	535	56	63.2	16.9	80.1	0.210
1	225	590	533	57	63.7	15.8	79.5	0.194
1	245	593	544	49	63.5	16.9	80.4	0.209
1	244	586	>600		62.3	17.4	79.6	0.219
1	247	593	>600		63.4	17.1	80.4	0.211
1	241	595	>600		64.0	16.5	80.4	0.202
1	239	593	>600		63.7	16.5	80.2	0.203
1	252	595	>600		63.5	17.2	80.8	0.212
1	290	601	>600		63.0	19.5	82.5	0.243
3		351	348	3	42.7		42.7	
3		350	347	3	42.6		42.6	
3		351	347	4	42.7		42.7	
3		319	308	11	39.9		39.9	
3		348	349	-1	42.4		42.4	
3		322	317	5	40.1		40.1	
3		321	317	4	40.0		40.0	
3		359	373	-14	43.4		43.4	
3		356	355	1	43.1		43.1	
3		361	363	-2	43.6		43.6	

Based on the size of the halite cube and vapor bubble still present at 600°C, total homogenization is estimated to occur at 605 to 615°C.

## Wee Three (W3-4) Prospect - Fluorite Fluid Inclusion Data

Type	Tm Sylv	Tm Halite	Th	Tm NaCl - Th	Weight%		Bulk Salinity	K/Na Ratio
					NaCl	KCl		
1	270	575	601	-26	59.2	20.2	79.4	0.267
1	283	569	600	-31	57.6	21.8	79.3	0.297
1	265	557	599	-42	56.3	21.3	77.6	0.297
1	269	563	600	-37	57.2	21.1	78.3	0.289
1	268	562	600	-38	57.0	21.1	78.1	0.290
1	223	561	545	16	58.8	17.7	76.5	0.236
1	251	558	535	23	57.1	20.0	77.2	0.275
1	268	553	596	-43	55.5	21.8	77.3	0.308
2	81	369	361	8	37.1	14.6	51.7	0.308
2	79	366	364	2	36.8	14.5	51.3	0.309
2	80	365	363	2	36.7	14.6	51.3	0.312
2	79	367	364	3	36.9	14.4	51.4	0.306
2	82	366	366	0	36.7	14.8	51.5	0.316
2	76	367	365	2	37.1	14.1	51.2	0.298
2	78	367	366	1	37.0	14.3	51.3	0.303
2	73	366	365	1	37.1	13.8	50.9	0.292
2	64	338	330	8	34.6	13.4	48.0	0.304
2	61	341	332	9	35.1	13.0	48.1	0.290
2	60	321	316	5	33.2	13.3	46.4	0.314
2	61	319	314	5	32.9	13.4	46.3	0.319
2	85	368	366	2	36.8	15.1	51.8	0.322
2	82	365	364	1	36.6	14.8	51.4	0.317
2	84	369	368	1	36.9	14.9	51.9	0.317
3		289	276	13	37.5		37.5	
3		286	279	7	37.3		37.3	
3		311	313	-2	39.2		39.2	
3		220	220	0	33.1		33.1	
3		218	218	0	33.0		33.0	
3		218	218	0	33.0		33.0	
3		219	218	1	33.0		33.0	
3		302	288	14	38.5		38.5	
3		295	271	24	38.0		38.0	
3		273	268	5	36.4		36.4	
3		275	266	9	36.5		36.5	
3		308	295	13	39.0		39.0	
3		300	303	-3	38.3		38.3	
3		297	253	44	38.1		38.1	
3		296	251	45	38.0		38.0	

## Wee Three (W3-4) Prospect - Smoky Quartz Fluid Inclusion Data

Type	Tm Sylv	Tm Halite	Th	Tm NaCl - Th	Weight%		Bulk Salinity	K/Na Ratio
					NaCl	KCl		
1	227	571	551	20	60.3	17.3	77.6	0.225
1	227	573	559	14	60.7	17.2	77.8	0.222
1	229	575	524	51	60.9	17.2	78.1	0.221
1	230	571	495	76	60.2	17.5	77.7	0.228
1	230	578	521	57	61.4	17.0	78.4	0.217
1	238	577	528	49	60.9	17.6	78.6	0.227
1	223	558	541	17	59.3	17.9	76.2	0.241
1	230	563	503	60	58.8	18.1	76.9	0.241
1	213	552	482	70	57.6	17.6	75.2	0.240
1	219	577	500	77	61.7	16.3	78.0	0.207
1	231	586	506	80	62.8	16.5	79.2	0.206
1	226	595	511	84	64.5	15.5	80.0	0.188
1	229	585	517	68	62.7	16.4	79.1	0.205
1	226	574	516	58	60.9	17.0	77.9	0.219
1	203	518	501	17	52.5	19.0	71.5	0.284
1	214	585	488	97	63.2	15.4	78.6	0.191
3		305	294	11	38.7		38.7	
3		291	287	4	37.7		37.7	
3		293	286	7	37.8		37.8	
3		227	214	13	33.5		33.5	
3		305	294	11	38.7		38.7	
3		302	287	15	38.5		38.5	

## **APPENDIX D**

### **Fluid Inclusion Crush-Leach Analysis - Experimental Procedures**

Bulk crush-leach analysis was performed on vein quartz to establish a semi-quantitative estimate of the inclusion fluid chemistry on samples from the MTE, Hot Hill, Wee Three (W3-3), CPU-2, Fuzzy Nut and CMX prospects. Vein quartz from other prospects was not analyzed due to lack of an adequate amount of sample to work with. Major elements on inclusion fluid leachates were checked by atomic absorption spectroscopy and anion chromatography. A leachate solution from MTE vein quartz was checked for REE's by ICP. Vein quartz samples from the MTE, W3-3 and CMX prospects contain greater than 90% type 1 inclusions. Vein quartz samples from the CPU-2, Hot Hill and Fuzzy Nut prospects contain greater than 75% type 1 inclusions. For these last three prospects, a dilution effect caused by the other types of inclusions may occur in the crush-leach results.

#### Sample Preparation for AA, ICP and Anion Chromatography Analyses

Vein quartz samples used for bulk crush-leach analysis were initially crushed to less than 1 cm size pieces. Quartz pieces containing significant amounts of impurities were discarded. Quartz pieces containing minor quantities of feldspar, plutonic rock or other impurities (samples from the CMX, W3-3 and CPU-2 prospects) were cleaned in warm, concentrated (48%) reagent grade hydrofluoric acid for two to four days. After cleaning with hydrofluoric acid, the samples were rinsed with tap water.

Samples were crushed to - 10 to + 40 mesh and hand-picked under a binocular microscope to remove any visible impurities. Samples were intermitantly boiled in concentrated reagent grade nitric acid for several days to remove any remaining

impurities (iron oxides, clays, surface dirt ...). Samples were rinsed with distilled water, oven-dried and re-checked under a binocular microscope to ensure all impurities have been removed. Samples were then boiled in concentrated nitric acid for two to three days, rinsed with distilled water, boiled in concentrated nitric acid for 24 hours, rinsed several times with distilled/deionized water (DIW) and boiled in DIW for several days with daily changes of water. The samples were finally cleaned in an electrolytic cell for two to four weeks according to the method of Roedder (1984). After cleaning, samples were oven-dried and stored in polypropylene bottles until ready for use.

#### Experimental Procedures for the Crush-Leach Method

Several methods were applied in order to determine which procedure was best suited for releasing the inclusion fluid contents contained within the vein quartz samples. Preliminary studies were applied on MTE vein quartz (a vein quartz which was abundant, relatively free of impurities and contained an abundance of type 1 inclusions) in order to determine the appropriate amount of quartz needed for a good crush-leach and to find a suitable leaching solution. Room temperature deionized/distilled water (DIW), hot (80°C) DIW, 0.13 N nitric acid and a 200 ppm  $\text{LaCl}_3$  in 0.13 N nitric acid (as prescribed by Bottrell et al., 1988) were used as leaching solutions.

All glassware used in the crush-leach experiments was previously soaked in 50% reagent grade nitric acid and rinsed with DIW prior to use. Approximately 5 to 25 gram samples of MTE quartz was crushed as a slurry with a specific leach solution in an alumina mortar and pestle. Crushing was done within three minutes. If a longer crushing time is used, the chance of contamination increases (contamination from mortar and pestle, hair/skin cells falling into the mortar and pestle, contamination from the air ...). The slurry was quantitatively transferred to

a 0.2 micron pore size Nalgene millipore disposable filter unit. The quartz slurry in the mortar and pestle was rinsed into the filter unit. The quartz in the filter unit was rinsed several times with the leaching solution until a leachate solution volume of 40 to 50 mL was obtained. For some samples, after collection of the first leachate solution, a second portion of leachate solution (samples MTE-201, MTE-203 and MTE-206) on the same sample was obtained by rinsing the crushed quartz residue with the appropriate leaching solution. This was done to ensure all ions were released from the crushed quartz and collected in the first portion of leachate solution. Leaching solutions were "crushed" without quartz in the mortar and pestle and filtered through the millipore filter unit to serve as blanks. DIW was filtered through the filter unit to check for contamination. Sample N-1 is a rinse of DIW through the filter unit, sample N-2 is a second rinse of DIW through the filter unit, sample N-3 is a fifth rinse of DIW through the filter unit. No contamination from the filter unit was observed.

Na, K, Ca, Mg, Mn, Fe, Zn, Ba, Ag, Cu and Pb were analyzed by atomic absorption spectroscopy using a Instrumentation Laboratory IL Video 12 AA/AE spectrophotometer. Operating parameters and calibration data for the standards are given in Table D1. Cl, SO<sub>4</sub>, NO<sub>3</sub> and F were analyzed by anion chromatography using a Dionex ion chromatograph series 4000i with a sulfuric acid ion suppressor and a NaHCO<sub>3</sub> eluant. Calibration data for the standards are given in Table D2.

MTE fluid inclusion leachates were found to contain significant amounts of Na, K, Ca and Cl and minor amounts of Fe, Mn, Mg, Zn, and SO<sub>4</sub>. Silver, Cu, Pb, Ba, F and NO<sub>3</sub> were not detected. Barium may not have been released into the leachate solution due to the insoluble nature of BaSO<sub>4</sub> (a potential daughter mineral). All leaching solutions used removed all the Na, K and Cl from the crushed quartz. The water and 0.13 N nitric acid leaching solutions did not release all of the +2 cations,



as evidenced by the higher concentrations of +2 cations in the  $\text{LaCl}_3$  leach solution. Bottrell et al. (1988) also noticed that simple water leaches were insufficient to remove all ions from crushed quartz. All pertinent experimental data related to the crush-leach analysis employing the various leaching solutions is listed in Table D5 and Tables 4A, B and C in the main text.

In order to achieve a complete bulk analysis on a single sample, the  $\text{LaCl}_3$  leach solution (which caused Cl contamination of the sample) was replaced by a similar leach solution which employs a +3 cation to act as an inhibitor for adsorption of desirable ions onto the crushed quartz. A 250 ppm Sc in 0.25 wt% nitric acid solution was used for all subsequent studies. A total of 17 quartz samples were crushed and leached using the Sc leach solution in a similar manner described above. Na, K, Ca, Mn, Mg, Fe and Zn were analyzed by atomic absorption spectroscopy and Cl and  $\text{SO}_4$  were analyzed by anion chromatography. Sulphate was nondetectable by anion chromatography due to interferences from the nitrate of the leaching solution. All pertinent experimental data related to the crush-leach analysis using the Sc leaching solution is listed in Table D6 and Tables 6A, B, C and D in the main text.. Operating parameters and calibration data for the standards for the atomic absorption analyses are given in Table D3. Calibration data for the anion chromatography analyses are given in Table D4.

#### Analysis of REE's by ICP - Experimental Procedure

A single sample of previously electrolytically cleaned quartz from the MTE prospect was checked for REE's by a Perkin Elmer Model 1000 Inductively Coupled Plasma spectrometer. Approximately 50 grams of quartz was crushed as a slurry, five grams at a time, in an alumina mortar and pestle and leached with a 250 ppm Sc in 0.13N  $\text{HNO}_3$  leaching solution. The slurry was transferred to a Nalgene 0.2 micron-size millipore filter unit and the leachate solution was filtered and collected.

The leachate solution was transferred to a teflon beaker and slowly evaporated until the leachate solution was about 10 mL and transferred to a 10 mL volumetric flask. The solution in the 10 mL volumetric flask was slowly heated to dryness. A 30% CdCl<sub>2</sub> internal standard solution was added to the volumetric flask to bring the volume up to 10 mL. A blank using the Sc leach solution was prepared as if it was a quartz sample. The blank and the MTE sample were checked for La, Ce and Hf by ICP. No REE's were detected by ICP (B. Popp, pers. comm., 1990).

## Hydrofluoric Acid Dissolution of MTE Vein Quartz

To avoid the problems of adsorption of +2 and +3 cations onto the surfaces of freshly crushed quartz and to avoid the problems of contamination (ie., mortar and pestle contamination) using the bulk crush-leach technique described previously, a hydrofluoric acid dissolution of electrolytically cleaned MTE vein quartz was attempted. The purity of MTE quartz and the abundance of primary/pseudosecondary inclusions allowed this type of technique to be employed. The idea behind this method was that it should be possible to chemically dissolve the quartz, liberate the fluid inclusion contents, dissolve all daughter mineral phases (including barite ?) and hence obtain a complete chemical analysis of all major cations and anions within the inclusion fluids. The limitations to this method were determined by the purity of the hydrofluoric acid used and the purity of the quartz host mineral.

Samples consist of one quartz blank (MTE-100), three MTE quartz samples containing abundant fluid inclusions (MTE-101, 102 and 103) and a hydrofluoric acid blank (MTE-104). 2.6 grams of inclusion-free quartz was obtained by breaking the terminated tips off of euhedral quartz crystals from single MTE quartz crystals. This sample was used as a check for contamination from the quartz host mineral. Five to ten grams of electrolytically cleaned MTE quartz was placed in a 250 mL teflon beaker (beakers were previously cleaned in 50% nitric acid). 40 to 60 mL (measured by weight) of ultrapure hydrofluoric (HF) acid was initially added to each beaker containing the quartz samples. About 25 mL of HF acid was added to a teflon beaker containing the inclusion-free quartz. 30 mL of the ultrapure HF acid was added to a teflon beaker without quartz to serve as a blank. The quartz samples were allowed to react with the HF acid for two days at 40°C on a hot plate. Additional aliquots of HF acid were added to the teflon beakers when the

initial amount of acid was nearly evaporated. Total amounts of HF acid added to each sample is recorded in Table D7. After all of the ultrapure HF acid from the stock solution was used up, the remaining amount of HF acid in the teflon beakers was allowed to evaporate to dryness. For samples MTE-101, 102 and 103, a small yellow residue was left in the beaker along with some unreacted quartz. The residue on any of the unreacted quartz was rinsed off into the teflon beaker with distilled/deionized water (DIW). The quartz grains were picked out of the beaker, oven-dried and weighed. The weights of the quartz before the acid was added and after the quartz was partially dissolved were used to calculate the percentage of quartz which dissolved. 60 to 77% of the quartz from samples MTE-101, 102 and 103 had dissolved. Only 24% of the inclusion-free quartz had dissolved. After the quartz had been picked out of the teflon beaker, about 20 mL of DIW (measured by weight) was added to the teflon beakers in order to dissolve the "salty" residues. The solution in the beaker was transferred to a 60 mL polyethylene bottle and weighed to obtain a solution weight. The samples were stored in the bottles until ready for analysis. The blank was prepared in a similar manner - the HF acid was allowed to evaporate to dryness, about 20 mL of DIW was added to the beaker in order to dissolve any residue and the solution was transferred to a 60 mL polyethylene bottle.

The samples were analyzed for major elements by atomic absorption and anion chromatography. Table D7 and Table 5 in the main text, summarizes all pertinent data related to the HF acid - quartz dissolution technique. The low Ca values (as compared to the Ca values from the  $\text{LaCl}_3$  leach solution method) from the HF acid - quartz dissolution method may be caused by precipitation of an insoluble residue,  $\text{CaF}_2$ . Barium was detected by this method, indicating the possibility of barite as a daughter mineral. A major problem with this technique was that fluoride from the HF acid was retained in the "salty residue" and hence carried over into the solution

which was analyzed. The large amount of fluoride interfered with the chloride peak in the anion chromatography analyses. As a result, chloride could not be detected. Because of this problem, and the low Ca values, the HF acid -quartz dissolution technique was abandoned.

## Crush-Leach Sample Descriptions

MTE 500-504: MTE prospect. Bulk sample consisting of cleaned chunks of 2 to 5cm clear quartz chunks/crystals. Most crystals exhibit Japanese-law twinning. Contains >95% type 1 inclusions.

MTE 501A: A second portion of leachate solution passed through sample MTE 501. This is a check to see if all of the cations/anions were leached and collected the first time.

W3-3A,B,C: Wee Three-3 trench in granite, southwestern Capitan Mountains. Bulk sample of 20-25 single, 1-2cm, smoky quartz crystals. Contains >90% type 1 inclusions.

W3-3A1: A second portion of leach solution passed through sample W3-3A.

CPU-2A,B,C: Prospect CPU-2. Trench in granite. Bulk sample of 0.1-1cm, clear quartz crystals. Quartz occurred as fracture coatings on the brecciated vein material. Contains >75% type 1 inclusions.

HH-100,101: Hot Hill prospect pit. Bulk analysis of smoky quartz taken from the brecciated vein material and 0.1-1cm crystals taken from fracture coatings on the brecciated material. Contains >90% Type 1 inclusions.

CMX-1A,B,C: CMX prospect. Bulk analysis of clear, 0.5-1.5cm quartz crystals, which occur as open-space fillings within 5-15cm smoky and clear quartz veins within the granite. Contains >90% type inclusions.

FN-1: Fuzzy Nut pit. Bulk analysis of clear, massive, brecciated vein quartz.

TABLE D1

Atomic Absorption Calibration Data for Preliminary  
Crush-Leach Analysis on MTE Quartz

Element	Calibration Data		Working Parameters		
	ppm	Absorbance	Wavelength (nm)	Lamp Current (mA)	Flame
Sodium	0.0	0.000	589.0	2.5	A-A
	1.0	0.036			
	2.0	0.083			
	5.0	0.222			
	10.0	0.450			
	15.0	0.657			
Potassium	0.0	0.000	766.5	2.8	A-A
	1.0	0.012			
	2.0	0.032			
	5.0	0.121			
	10.0	0.279			
Calcium	0.0	0.000	422.7	4.0	NO-A
	0.5	0.032			
	1.0	0.057			
	3.0	0.145			
Iron	0.0	0.000	248.3	5.5	A-A
	0.5	0.041			
	1.0	0.087			
	2.5	0.220			
Magnesium	0.0	0.000	202.5	3.0	A-A
	0.5	0.014			
	1.0	0.025			
	5.0	0.099			
	10.0	0.196			
Manganese	0.0	0.000	279.5	4.0	A-A
	0.5	0.072			
	1.0	0.139			
	5.0	0.604			
Zinc	0.0	0.000	214.9	4.0	A-A
	0.1	0.022			
	0.5	0.049			
	1.0	0.101			

TABLE D1 (continued)

Element	Calibration Data		Working Parameters		
	ppm	Absorbance	Wavelength (nm)	Lamp Current (mA)	Flame
Copper	0.0	0.000	324.7	3.5	A-A
	0.1	0.017			
	0.5	0.126			
	1.0	0.250			
	2.5	0.606			
Barium	0.0	0.000	553.5	10.0	NO-A
	1.0	0.011			
	2.5	0.018			
	5.0	0.039			
	10.0	0.107			
Silver	0.0	0.000	328.1	3.0	A-A
	0.5	0.045			
	1.0	0.100			
	5.0	0.538			
Lead	0.0	0.000	217.0	5.0	A-A
	0.5	0.020			
	1.0	0.057			
	5.0	0.244			

## Comments

A-A Flame = Air-Acetylene Flame

NO-A Flame = Nitrous Oxide-Acetylene Flame



TABLE D2

Anion Chromatography Calibration Data for Preliminary Crush-Leach  
Analysis on MTE Quartz  
May 16, 1990

## CHLORIDE

<u>Conc (ppm)</u>	<u>Peak Height (mm)</u>	<u>Peak Area</u>	<u>Retention Time (min)</u>
10	23.5	869417	1.45
20	49.0	1861188	1.45
30	77.8	3046242	1.46
40	97.7	4017760	1.46
50	117.8	5044614	1.47

## NITRATE

<u>Conc (ppm)</u>	<u>Peak Height (mm)</u>	<u>Peak Area</u>	<u>Retention Time (min)</u>
10	7.1	415163	2.39
20	13.8	872529	2.37
30	20.9	1397584	2.35
40	27.1	1896237	2.34
50	33.6	2421824	2.33

## SULPHATE

<u>Conc (ppm)</u>	<u>Peak Height (mm)</u>	<u>Peak Area</u>	<u>Retention Time (min)</u>
10	7.5	636007	3.64
20	14.0	1171632	3.62
30	22.1	1919260	3.61
40	28.5	2492308	3.59
50	35.7	3186942	3.58

Peak Area is obtained from integration of peak areas

TABLE D3  
Atomic Absorption Calibration Data for Fluid Inclusion Leachate  
Solutions on Vein Quartz Using a 250 ppm Sc in 0.25 wt% HNO<sub>3</sub>  
Leaching Solution

Element	Calibration Data		Working Parameters		
	ppm	Absorbance	Wavelength (nm)	Lamp Current (mA)	Flame
Sodium	0.0	0.000	589.0	2.5	A-A
	1.0	0.003			
	5.0	0.017			
	10.0	0.030			
	25.0	0.081			
	50.0	0.155			
Potassium	0.0	0.000	766.5	2.8	A-A
	1.0	0.038			
	3.0	0.115			
	5.0	0.195			
	10.0	0.383			
Calcium	0.0	0.000	422.7	4.0	NO-A
	1.0	0.034			
	3.0	0.112			
	5.0	0.221			
	10.0	0.443			
	15.0	0.681			
Iron	0.0	0.000	248.3	5.5	A-A
	0.5	0.066			
	1.0	0.110			
	3.0	0.287			
Magnesium	0.0	0.000	202.5	3.0	A-A
	0.5	0.065			
	1.0	0.131			
	3.0	0.352			
Manganese	0.0	0.000	279.5	4.0	A-A
	0.5	0.106			
	1.0	0.207			
	3.0	0.569			
Zinc	0.0	0.000	214.9	4.0	A-A
	0.1	0.020			
	0.5	0.066			
	1.0	0.099			

A-A Flame = Air-Acetylene Flame; NO-A Flame = Nitrous Oxide-Acetylene Flame

TABLE D4  
 Anion Chromatography Calibration Data for Fluid Inclusion  
 Leachates on Vein Quartz Using a 250 ppm Sc in 0.25 wt%  
 HNO<sub>3</sub> Leaching Solution

CHLORIDE (9-7-90)

<u>Conc (ppm)</u>	<u>Peak Height (mm)</u>	<u>Peak Height</u>	<u>Retention Time (min)</u>
5	8.3	47245	1.39
10	18.1	104653	1.39
25	52.5	302989	1.40
50	102.6	589075	1.41

SULPHATE (9-7-90)

<u>Conc (ppm)</u>	<u>Peak Height (mm)</u>	<u>Peak Height</u>	<u>Retention Time (min)</u>
5	2.4	12086	3.30
10	4.8	25802	3.29
25	13.8	78388	3.28
50	27.0	154225	3.25

CHLORIDE (9-10-90)

<u>Conc (ppm)</u>	<u>Peak Height (mm)</u>	<u>Peak Height</u>	<u>Retention Time (min)</u>
5	27.4	161115	1.38
10	52.8	307044	1.38
25	150.6	866965	1.38

SULPHATE (9-10-90)

<u>Conc (ppm)</u>	<u>Peak Height (mm)</u>	<u>Peak Height</u>	<u>Retention Time (min)</u>
5	17.3	99983	3.25
10	26.2	152171	3.24
25	52.2	301555	3.22

The second peak height was determined by peak integration

TABLE D5

Preliminary Crush-Leach Data Using MTE Quartz and  
Various Leaching Solutions

Sample	Sample wt (g)	Solution wt (g)	Leachate Solution	Conc. in ppm (after blank subtraction)								
				Na	K	Ca	Fe	Mn	Mg	Zn	Cl	SO <sub>4</sub>
MTE-200	5.0	54.9	A	5.6	2.3	1.2	0.2	0.3	0	0	12.4	0.3
MTE-201	(3)	38.1	A	0	0	0	0	0	0	0	0.2	0.3
MTE-202	10.0	53.6	B	9.8	4.2	0.5	0.6	0.4	0	0.1	5.8	(1)
MTE-203	(4)	44.0	B	0	0	0	0	0	0	0	0	(1)
MTE-204	10.1	59.1	B	8.7	3.7	0.8	0.4	0.3	0.2	0.1	10.5	(1)
Blank			B	0	0	0	0	0	0.1	0	0	(1)
MTE-205	10.1	40.9	C	12.9	5.4	6.9	0.6	0.6	0.4	0.1	(2)	(1)
MTE-206	(5)	48.7	C	0	0	0.2	0	0	0	0	(2)	(1)
MTE-207	6.4	37.8	C	9.1	3.8	4.6	0.4	0.5	0.3	0.1	(2)	(1)
Blank			C	0	0	0	0	0	0.1	0	(2)	(1)
MTE-208	5.0	52.6	D	5.4	2.4	0.9	0.3	0.3	0	0.1	12.2	1.1
MTE-209	10.6	57.3	D	11.8	5.0	2.4	0.8	0.7	0	0.1	23.6	1.4
MTE-210	25.1	59.2	D	15.6	6.5	2.9	0.9	0.9	0.1	0.1	29.9	1.3
Blank			D	0	0	0	0	0	0.1	0	0.8	1.7
N-1		53.2	A	0	0	0	0	0	0.1	0	0	0
N-2		57.2	A	0	0	0	0	0	0	0	0	0
N-3		57.8	A	0	0	0	0	0	0	0	0	0

## Leaching Solutions

A = Distilled/Deionized Water; B = 0.13 N HNO<sub>3</sub>C = 200 ppm LaCl<sub>3</sub> in 0.13 N HNO<sub>3</sub>; D = Hot (80) Distilled/Deionized Water

- (1) Sulphate nondetectable due to interference with nitrate from leaching solution  
 (2) Chloride nondetectable due to contamination from chloride in leaching solution  
 (3) Sample MTE-201 is a releach of crushed quartz from sample MTE-200  
 (4) Sample MTE-203 is a releach of crushed quartz from sample MTE-202  
 (5) Sample MTE-206 is a releach of crushed quartz from sample MTE-205

**TABLE D6**  
**Experimental Data on Fluid Inclusion Crush-Leach Analyses of**  
**Vein Quartz Using a 250 ppm Sc Solution in 0.25 wt% HNO<sub>3</sub>**

Sample	Sample wt (g)	Leachate Solution wt (g)	Conc. in ppm (after blank subtraction)							
			Na	K	Ca	Fe	Mn	Mg	Zn	Cl
MTE-500	5.04	28.1	12.2	5.0	3.6	0.7	0.7	0	0.1	12.8
MTE-501	5.20	32.9	10.7	4.3	2.5	0.6	0.6	0	0.1	10.5
MTE-501A	(1)	55.4	0	0	0	0	0	0	0	0
MTE-502	5.01	25.5	12.6	5.2	3.7	0.8	0.6	0	0.1	15.1
MTE-503	5.24	31.1	8.9	4.1	2.4	0.6	0.5	0	0	10.8
MTE-504	5.45	32.6	8.4	3.7	2.3	0.5	0.5	0	0	10.2
W3-3A	5.20	26.7	19.4	7.5	4.7	0.5	1.1	0.1	0.2	21.4
W3-3A1	(2)	37.8	0.6	0	1.1	0	0	0	0	0
W3-3B	5.27	26.0	18.8	7.2	4.2	0.4	1.1	0.1	0.1	21.7
W3-3C	5.21	27.2	14.2	5.4	4.2	0.3	0.8	0.2	0.1	15.6
HH-100	5.15	27.0	17.3	5.8	5.0	1.0	1.3	0.3	0.2	20.0
HH-101	7.08	24.1	24.3	8.2	7.0	1.7	1.8	0.5	0.2	23.1
CMX-1A	5.83	31.9	12.2	4.8	2.9	0.3	0.6	0	0.1	12.9
CMX-1B	5.39	28.4	12.1	4.9	2.8	0.3	0.7	0	0.1	12.4
CMX-1C	6.07	33.4	9.0	4.0	2.2	0.2	0.5	0	0.1	9.4
FN-1	5.19	23.6	27.0	10.6	6.6	2.0	1.7	0.3	0.2	29.2
CPU-2A	5.40	28.9	6.7	2.0	2.0	0.4	0.4	0.1	0.1	7.7
CPU-2B	5.34	32.8	5.5	1.9	1.6	0.3	0.3	0	0.1	4.3
CPU-2C	5.38	27.5	6.5	2.3	2.1	0.4	0.4	0.1	0.1	5.0
Sc Solution	(3)		0	0	0	0.3	0	0	0	0
Blank	(4)		0.3	0	2.1	0.4	0	0.6	0	0

(1) Sample MTE-501A is a re-leach of sample MTE-501

(2) Sample W3-3A1 is a re-leach of sample W3-3A

(3) The Sc solution is the stock solution used as the leaching solution

(4) The blank is the Sc leaching solution that is "crushed" in the alumina mortar and pestle and passed through the filter unit. This was done to check for contamination in the procedure.

Samples W3-3A, B and C are from the Wee Three (W3-3) prospect

Samples HH-100, 101 are from the Hot Hill prospect

Sample FN-1 is from the Fuzzy Nut prospect

TABLE D7

Experimental Data for the Hydrofluoric Acid-Quartz Dissolution  
Technique

Sample	Sample wt (g)	Amount of HF Added (g)	Percent Quartz Reacted	Analyzed Solution Wt (g)
MTE-100	2.6	71.0	23.5	19.0
MTE-101	5.1	58.9	77.2	18.6
MTE-102	10.0	68.7	61.6	16.8
MTE-103	10.0	77.7	66.7	18.1
MTE-104	Blank	25.0		15.4

Sample MTE-100 is inclusion-free MTE vein quartz  
Sample MTE-104 is a hydrofluoric acid blank

Concentrations in ppm (after blank subtraction)

Sample	Na	K	Ca	Fe	Mn	Mg	Zn	Ba	Cl	SO <sub>4</sub>	Molar Ratio	
											K/Na	Ca/Na
MTE-100	0.2	0	0.1	0.1	0	0	0	0	(1)	0		
MTE-101	20.2	10.9	0.4	4.0	0.7		0.2	0	(1)		0.32	0.01
MTE-102	39.2	20.2	1.4	7.7	2.1	0.3	0.3	1.6	(1)	6.1	0.30	0.02
MTE-103	34.7	17.9	0.5	6.5	1.5	0.1	0.3	1.2	(1)	4.2	0.30	0.01
MTE-104	0.1	0	0	0.1	0	0.1	0	0	(1)	0		

(1) Chloride nondetectable due to peak overlap interference with fluoride

Low Ca values for samples may be due to formation of an insoluble residue, CaF<sub>2</sub>

This technique was the only method which detected Ba

## Appendix E

### Delta O-18 on Silicates - Experimental Procedure

A silicate extraction line employing chlorine trifluoride ( $\text{ClF}_3$ ) as the fluorinating reagent was used for extracting oxygen samples from quartz, adularia and whole rock samples. Detailed procedures for the operation of the silicate line are given in Pierson and Phillips (1990).

Quartz and adularia samples for oxygen isotope analyses were handpicked from vein material. Pure, millimeter-size samples were obtained by 1) scrubbing the sample with soap and water to remove any surface dirt, rinsed with distilled water and oven-dried, and/or 2) smashing the sample in order to obtain a clean and pure interior portion of the mineral. Whole rock samples for oxygen isotope analyses were obtained by breaking fist-size samples and obtaining millimeter-size pieces of the interior portions from the broken sample. The millimeter-size portions of the quartz, adularia and whole rock samples were crushed to a - 80 mesh powder in an agate mortar and pestle. The samples were stored until ready for use.

Ten to twenty milligram portions of the - 80 mesh silicate samples were loaded into sample containers and oven-dried at  $120^\circ\text{C}$  for six to eight hours prior to being loaded into the nickel reaction vessels on the silicate line. Quartz samples were loaded into nickel reaction vessels and prefluorinated for five minutes at  $150^\circ\text{C}$  to remove any water that may have adsorbed onto the surface of the quartz during the loading process. Adularia and whole rock samples were loaded into nickel reaction vessels and heated to  $150^\circ\text{C}$  under vacuum for ten minutes to remove any water. The silicate samples in the nickel reaction vessels were evacuated and then reacted with the  $\text{ClF}_3$  reagent at 450 to  $500^\circ\text{C}$  for eight hours.

The liberated oxygen from the silicate samples was converted to  $\text{CO}_2$  with a heated graphite rod. The  $\text{CO}_2$  pressures were measured and the gases stored in

collection vessels. CO<sub>2</sub> yields from the extraction process range from 93 to 112% for quartz, with the majority at  $100 \pm 4\%$ . CO<sub>2</sub> yields for adularia range from 107 to 128%.

Oxygen isotope ratios, with respect to SMOW, were measured on the CO<sub>2</sub> samples with a Finnigan Mat delta E mass spectrometer. Precision for silicates using an NBS standard (NBS-28) was  $\pm 0.07\text{‰}$ . Precision for silicate samples using an in-house standard (Capitan quartz) was  $\pm 0.10\text{‰}$  (Pierson and Phillips, 1990). Precision for duplicate/triplicate runs on other quartz samples was usually greater than  $\pm 0.10\text{‰}$ .

Occasionally, low CO<sub>2</sub> yields and/or bad oxygen isotope ratios on the silicate samples were obtained. This was attributed to several factors.

- 1) An incomplete liberation of O from the silicate sample as a result of a heater breaking during the course of the eight hour run.
- 2) Contamination of the nickel reaction vessel from a previous sample which had reacted incompletely.
- 3) A bad O<sub>2</sub> to CO<sub>2</sub> conversion - which happened when none of the O<sub>2</sub> converted to CO<sub>2</sub>, or when it took greater than five minutes (sometimes 15 to 20 minutes) for all of the O<sub>2</sub> to convert to CO<sub>2</sub>. It is unclear why bad O<sub>2</sub> to CO<sub>2</sub> conversions occur.

Tables E1 to E4 list all the pertinent data for quartz, adularia and whole rock samples which were analyzed in this project. Descriptions for all of the silicate samples are given immediately preceding this section.



## Oxygen Isotope Sample Descriptions for Quartz

### BS Prospect

Sample consists of clear/milky massive vein quartz from a 0.5 cm quartz vein cutting granite. float/dump material.

### CM 104 Prospect

Sample of clear, euhedral, 1 to 3 mm quartz crystals attached to brecciated vein material.

### CM 235 Prospect

Samples of clear, euhedral, 1 to 4 mm quartz crystals in vugs from brecciated granite.

### CM 242

Small, clear, euhedral quartz crystals from a 1 cm quartz vein in alaskite.

### CM 301

Sample consists of several 1 to 3 mm clear, euhedral quartz crystals from a 5 mm wide vuggy quartz vein in granite. Float material.

### CMX Prospect

Sample CMX-1 consists of clear, euhedral, 1 cm quartz crystals from a quartz vein cutting through the granite. Sample CMX-2 consists of smoky, euhedral, 1 cm quartz crystals from a quartz vein cutting through the granite.

### CPU-2 Prospects

Sample CPU-2A consists of smoky quartz crystals lining vugs in a vein cutting the granite. Sample CPU-2B consists of single, clear, euhedral quartz crystals from a vuggy quartz vein. Sample CPU-2C consists of clear, massive vein quartz in brecciated granite. Sample CPU-2D consists of euhedral, smoky quartz crystals lining fractures in brecciated granite. Sample CPU-2E consists of clear, massive vein quartz in brecciated granite.

### Fuzzy Nut Prospect

Sample FN-2 consists of clear quartz in veins within brecciated granite. Sample FN-5 consists of clear, vuggy quartz in a 2 cm vein cutting granite. Sample FN-6 consists of clear, massive quartz in a 1 cm quartz vein cutting granite.

### Hot Hill Prospect

Sample HH-1 consists of smoky quartz crystals from a smoky quartz vein in brecciated granite. Sample HH-2 consists of single, clear euhedral quartz crystals in a clear quartz veinlet cutting through the granite. Sample HH-8 is a single smoky quartz crystal from a smoky quartz vein west of the main pit.

### Koprian Springs Prospect

Sample KS-1C consists of clear quartz crystals along fracture fill on granite.

### McCory Prospect

Sample McC-5 consists of two smoky quartz crystals lining fractured granite.

Mina Tiro Estrella (MTE) Prospect

Sample MTE-1 is a bulk sample of clear, massive vein quartz. Sample MTE-2 consists of single, clear, 2cm vuggy quartz crystals. Sample MTE-3 is a single, clear, 2 cm Japanese-law twinned quartz crystal.

Piney Prospect

Sample consists of three, 3 mm smoky crystals lining fractured surfaces of vein material.

Wee Three Prospects

Sample W3-1 is a single smoky quartz crystal from brecciated granite. Sample W3-2A consists of 1 to 5 mm smoky quartz crystals in veinlets from brecciated granite. Sample W3-2B consists of smoky quartz crystals in veinlets. Sample W3-3A is a single, 2 cm smoky quartz crystal from a fracture zone in the granite. Sample W3-3B is another 2 cm smoky quartz crystal. W3-3C is a single, clear quartz crystal from a vuggy quartz vein in brecciated granite. Sample W3-4A consists of smoky quartz crystals from open-space/fracture-fill in brecciated vein material. Sample W3-5 consists of smoky quartz crystals in veinlets of brecciated granite. Sample W3-7 is a single, clear quartz crystal from a quartz vein in granite.

TABLE E 1  
Oxygen Isotope Data for Quartz

Sample	Lab Number	Sample wt (mg)	O <sub>2</sub> to CO <sub>2</sub> Conversion	CO <sub>2</sub> μmoles	CO <sub>2</sub> % Yield	Δ <sup>18</sup> O-18	ClF <sub>3</sub> Pressure	Rxn Temp
BS	Si-52-10	12.2	good	209.2	103.1	9.12	2.89	450
CM 104	Si-45-12	11.9	good	188.6	95.2	8.86	2.56	450
CM 235	Si-23-1	10.7	good	183.7	103.0	9.04	3.51	530
CM 235	Si-37-7	11.3	bad	184.9	98.3	12.10	2.65	475
CM 235	Si-41-5	10.8	good	178.4	99.3	9.46	2.50	450
CM 242	Si-23-7	9.5	good	153.7	97.1	9.08	2.51	530
CM 242	Si-37-10	9.8	good	183.3	112.4	9.94	2.65	475
CM 242	Si-41-4	11.1	good	181.2	98.2	9.62	2.50	450
CM 301	Si-49-11	10.1	good	172.4	101.5	9.07	2.50	450
CMX-1	Si-23-4	10.6	good	173.8	98.3	9.17	3.51	530
CMX-1	Si-37-8	12.8	good	218.7	102.7	9.14	2.65	475
CMX-2	Si-23-5	10.3	good	172.6	100.5	9.04	3.51	450
CMX-2	Si-37-9	10.4	good	180.8	104.4	8.82	2.65	450
CPU-2A	Si-45-4	10.9	bad	152.7	84.2	11.19	2.56	450
CPU-2A	Si-46-2	10.3	good	163.4	95.4	9.54	2.62	450
CPU-2B	Si-46-9	10.1	good	173.0	102.9	9.11	2.62	450
CPU-2C	Si-46-12	10.1	good	173.8	103.4	9.39	2.62	450
CPU-2D	Si-45-10	12.4	good	197.3	95.6	9.62	2.56	450
CPU-2E	Si-46-11	11.6	good	203.7	105.5	8.55	2.62	450
FN-2	Si-45-5	11.8	bad	127.8	65.1	9.73	2.56	450
FN-2	Si-46-3	10.8	good	171.4	95.4	10.16	2.62	450
FN-5	Si-45-2	11.0	good	183.9	100.4	8.82	2.56	450
FN-6	Si-46-8	10.0	good	166.6	100.1	9.42	2.62	450
HH-1	Si-41-6	10.8	good	183.1	101.9	8.73	2.50	450
HH-2	Si-45-1	10.8	good	172.8	96.2	9.43	2.56	450
HH-8	Si-45-11	11.2	good	178.0	95.5	8.99	2.56	450
KS-1C	Si-52-11	10.7	good	182.3	102.4	9.22	2.89	450
McC-5	Si-45-3	10.5	good	165.0	94.5	9.59	2.56	450
MTE-1	Si-22-7	12.0	good	204.5	102.2	9.10	3.51	530
MTE-1	Si-37-4	10.6	bad	166.0	94.1	10.21	2.65	475

Table E1 Continued

Sample	Lab Number	Sample wt (mg)	O <sub>2</sub> to CO <sub>2</sub> Conversion	$\mu$ moles CO <sub>2</sub>	CO <sub>2</sub> % Yield	Del O-18	ClF <sub>3</sub> Pressure	Rxn Temp
MTE-1	Si-41-2	12.5	good	209.4	100.7	8.99	2.50	450
MTE-2	Si-22-9	11.0	good	184.3	100.5	8.81	3.51	530
MTE-2	Si-37-5	10.5	bad	184.7	105.7	11.16	2.65	475
MTE-2	Si-41-3	15.0	good	260.2	104.2	8.94	2.50	450
MTE-3	Si-22-11	11.8	good	181.7	92.4	9.21	3.51	530
MTE-3	Si-37-6	14.1	good	245.4	104.6	8.85	2.65	475
Piney-1	Si-49-12	11.4	good	197.7	104.2	9.05	2.50	450
W3-1	Si-45-7	11.6	good	187.0	96.8	10.46	2.56	450
W3-2A	Si-23-9	11.4	good	189.7	99.9	9.15	3.51	530
W3-2A	Si-37-11	10.9	good	173.4	95.6	8.84	2.65	475
W3-2B	Si-23-11	10.7	good	181.9	102.0	9.24	3.51	530
W3-2B	Si-37-12	13.9	good	248.3	107.4	8.78	2.65	475
W3-3A	Si-22-4	12.8	good	218.3	102.3	9.34	3.51	530
W3-3A	Si-37-2	10.1	bad	146.3	87.0	7.80	2.65	475
W3-3A	Si-41-1	14.4	bad	159.2	66.4	9.36	2.50	450
W3-3B	Si-22-5	12.7	good	215.8	101.9	9.06	3.51	530
W3-3B	Si-37-3	10.3	good	159.0	92.7	9.01	2.65	475
W3-3C	Si-46-10	11.1	good	182.7	98.9	9.05	2.62	450
W3-4A	Si-45-6	12.2	good	208.0	102.5	10.16	2.56	450
W3-5	Si-46-6	10.4	good	171.4	99.0	9.37	2.62	450
W3-7	Si-46-7	12.7	good	202.6	95.8	9.58	2.62	450

FN = Fuzzy Nut, HH = Hot Hill, KS = Kopian Springs, McC = McCory,  
W3 = Wee Three

All isotope values are in o/oo units and are reported with respect to SMOW.  
See Figure 1 or Appendix B for prospect/sample localities.

A good CO<sub>2</sub> conversion is defined when all of the O<sub>2</sub> converts to CO<sub>2</sub> in a short period of time (less than five minutes). A bad conversion is when the O<sub>2</sub> does not all convert to CO<sub>2</sub>, or if it takes a long time (greater than five minutes) to convert all of the O<sub>2</sub> to CO<sub>2</sub>.

The ClF<sub>3</sub> pressure and reaction temperature are the conditions at which oxygen was liberated from the sample.

The CO<sub>2</sub> % Yield is based on the molecular weight of quartz (60 g/mole).

## Oxygen Isotope Descriptions for Adularia

### CPU-2 Prospect

Sample CPU-2F consists of two single, pink euhedral adularia crystals. The adularia occurs as fracture fill within brecciated alkali granite. Sample CPU-2G consists of whiteish-pink adularia crystals lining fractures within brecciated alkali granite.

### Fuzzy Nut Prospect

Sample FN-10 consists of small, pink euhedral adularia crystals which occur as coatings on fractured surfaces of brecciated granite. Adularia is slightly iron-stained.

### Hot Hill Prospect

Sample HH-10 is a single, pink euhedral adularia crystal taken from a vug from the main part of the trench.

### Koprian Springs Prospect

Sample KS-1B consists of a cluster of white adularia crystals taken from brecciated and hematite-cemented granite of the main pit.

### McCory Prospect

Sample McCory-6 is a single, pink euhedral adularia crystal from a fracture.

### Mina Tiro Estrella (MTE) Prospect

Sample MTE-4 consists of massive pink adularia from the vein material which is composed mostly of adularia and quartz. Sample is from the dump material.

Wee Three Prospects

Sample W3-2C consists of white euhedral adularia crystals from brecciated granite. Sample W3-4B is a pink adularia crystal from the brecciated granite.

TABLE E 2  
Oxygen Isotope Data for Vein Adularia

Sample	Lab ID Number	Sample wt (mg)	O <sub>2</sub> to CO <sub>2</sub> Conversion	μ moles CO <sub>2</sub>	CO <sub>2</sub> % Yield	Del O-18	ClF <sub>3</sub> Press	Rxn Temp
CPU-2F	Si-52-2	10.5	good	161.3	106.9	9.19	2.89	450
CPU-2G	Si-52-9	12.8	good	201.2	109.4	8.76	2.89	450
FN-10	Si-52-5	9.6	good	161.5	117.0	7.94	2.89	450
HH-10	Si-50-12	12.1	good	194.2	111.7	10.05	2.51	450
KS-1B	Si-52-4	11.8	good	191.9	113.1	8.47	2.89	450
McC-6	Si-46-1	13.4	good	215.8	112.1	8.29	2.62	450
MTE-4	Si-50-11	11.6	good	213.5	128.1	9.05	2.51	450
W3-2C	Si-52-3	12.2	good	190.3	108.6	9.63	2.89	450
W3-4B	Si-52-7	10.8	good	178.6	115.1	10.09	2.89	450

FN = Fuzzy Nut, HH = Hot Hill, McC = McCory, W3 = Wee Three

All isotope values are in ‰ units and are reported with respect to SMOW

See Figure 1 for prospect localities.

A good CO<sub>2</sub> conversion is defined when all of the O<sub>2</sub> converts to CO<sub>2</sub> in a period of time less than five minutes.

The ClF<sub>3</sub> pressure and reaction temperature are the conditions at which oxygen was liberated from the sample.

The CO<sub>2</sub> % Yield is based on the molecular weight of adularia (278.4 g/mole).



## Oxygen Isotope Descriptions for Pluton Whole Rocks

- CM 100: Sample of unaltered granophyric granite.
- CM 103: Sample of slightly altered aplitic granite.
- CM 211: Sample of unaltered porphyritic granite.
- CM 225: Sample of unaltered granophyric granite.
- CM 228: Sample of slightly altered granophyric granite.
- CM 241: Sample of unaltered granophyric granite.
- CM 243: Sample of unaltered aplitic granite.
- CM 246: Sample of unaltered porphyritic granite.
- CM 249: Sample of slightly altered porphyritic granite.

Textural classifications are from V. McLemore (pers. comm., 1990)

TABLE E 3  
Oxygen Isotope Data for Pluton Whole Rocks

Sample	Lab ID Number	Sample wt (mg)	O <sub>2</sub> to CO <sub>2</sub> Conversion	μ moles CO <sub>2</sub>	CO <sub>2</sub> % Yield	Del O-18	ClF <sub>3</sub> Press	Rxn Temp
CM 100	Si-50-2	11.7	good	196.0	100.6	9.12	2.51	450
CM 103	Si-50-3	12.4	good	204.5	99.1	9.02	2.51	450
CM 211	Si-50-7	12.4	good	199.5	96.6	9.22	2.51	450
CM 225	Si-50-8	10.3	good	174.0	101.5	8.86	2.51	450
CM 228	Si-50-9	12.1	good	202.6	100.6	7.96	2.51	450
CM 241	Si-50-4	13.2	good	177.3	80.7	8.73	2.51	450
CM 243	Si-50-6	12.1	good	202.2	100.4	7.64	2.51	450
CM 246	Si-50-10	12.3	good	204.3	99.8	7.85	2.51	450
CM 249	Si-50-5	13.5	good	211.1	94.0	8.97	2.51	450

CO<sub>2</sub> % Yield is based on the molecular weight of quartz (60 g/mole).

A good O<sub>2</sub> to CO<sub>2</sub> conversion implies that that conversion was nearly 100% and took place over a short time interval (less than 5 minutes).

ClF<sub>3</sub> Pressure and Reaction Temperature were the conditions at which the O<sub>2</sub> was formed.

## **Oxygen Isotope Sample Descriptions for Whole Rocks on Vein Clasts and Plutonic Rock Adjacent to Veins**

### CM 235 Prospect

Sample CM 235-10 is a 8 cm-size clast of brecciated granophyric granite in the central part of the vein. Minor amounts of Mn-Fe staining are on the sample.

### CPU-2 Prospect

Sample CPU-2H is a fist-size altered granophyric granite clast from the main part of the fracture zone. The clast contains Mn-Fe staining and minor amounts of smoky quartz.

### Fuzzy Nut

Sample FN-11 is a clast of granophyric granite in the brecciated vein.

### Hot Hill Prospect

Sample HH-5 is aplitic granite 10 cm from the brecciated zone in the main trench. Sample HH-6 is a fist-size clast of aplitic granite from the main part of the brecciated zone in the main trench. Sample HH-6 is slightly more altered than HH-5. Sample HH-9 is a sample of mineralized aplitic granite in the vein and contains small amounts of fluorite, calcite and brown nodular/tabular masses.

### McCory Prospect

Sample McC-2 is a fist-size granite clast in the brecciated vein material.

### Mina Tiro Estrella (MTE) Prospect

Sample MTE-5 is a fist-size piece of aplitic granite adjacent to the vein.

Wee Three Prospect

Sample W3-4C is a 4 cm clast of granite in the brecciated vein material. Sample is in contact with smoky quartz veins. Sample does not appear to be very altered.

TABLE E 4

Oxygen Isotope Data for Whole Rock Vein Clasts and  
Plutonic Rock Adjacent to Veins

Sample	Lab ID Number	Sample wt (mg)	O <sub>2</sub> /CO <sub>2</sub> Convert	μmoles CO <sub>2</sub> %	CO <sub>2</sub> Yield	De <sub>l</sub> O-18	ClF <sub>3</sub> Press	Rxn Temp
CM 235-10	Si-66-8	12.3	bad	146.1	71.3	6.47	2.50	450
CPU-2H	Si-66-3	13.1	good	122.6	56.1	8.23	2.50	450
FN-11	Si-66-12	11.9	good	202.4	102.0	8.97	2.50	450
HH-5	Si-66-5	11.9	good	201.4	101.5	8.49	2.50	450
HH-6	Si-66-6	12.4	good	208.6	100.9	8.61	2.50	450
HH-9	Si-66-7	16.0	good	238.2	89.3	9.68	2.50	450
McC-2	Si-66-9	12.5	good	226.3	108.6	8.77	2.50	450
MTE-5	Si-66-10	16.8	good	265.5	94.8	11.14	2.50	450
MTE-5	Si-66-11	15.7	good	264.5	101.1	10.84	2.50	450
W3-4C	Si-66-4	15.7	bad	163.2	62.4	5.90	2.50	450

FN = Fuzzy Nut, HH = Hot Hill, McC = McCory, W3 = Wee Three.

All isotope values are in o/oo units and are with respect to SMOW.

See Figure 1 for prospect localities.

A good CO<sub>2</sub> conversion is defined when all of the O<sub>2</sub> converts to CO<sub>2</sub> in a short period of time (less than five minutes). A bad conversion is when the O<sub>2</sub> does not all convert to CO<sub>2</sub>, or if it takes a long time (greater than five minutes) to convert all of the O<sub>2</sub> to CO<sub>2</sub>.

The ClF<sub>3</sub> pressure and reaction temperature are the conditions at which oxygen was liberated from the sample.

The CO<sub>2</sub> % Yield is based on the molecular weight of quartz (60 g/mole).

## **Delta D Analyses on Fluid Inclusion Waters - Experimental Data**

Hydrogen samples on inclusion fluids of vein quartz and fluorite were determined by using 10 to 25 grams of 0.2 to 1 cm size pieces of material. The samples and steel crushing tubes used to crush the quartz or fluorite are oven-dried at 120°C prior to use. The samples are loaded into the steel crushing tubes and the tubes are connected to a vacuum line. The tubes plus sample are evacuated and pumped on for 20 to 30 minutes. The valves on the crushing tubes are closed for 5 to 10 minutes and reopened to check for leaks. [Crushing tubes which show a significant leak are taken apart at the valve-tube connection, reassembled and checked again for leaks. Crushing tubes which continually leak are discarded. Generally, a crushing tube can be reused four or five times before it must be discarded. After the crushing tubes have been leak-checked, they are evacuated for 5 more minutes. The tubes are then closed, taken off the vacuum line and the sample is crushed with a hydraulic press. The steel crushing tubes are placed back onto the vacuum line. The lower portion of the crushing tube is cooled with liquid nitrogen in order to freeze the inclusion fluid within the crushing tube. The crushing tube is opened under vacuum and leak-checked. If a major leak has occurred during crushing, the sample is discarded. For minor leaks, the tube is re-evacuated with the liquid nitrogen still on the lower portion of the crushing tube. The valve on the crushing tube is closed and the tube is warmed with a heat gun. The water sample is then transferred over to a hydrogen reaction vessel by placing liquid nitrogen onto the lower portion of the hydrogen reaction vessel and freezing the water into it. [The hydrogen reaction vessel contains 0.25 to 0.3 grams of specially prepared zinc metal. Prior to freezing the water into the reaction vessel, the reaction vessel with the zinc metal in it is evacuated under vacuum, heated with a heat gun for five minutes, and pumped on for at least 15 minutes.] After the water has been frozen

into the hydrogen reaction vessel, the vessel is closed, taken off the vacuum line and placed in a specially designed hot plate for 30 minutes at 450 to 500°C. The hydrogen formed by this technique was measured to obtain the hydrogen isotope ratio of the inclusion fluids on a Finnigan Mat delta E mass spectrometer. Hydrogen isotope values were corrected with respect to SMOW ( $\delta D = 0\text{‰}$ ), GISP ( $\delta D = -189.7\text{‰}$  vs SMOW) and SLAP ( $\delta D = -428\text{‰}$ ). The equation for obtaining the correction factor is  $y = 1.041x + 19.8$ , where  $x$  is the uncorrected hydrogen isotope value and  $y$  is the corrected value.

In one sample, CMX-2, the sample was heated under vacuum prior to crushing. This was done in order to see if any secondary ( lower temperature) inclusions could be decrepitated and analyzed separately from the higher temperature inclusions. After the initial heating, the sample was crushed, extracted and analyzed as a regular sample. Not much difference was seen in the hydrogen values,  $-114\text{‰}$  for heating only versus  $-103\text{‰}$  for crushing.

Depleted hydrogen isotope values, values less than  $-90\text{‰}$ , were usually obtained on samples which evolved small amounts of water during the crushing process, or on runs which showed moderate to major leaks during the crushing process. It was also noted that the heavier hydrogen values, values greater than  $-85\text{‰}$ , were obtained on larger chunks of material.

Table E5 lists all pertinent data for the fluid inclusion water samples which were analyzed in this project. Following is a summary of the quartz and fluorite samples which were used.

## **Hydrogen Isotope Sample Descriptions for Quartz and Fluorite**

### CM 301

Sample consists of 1 cm pieces of quartz from a 5 mm quartz vein cutting porphyritic granite. The quartz consists of 1 to 3 mm clear, euhedral crystals (a crystal mush of quartz crystals). Sample is a float specimen.

### CMX Prospect

Sample CMX-1 consists of clear quartz crystals from a quartz vein along a fracture zone in the aplitic granite. Sample CMX-2 consists of smoky quartz crystals from a smoky quartz vein along the same fracture zone as the clear quartz vein.

### CPU-1 Prospect

Samples consist of 0.2 to 1 cm pieces of green vein fluorite.

### CPU-2 Prospect

Sample CPU-2 consists of clear, massive vein quartz and clear quartz crystals lining fractured surfaces of the granophyric granite. Some of the quartz pieces contain alkali granite on their surfaces, which may be a source of impurity during the crushing of the quartz.

### Fuzzy Nut Prospect

Samples consist of massive vein quartz within fractures of brecciated granophyric granite.



Hot Hill Prospect

Samples consist of smoky, massive vein quartz and smoky quartz crystals which protrude from the massive smoky quartz veins.

Mina Tiro Estrella (MTE) Prospect

Samples consist of large, 1 to 2 cm, crystals of clear Japanese-law twinned quartz. Samples are all from the dump material.

Wee Three Prospects

Samples W3-3 are 1 to 2 cm smoky quartz crystals from open spaces within fractured aplitic granite of the W3-3 prospect. Sample W3-4 consists of small pieces of vein fluorite from the W3-4 prospect. Small amounts of adularia are intergrown with the fluorite and may act as impurities in the crushing process.

TABLE E 5

## Hydrogen Isotope Data for Quartz and Fluorite

Sample	Lab ID Number	Description	Sample wt (g)	Uncorrected $\delta D$ (o/oo)	Corrected $\delta D$ (o/oo)	Comments
CM 301	H-48-11	cl quartz	25.16	-127.6	-113	1, 4
CM 301	H-79-12	cl quartz	18.48	-115.3	-100	2, 4
CMX-1	H-47-11	cl quartz	14.69	-83.5	-67	4
CMX-1	H-48-6	cl quartz	13.21	-82.4	-66	0, 5
CMX-1	H-50-2	cl quartz	10.16	-88.8	-73	0, 4
CMX-1	H-53-10	cl quartz	16.47	-96.0	-80	1, 5
CMX-1	H-79-4	cl quartz	10.25	-66.8	-50	0, 6, 7
CMX-1	H-79-11	cl quartz	11.88	-95.5	-79	3, 4
CMX-2	H-48-3	sm quartz	11.09	-101.5	-86	1, 5
CMX-2	H-48-8	sm quartz	12.25	-117.9	-103	1, 5
CMX-2	H-51-2a	sm quartz	10.16	-129.4	-114	8
CMX-2	H-51-2b	sm quartz	-----	-118.4	-103	9
CMX-2	H-53-11	sm quartz	15.64	-167.3	-154	3
CMX-2	H-79-8	sm quartz	14.40	-114.6	-100	2, 4
CPU-1	H-46-17	fluorite	14.73	-121.8	-106	2, 5
CPU-1	H-47-1	fluorite	19.37	-117.7	-103	1, 5
CPU-1	H-47-8	fluorite	20.57	-128.1	-113	1, 4
CPU-1	H-53-13	fluorite	16.79	-110.0	-95	7
CPU-1	H-79-9	fluorite	14.76	-112.6	-98	2, 4
CPU-1	H-79-10	fluorite	21.73	-117.9	-103	2, 4
CPU-2	H-48-4	cl quartz	13.89	-159.9	-147	2, 4
CPU-2	H-48-7	cl quartz	17.31	-145.3	-131	1, 4
CPU-2	H-48-12	cl quartz	7.97	-139.3	-125	0, 4
CPU-2	H-53-12	cl quartz	12.29	-123.2	-108	0, 4
CPU-2	H-79-5	cl quartz	15.50	-113.9	-99	2, 4
Fuzzy Nut	H-48-2	cl quartz	18.65	-129.1	-114	1, 5
Fuzzy Nut	H-48-10	cl quartz	19.05	-112.0	-97	1, 5
Fuzzy Nut	H-53-9	cl quartz	12.83	-93.6	-67	0, 5
Fuzzy Nut	H-53-14	cl quartz	12.17	-100.7	-75	1, 5
Hot Hill	H-47-9	sm quartz	7.85	-128.3	-103	1, 4

TABLE E 5 (Continued)

Sample	Lab ID Number	Description	Sample wt (g)	Uncorrected $\delta D$ (o/oo)	Corrected $\delta D$ (o/oo)	Comments
Hot Hill	H-48-1	sm quartz	10.35	-150.9	-137	3,4
Hot Hill	H-48-9	sm quartz	12.34	-130.9	-117	1, 4
Hot Hill	H-79-7	sm quartz	13.22	-122.8	-107	3, 4
MTE	H-35-7	cl quartz	8.12	-66.7	-50	1, 6, 7
MTE	H-37-8	cl quartz	?	229		10
MTE	H-37-12	cl quartz	?	-100.7	-85	10
MTE	H-46-13	cl quartz	11.25	-54.5	-36	0, 6, 7
MTE	H-46-14	cl quartz	14.30	-52.1	-34	1, 6, 7
MTE	H-48-5	cl quartz	12.56	-65.9	-49	1, 6
MTE	H-53-8	cl quartz	11.55	-164.5	-151	3
MTE	H-79-1	cl quartz	15.26	-39.9	-22	1, 6, 7
MTE	H-79-2	cl quartz	11.74	-43.1	-25	0, 6, 7
W3-3	H-46-16	sm quartz	9.93	-85.4	-69	2, 5
W3-3	H-47-2	sm quartz	13.72	-63.1	-46	0, 6, 7
W3-3	H-47-10	sm quartz	11.21	-64.7	-48	1, 6, 7
W3-4	H-79-6	fluorite	18.37	-129.1	-114	3, 4

## Comments

- (0) No leak during crushing
- (1) Small leak during crushing
- (2) Moderate leak during crushing
- (3) Large leak - to atmosphere - during crushing
- (4) Low water yield on pressure gauge
- (5) Moderate water yield on pressure gauge
- (6) High water yield on pressure gauge
- (7) Good run overall
- (8) Sample heated by heat gun to decrepitate lower temperature inclusions
- (9) Sample was crushed after being heated
- (10) Hydrogen reaction vessel contaminated from a previous enriched sample

See Figure 1 for prospect localities

cl quartz = clear quartz, sm quartz = smoky quartz

A correction was applied to the hydrogen isotope values based on SMOW, GISP and SLAP standards. The correction is  $y = 1.041x + 19.8$ , where  $y$  is the corrected hydrogen isotope value and  $x$  is the uncorrected value.

## Oxygen and Carbon Isotopes on Carbonates - Experimental Data

Carbonate samples for carbon and oxygen isotope analyses were handpicked from vein material and from fresh, massive limestone. Ten to twenty milligrams of sample were placed on one side of a partitioned carbonate reaction vessel. About 5 mL of 105% phosphoric acid was pipeted into the other side of the partitioned carbonate reaction vessel. The carbonate reaction vessel with the sample and acid were placed on a vacuum line and pumped out for six hours. This was done in order to ensure all gases ( $\text{CO}_2$ ,  $\text{H}_2\text{O}$ ,  $\text{N}_2$ ) were liberated from the acid. The reaction vessel was closed, tipped and the carbonate sample was reacted with the acid at a temperature of  $24^\circ\text{C}$  for at least 10 hours to liberate the  $\text{CO}_2$ . The amount of  $\text{CO}_2$  liberated from the sample was measured on a mercury manometer and the sample was transferred to a collection vessel.

Carbon and oxygen isotope ratios on the  $\text{CO}_2$  samples were measured on a Finnigan Mat delta E mass spectrometer. An isotope fractionation factor for the reaction of the carbonates with the phosphoric acid was determined using NBS standards (NBS-18, NBS-19 and NBS-20). A value of - 10.62 ‰ was added to all oxygen values for the vein carbonates and a value of - 10.32 ‰ was added to the oxygen values for the limestones.

Table E6 lists all the pertinent data for the carbonate samples which were analyzed in this project. Descriptions for all of the carbonate samples are given immediately preceding this section.

## **Carbon and Oxygen Isotope Sample Descriptions of Vein Carbonates and Limestones**

### Fuzzy Nut Prospect

Sample FN-20 is a late-stage, white crystalline calcite which occurs within vuggy brecciated vein material as a thin overgrowth on a brown, massive carbonate. The brown carbonate may be iron-stained calcite. Sample FN-21 is a brown massive carbonate, as mentioned above. Sample FN-22 is a massive pink carbonate in the brecciated vein material.

### Hopeful (HC) Prospect

Sample HC-20 is a late-stage, white crystalline calcite, which occurs as an overgrowth on a brown tabular mineral. Sample HC-21 is a brown tabular mineral believed to be an iron-stained carbonate.

### Hot Hill Prospect

Sample HH-20 is a late-stage, white crystalline calcite, which occurs as an overgrowth on a brown tabular mineral. Sample HH-21 is a brown tabular mineral which occurs within the mineralized zone in the main part of the trench. The brown carbonate is probably iron-stained calcite.

### San Andres Limestone

Samples LS-2A and LS-2B are from fresh, massive limestone of the San Andres formation. Both samples are from the same roadcut near mile marker 6 on highway 48. Samples LS-3A and LS-3B are from massive (unaltered?) limestone of the San Andres formation. Both samples are from the limestone roof pendant on top of the northwestern part of the Capitan Mountains.

TABLE E 6

## Carbon and Oxygen Isotope Data on Vein Carbonates and Limestone

Sample	Lab ID	Sample	$\mu$ moles	CO <sub>2</sub>	Uncorrected		Corrected	
	Number	wt (mg)	CO <sub>2</sub>	% Yield	$\delta^{18}\text{O}$	$\delta^{13}\text{C}$	$\delta^{18}\text{O}$	$\delta^{13}\text{C}$
FN -20	CO2-144-10	13.1	96.1	73.4	33.05	-7.63	22.43	-7.74
FN-20	CO2-144-9	13.6	111.0	81.6	32.77	-7.64	22.15	-7.76
FN-21	CO2-144-11	11.2	67.2	60.0	31.78	-4.68	21.16	-4.80
FN-21	CO2-144-12	12.7	75.0	59.1	31.72	-4.76	21.10	-4.88
FN -22	CO2-145-1	12.4	88.1	71.0	32.49	-7.90	21.87	-8.02
HC-20	CO2-145-2	15.4	128.9	83.7	32.58	-7.56	21.96	-7.68
HH-20	CO2-144-5	13.6	105.5	77.6	33.66	-7.04	23.04	-7.16
HH-20	CO2-144-6	10.6	53.2	50.2	33.79	-7.01	23.17	-7.13
HH-21	CO2-144-7	16.9	92.1	54.5	33.46	-2.19	22.84	-2.31
HH-21	CO2-144-8	15.5	82.8	53.4	33.24	-2.12	22.62	-2.24
NBS-18	CO2-144-1	12.4	62.1	50.1	17.83	-4.86	7.20	-5.00
NBS-18	CO2-144-2	11.0	64.7	58.8	17.81	-4.90	7.20	-5.00
NBS-19	CO2-144-3	11.0	57.0	51.8	39.26	2.05	28.65	1.92
NBS-20	CO2-144-4	12.7	105.5	83.1	37.26	-0.97	26.64	-1.06
LS-2A	CO2-148-9	20.3	20.2	9.9	36.44	2.54	26.13	2.32
LS-2B	CO2-148-10	19.3	20.2	10.5	37.46	2.48	27.14	2.25
LS-3A	CO2-148-11	21.3	68.5	32.2	31.33	2.23	21.01	2.00
LS-3B	CO2-148-12	18.6	59.6	32.0	30.43	1.71	20.12	1.48
NBS-18	CO2-148-13	14.2	84.1	59.2	17.52	-4.77	7.20	-5.00

FN = Fuzzy Nut, HC = Hopeful Claim, HH = Hot Hill. See Fig. 1 for localities.

Carbon isotope values with respect to PDB. Oxygen isotope values with respect to SMOW.

All isotope values are reported as ‰ units.

Oxygen isotope values are corrected for acid fractionation using NBS standards. Carbonates and limestones were run on different days and therefore have different corrections. Acid fractionation factor for oxygen =  $-10.62\text{‰}$  for the carbonates (calcites) and  $-10.32\text{‰}$  for the limestone samples.

A correction factor of  $-0.12\text{‰}$  was applied to the calcites and  $-0.23\text{‰}$  for the limestones for all carbon values in order to report all values relative to the NBS standards. This correction relates to the "zero enrichment" run on the mass spectrometer.

## APPENDIX F

### **Construction of a P-T Diagram to Illustrate the Phase Equilibria for the Capitan Halite Trend Inclusions**

The construction of the pressure-temperature phase diagram is followed according to the method of Cloke and Kesler (1979). The phase diagram construction is by no means original work of this author; therefore, unless other references are cited, all of the information in this section is taken directly from Cloke and Kesler (1979).

Figure 28, main text, shows the necessary cotectic lines, isotherms and isobars in the NaCl-KCl-H<sub>2</sub>O system used to construct the P-T phase diagram. For isobars greater than 200 bars, the isobars have been extrapolated to 300 bars by this author. The experimental data from this figure was obtained in the presence of vapor and therefore lies on solubility surfaces. For Figure 28, a straight line is drawn along the direction of the Capitan halite trend for the type 1 and 2 inclusions. From the straight line of Figure 28, the NaCl-KCl-H<sub>2</sub>O solubility curve along the direction of the halite trend is drawn, see Figure 31, main text. The lines L + H/L show the boundary between the two-phase L + H field and one-phase L only field. Two lines for salinities at 55 and 80 eq wt% NaCl + KCl are shown and one line for 35 eq wt% NaCl is shown. The first two lines were derived from Figure 28. The third line was estimated from Roedder and Bodnar (1980). At low pressures and high temperatures, the liquid field is bounded by the two-phase L + V field. The boundaries are shown by the lines L/L + V. A single L/L + V boundary for 80 and 55 wt% NaCl + KCl and 35 eq wt% NaCl are shown in Figure 31. This line does not represent data from the Capitan Mountains. See Cloke and Kesler (1979) for more details on the origin of the L/L + V boundaries. The resulting Figure 31 is a P-T phase diagram for the Capitan halite trend inclusions. It should be mentioned that the pressures are minimum pressures taken from Figure 28 which were used to calculate the P-T diagram.



### References Cited in Appendices

- Bodnar, R. J., Sterner, S. M., and Hall, D. L., 1989, SALTY: A FORTRAN program to calculate compositions of fluid inclusions in the system NaCl-KCl-H<sub>2</sub>O: *Comp. and Geoscience*, v. 15, p. 19-41.
- Bottrell, S. H., Yardley, B., and Buckley, F., 1988, A modified crush-leach method for the analysis of fluid inclusion electrolytes: *Bull. Mineral.*, v. 111, p. 279-290.
- Brown, P. E., and Lamb, W. M., 1989: P-V-T properties of fluids in the system H<sub>2</sub>O ± CO<sub>2</sub> ± NaCl: New graphical presentations and implications for fluid inclusion studies: *Geochim. et Cosmochim. Acta*, v. 53, p. 1209-1221.
- Cloke, P. L., and Kesler, S. E., 1979, The halite trend in hydrothermal solutions: *ECON. GEOL.*, v. 74, p. 1823-1831.
- Griswold, G. B., 1959, Mineral deposits of Lincoln County, New Mexico: New Mexico Bureau of Mines and Mineral Resources Bulletin no. 67, 117p.
- Hanson, T., 1989, Mina Tiro Estrella: *Mineralogical Record*, v. 20, p. 51-53.
- Kelley, V. C., 1949, Geology and economics of New Mexico iron-ore deposits: University of New Mexico, Publications in Geology, no. 2, 246p.
- Pierson, P., and Phillips, R., 1990, Calibration, precision and operating parameters for a new silicate line at the New Mexico Tech Stable Isotope Lab: Class Project for Geochemistry 571, 33p.
- Roedder, E., 1984, ed., Fluid Inclusions: Reviews in Mineralogy volume 12, Mineralogical Society of America, 646 p.
- Roedder, E. and Bodnar, R. J., 1980, Geologic pressure determinations from fluid inclusion studies: *Ann. Rev. Earth Planet. Sci.*, v. 8, p. 263-301.
- Tuftin, S., 1984, Mineral investigation of the Capitan Mountains Wilderness Area, Lincoln County, New Mexico: United States Department of the Interior, Bureau of Mines, Open-File Report MLA 20-84, 20 p.

This thesis is accepted on behalf of the faculty  
of the Institute by the following committee:

*Andrew Campbell*

Adviser

*Philip Kyle*

*Virginia T. McNamee*

12/7/90

Date